



KARMA



Karst Aquifer Resources availability and quality in the **Mediterranean Area**

Spring discharge monitoring

Deliverable 2.6

Authors:

Juan Antonio Barberá Fornell (UMA), Christelle Batiot-Guilhe (UMO), Simon Frank (KIT), Nadine Goeppert (KIT), Nikolai Fahrmeier (KIT), Nico Goldscheider (KIT), Sharon Rakowski (KIT), Hervé Jourde (UMO), Bartolomé Andreo Navarro (UMA), Jaime Fernández Ortega (UMA), Fairouz Slama (ENIT), Emna Gargouri-Ellouze (ENIT), Rachida Bouhlila (ENIT), Pascal Brunet (UMO), Guillaume Cinkus (UMO), Vianney Sivelles (UMO), Francesco Ulloa (UMO), Marco Petitta (URO), Valeria Lorenzi (URO), Domenico Barbiero (URO), Jihad Othman (AUB), Mohamed Al Ali (AUB), Joanna Doummar (AUB)

Date: May 2022



This project has received funding from the European Union's PRIMA research and innovation programme



Project Partners



(Coordinator)



SAPIENZA
UNIVERSITÀ DI ROMA



Executive Summary

WP2 is in charge to evaluate water availability at five KARMA test sites using different hydrodynamic approaches. The previous deliverables included (1) a preliminary assessment of the water budget (recharge/discharge) for each test site, so that a first estimation of karst groundwater resources at each test site was established; (2) an analysis of water stable isotopes, in order to validate indirect recharge assessment methods and (3) tracer test experiments, which deliver quantitative information on contaminant transport and represent an important input to WP3. A total of 14 springs are being monitored through the use of different tools and techniques in the framework of KARMA project. Almost half of those are used for populations drinking water supply, of different sizes like Montpellier (Lez spring, 350.000 inhabitants), France or Serrato, Spain (Cañamero spring, 470 inhabitants); or even (boreholes) used for mineral water commercialization (Tunisia). Thus, the analysis of the recharge and discharge processes of the aquifer systems constitutes an essential tool for the correct management of water resources.

In this report, KARMA project partners show the main characteristics of their spring discharge monitoring network, including the description of the measuring station, rating curves, main statistical descriptors and record time. KARMA karst springs present different geological and hydrogeological characteristics representative of the Mediterranean area, such as recharge areas range from 25 to 1034 km² with mean altitudes between 1200 and 1600 m a.s.l. and annual precipitation between 800 and 1800 mm. In the hydrographs obtained during the project execution, maximum spring discharge values have been recorded between 6-15 m³/s in permanent and overflow springs, however, the average flow of the monitored springs is 0.81 m³/s. A total of 5 springs were monitored in Italy (Gran Sasso aquifer) and show mean discharges that vary between 0.12-0.93 m³/s except for TI1 spring, which shows an average discharge of 5.27 m³/s. In Spain, 3 springs were monitored in Eastern Ronda Mountains and 3 more were also controlled in Ubrique test site. The highest average discharge rates were registered in Garciago (overflow) spring up to 0.3 m³/s during KARMA period and all of them were classified as a “complex and large system” (IV) according to Mangin's classification criteria. Spring discharge monitoring in Lez spring (France) has been realized since approximately 2010 and includes the control of a wide variety of hydrochemical parameters (Turbidity, DOM, Cl⁻, etc.) in addition to hydrodynamic control. Such long records allowed the application of specific techniques like Spectral and Correlation analysis or Mangin recession analysis. Sägebach and Aubach (overflow) springs in Austria were monitored during July and August 2020 and showed maximum discharge peaks of 3.5 and 6 m³/s respectively. However, the application of numerical modeling in this area is limited by the lack of meteorological data with high spatial resolution. The case of Jebel Zaghouan aquifer (Tunisia) shows the lack of spring discharge data corresponding to the natural flow until the installation of control valves inside the galleries, so that the system is no longer natural in Zaghouan massif and discharge regime has been highly disturbed. Finally, spring discharge record since 2014 is available at Qachqouch spring (Lebanon) and a description of data correction process is included. The application of cross correlation and autocorrelation approaches allowed to identify the memory effect of the spring of 60 days indicating a latent behavior of the spring.

Table of Contents

Technical References	1
Version History.....	1
Project Partners	1
Executive Summary.....	2
Table of Contents.....	3
1 Introduction	5
1.1 Direct spring discharge measurements	5
1.2 Features of the monitoring networks.....	6
1.3 Hydrodynamic data analysis	7
1.4 References	7
2 Gran Sasso aquifer (Case Study Italy)	9
2.1 Hydrogeological setting	9
2.2 The monitoring network	11
2.3 Results and Discussion	13
2.4 Bibliography	24
3 Ubrique test site (case study Spain).....	25
3.1 General description of the test sites.....	25
3.2 Equipment and methods	27
3.3 Results.....	30
3.3.1 Main statistical descriptors of spring discharge	30
3.3.2 Analysis of recession curves (Mangin, 1970 1975)	32
3.4 Discussion and conclusion	34
3.6 References	34
4 The Lez Karst Catchment (case study France).....	36
4.1 General description of the test site	36
4.1.2 Characteristics of the monitoring station at Lez spring	40
4.1.3 Objectives.....	41
4.2 Equipment and methods used.....	42
4.3 Results.....	44
4.3.1 Time Series of the Lez spring karst system	44
4.3.1.1 Main statistical description.....	44
4.3.1.2 Yearly discharge analysis.....	45

4.3.2	Recession curves analysis	45
4.3.3	Description of hydrological cycle	47
4.3.4	Correlation analysis.....	48
4.3.5	Spectral analysis.....	50
4.4	Discussion.....	50
4.5	References	51
5	Hochiften-Gottesacker karst area (test site in Austria).....	53
5.1	General description of the monitoring network for spring discharge monitoring	53
5.2	Equipment and methods used	54
5.3	Results.....	54
5.4	Discussion.....	56
5.5	Conclusions	56
5.3	Literature	57
6	Jebel Zaghouan aquifer	58
6.1	Study area	58
6.2	Water resources.....	59
6.3	Historical flow data	60
6.4	Current situation.....	60
6.5	References	60
7	The Qachqouch aquifer (Case study-Lebanon).....	62
7.1	Introduction	62
7.2	Equipment and methods	64
7.3	Results.....	66
7.3.1	Time series	66
7.3.2	Data Correction.....	67
7.3.3	Discharge auto- and cross correlation	68
7.4	Conclusions	69
7.5	References	69
8	Conclusions	70
8.1	References	70

1 Introduction

The overarching objective of the KARMA project is to achieve substantial progress in the hydrogeological understanding and sustainable management of karst groundwater resources in the Mediterranean area in terms of water availability and quality. Spring discharge in natural regime provides information about the hydrodynamic functioning of whole system and its analysis constitutes an essential approach to understand the natural processes of the environment. One of the main objectives of this task consist on analyzing the short-term variations of groundwater availability, given that in future climate scenarios such short/mid-term availability represents an important drinking water source to be protected and correctly managed. In the following sections, the most relevant results in each study area are shown, and will serve as major input for tasks 2.4, 3.2 and 4.2. Karst hydrogeology studies have traditionally been based on the analysis of the hydrodynamic response of the springs (represented through hydrographs), which constitute the basis for the elaboration of the different hypotheses about the structure and functioning of the system. These studies have been done on the shape of the rising and falling limbs and on the global hydrograph response and base times. This deliverable constitutes the main activity of Task 2.2 “Spring discharge monitoring”, as it comprises (1) the direct spring discharge measurements for establishing rating curves; (2) the main features of the monitoring stations as well as used sensors and (3) the analysis of the acquired hydrodynamic information.

1.1 Direct spring discharge measurements

The salt dilution technique is a widely used technique to measure spring discharge or turbulent streams but also to calculate the time of travel of pollutants. The approach consists on introducing a known amount of salt in the stream and measure the variation of Electrical Conductivity in order to establish a correlation between the last parameter and salt concentration and the discharge (Q) is derived from the standard equation described by Wood and Dykes (2002).

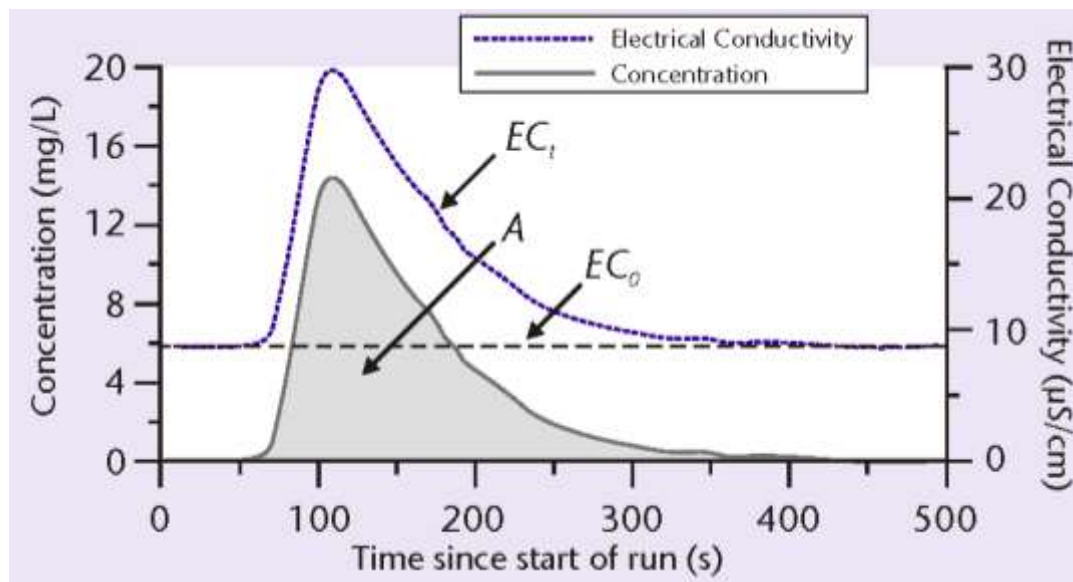


Figure 1.1. Salt dilution measurement at Russell Creek, October 2003. The shaded area is the quantity A that represents the injected mass (taken from Hudson et al; 2008).

On the other hand, the velocity-area method for the determination of discharge in laminar flows consists of measurements of stream velocity at different depths and distance across the river sections. The velocity is measured by a previously calibrated current-meter and an average velocity determined in each vertical and the discharge is calculated by the sum of partial discharges over the N subsections of the river section. Commonly used current-meters include mechanical (propellers), electro-magnetic (Hall effect based), or acoustic (Doppler effect based) (Le Coz et al; 2012).

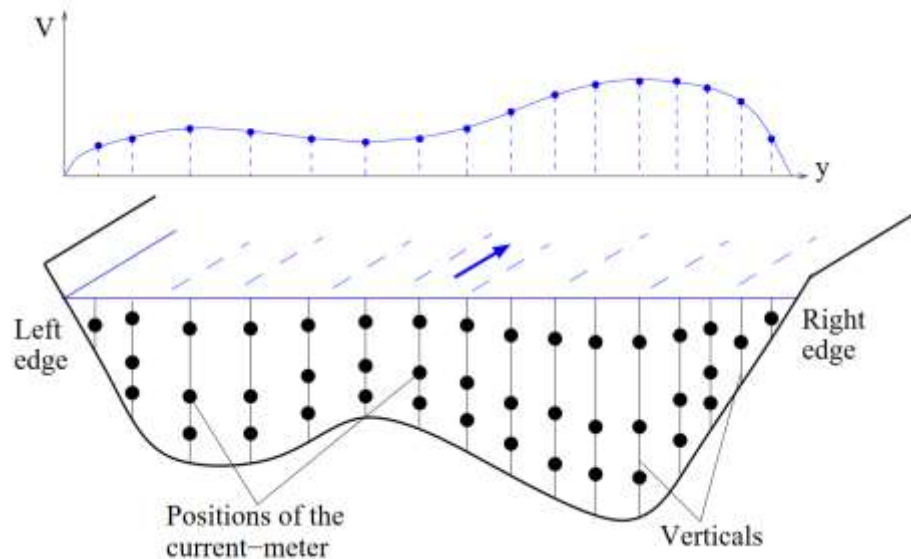


Figure 1.2. Principle of the velocity-area method: discrete sampling of velocity and depth throughout a cross-section, and the corresponding profile of depth-averaged velocity Le Coz et al; 2012.

1.2 Features of the monitoring networks

As karst springs show rapid reactions to precipitation events, in terms of quantity and quality, monitoring at high temporal resolutions is essential to characterize the dynamic behaviour (Hartmann, 2014). Two concepts are mainly used on this task: (1) stage height, or the level of a water surface at some point along the stream above an arbitrarily determined datum, and (2) discharge, which is the volume of water flowing past a cross section of the stream per time (Goldscheider and Drew, 2007). Flow measurements are required to calibrate the continuous records of stage height obtained by water level loggers through the application of rating curves, which serve for simple estimation of continuous spring discharge.

The first devices used for continuous spring discharge monitoring consisted on a weight and float attached to a wire draped over a cylinder that rotates as the float moves up or down with rising or falling stage (Goldscheider and Drew, 2007). Nowadays, the most common infrastructures implemented for continuous measurements usually consist on wireless sensors which use capacitive, pressure or even barometric compensation systems to measure water level. Such devices are installed in a stable stream section in order to avoid variations in the flow-through section.

1.3 Hydrodynamic data analysis

The quantitative analysis of the obtained data provides information about the physical processes related to karst aquifers and recharge processes. Karst spring recession analysis are essential for interpreting the aquifer geometry since the shape of spring hydrograph reproduces the arrival of groundwater from different recharge pathways or aquifer sectors (Ford and Williams 2007). Mangin's method (1970, 1975) is one of the most applied because it was specifically developed for karst aquifers and it considers the entire recession curve. This method is based on the distinction of two subsystems within the karst aquifer: (1) the infiltration subsystem, drainage of the unsaturated zone and the saturated zone during the decrease and (2) the saturated subsystem, drainage of the saturated zone in stationary regime.

Other methods are also used for this task, among which correlative and spectral analysis are found. They consider the complete data series and can be applied in the domain of time (correlatory analysis) and in the domain of frequency (spectral analysis). Mangin (1981, 1984) was the first to apply this methodology for investigating discharge variations in karst aquifers. Correlation and spectral analysis are used to investigate the frequency content of a signal (often referred to as “simple analysis”) and the dependency relationships among signals (usually an input and an output signal, referred to as “cross-analysis”) (Massei et al., 2006). Nowadays, the application of modelling techniques allows to rapidly process comparative analysis of karst spring systems using large number of data series which would otherwise be a complex task to execute (Olarinoye et al., 2021). Furthermore, numerical approaches avoid subjectivity and errors introduced by manual procedures. Throughout the last decades, karst models have been presented as a powerful tool for water quality and contamination vulnerability simulations and the prediction of karst water resources. For these reasons, spring discharge monitoring is essential for understanding the aquifer functioning and for sustainable karst groundwater management.

1.4 References

- Ford D, Williams P (2007) *Karst Hydrogeology and Geomorphology*. John Wiley and Sons, Ltd
- Goldscheider, N. and Drew, D. -Eds- (2007) *Methods in Karst Hydrogeology*. Taylor & Francis, London (UK). 264 pages.
- Hartmann, A., Goldscheider, N., Wagener, T., Lange, J. and Weiler, M. (2014) Karst water resources in a changing world: Review of hydrological modeling approaches. *Reviews of Geophysics*, 52(3), 218–242
- Hudson, R. O., John F. (2008) Introduction to Salt Dilution Gauging for Streamflow Measurement Part IV: The Mass Balance (or Dry Injection) Method. *Streamline Watershed Management Bulletin Vol. 9/No. 1*, Fall 2005
- Le Coz, J., Camenen, B., Peyrard, X., Dramais, G. (2012) Uncertainty in open-channel discharges measured with the velocity-area method. *Flow Measurement and Instrumentation* 26: 18-29.
- Mangin, A. (1970) Contribution à l'étude des aquifères karstiques à partir de l'analyse des courbes de décrue et tarissement. *Annales Spéleologie* 25 (3), 581-610.
- Mangin, A. (1975) Contribution à l'étude hydrodynamique des aquifères karstiques (I). PhD Thesis. Dijon University (France). *Annales Spéleologie* 29 (3), 283-332; 29 (4), 495-601; 30 (1), 21-214.

Mangin, A. (1981) Utilisation des analyses corrélatrices et spectrales dans l'approche des systèmes hydrologiques. C.R. Acad. Sci. Paris 293, 401–404.

Mangin, A. (1984) Pour une meilleure connaissance des systèmes hydrologiques à partir des analyses corrélatrices et spectrales. J. Hydrol. 67, 25–43.

Massei, N., Dupont, J.P., Mahler, B.J., Laignel, B., Fournier, M., Valdes, D., Ogier, S. (2006) Investigating transport properties and turbidity dynamics of a karst aquifer using correlation, spectral, and wavelet analyses. Journal of Hydrology 329, 244– 257

Olarinoye, T., Gleeson, T., and Hartmann, A.: Karst spring recession curve analysis: efficient, accurate methods for both fast and slow flow components. Hydrol. Earth Syst. Sci. Discuss. [preprint]

Wooda, P.J., Dykesb A.P. (2002) The use of salt dilution gauging techniques: ecological considerations and insights. Water Research 36, 3054–3062

2 Gran Sasso aquifer (Case Study Italy)

2.1 Hydrogeological setting

The Gran Sasso aquifer, a karstic aquifer about 1034 km² of surface, is one of the most representative karst aquifers of the Apennines, defined as a single basal regional aquifer with high permeability for fracturing and karstification (Amoruso et al., 2013). Its relevance is due to the groundwater resources deeply exploited for any purpose, the interaction between groundwater and underground works (tunnels and underground lab) and the position inside a protected area (National Park) (Monjoie, 1980; Adinolfi Falcone et al., 2008). The Gran Sasso hydrogeological system is defined by Meso-Cenozoic carbonate units (aquifer). It is bounded by terrigenous units represented by Miocene flysch (regional aquiclude) along its northern side, and by Quaternary continental deposits (regional aquitard), along its southern side (Amoruso et al., 2013). Permeability limits are constituted to the main overthrust, located in the northern and eastern areas, with direction E-W and then N-S, dipping respectively to the South and West (Figure 2.1) (Amoruso et al., 2013). The hydrogeological system can be divided into several hydrogeological complexes determined according to different characteristics such as lithology, porosity and permeability.

At the massif core, an endorheic basin having a tectonic-karst origin, called Campo Imperatore, acts as a preferential recharge area of the Gran Sasso aquifer, fed by high rainfall and snow rate.

The Gran Sasso aquifer feeds major basal springs, characterised by high and steady discharge rates and located on the margins of the massif along the low permeability boundary, in contact between the carbonate rocks and the impermeable land sediments (Petitta et al., 2015). The springs have a total discharge between 18 m³/s (Amoruso et al., 2011) and 25 m³/s, corresponding to a net infiltration of about 800 mm/year (Amoruso et al., 2013). Discharge from the Gran Sasso springs has decreased significantly after tunnel excavation in the 1980s and subsequent groundwater drainage has been realized (Amoruso et al., 2014). In the following years, spring discharge has risen slightly, indicating that the aquifer groundwater has reached a new steady state thanks to drainage by the tunnels (Amoruso et al., 2013). The main springs have been organised into six groups based on groundwater flow and hydrochemical characteristics, as illustrated in Figure 2.1 (A-F) (Amoruso et al., 2013).

The springs were also subdivided according to the characteristics of the chemical-physical parameters, monitored mainly to check the quality of the water tapped for drinking and hydroelectric purposes (Amoruso et al., 2013). Petitta and Tallini (2002) processed temperature and electrical conductivity data over a long period (1970-2000) using statistical methods and seasonal trends can be observed for some springs.

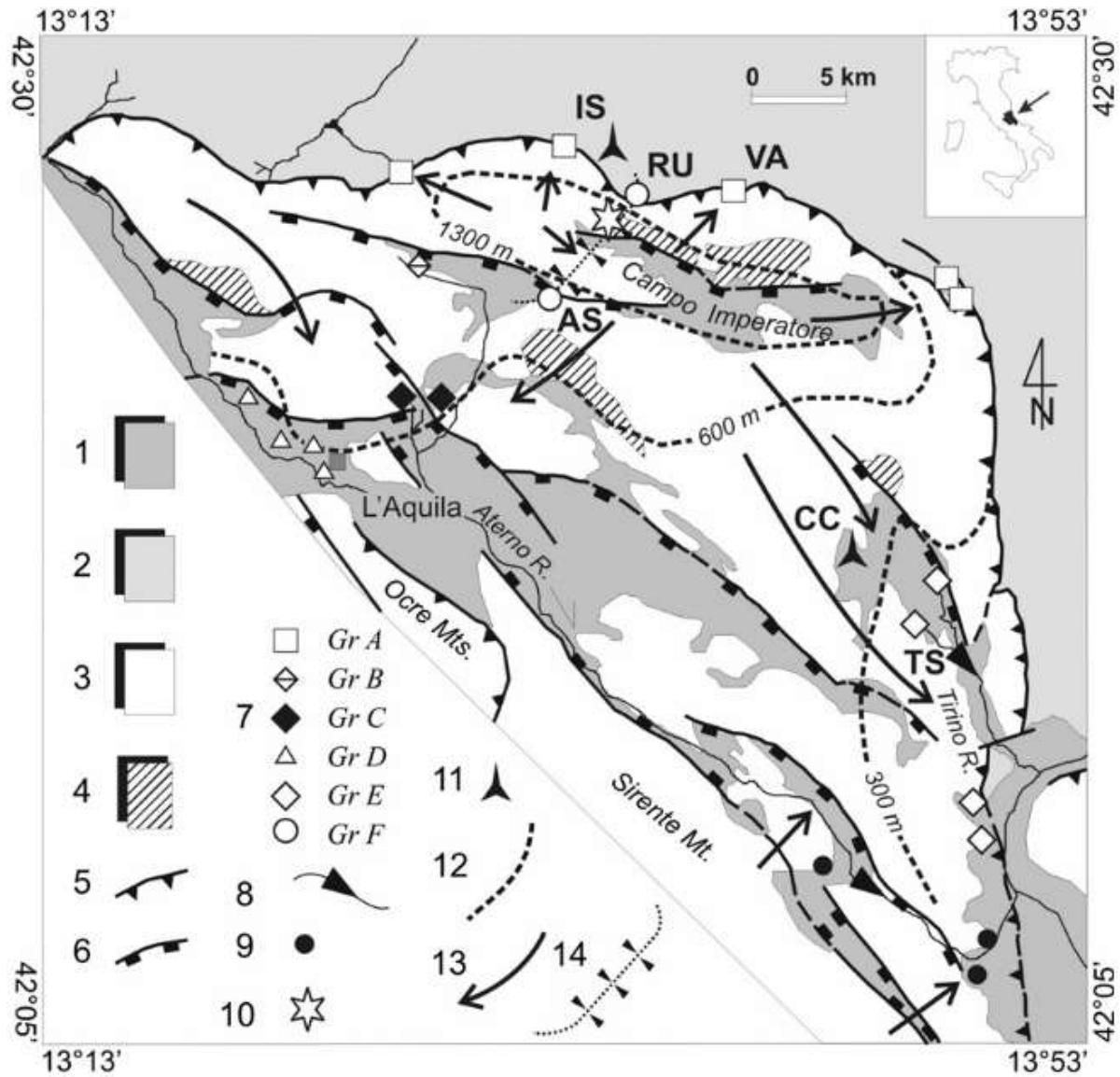


Figure 2.1. Gran Sasso hydrogeological outline. 1: aquitard (continental detrital units of intramontane basins, Quaternary); 2: aquiclude (terrigenous turbidites, Mio-Pliocene); 3: aquifer (calcareous sequences of platform Meso-Cenozoic); 4: low permeability substratum (dolomite, upper Triassic); 5: thrust; 6: extensional fault; 7: main spring; AS: Assergi drainage; RU: Ruzzo drainage; VA: Vacelliera spring; TS: Tirino springs; symbols refer to the six spring groups identified in Barbieri et al. (2005); 8: linear spring; 9: springs belonging to a nearby aquifer; 10: INFN underground laboratories (UL in the text); 11: meteorological gauge (IS: Isola Gran Sasso, CC: Carapelle Calvisio); 12: presumed water table in m asl; 13: main groundwater flow path; 14: highway tunnels drainage. [Amoruso, 2013].

2.2 The monitoring network

Considering the hydrogeological and hydrogeochemical setting of the Gran Sasso aquifer (Amoruso et al., 2013), five monitoring gauges are installed for the continuous measurement of the hydrometric level, temperature and electrical conductivity. The gauges are installed in Mavone (MA1), Ruzzo (RU1), Tavo (TA2), Tirino (TI1) and Aterno (TE1) river basins (Figure 2.2).

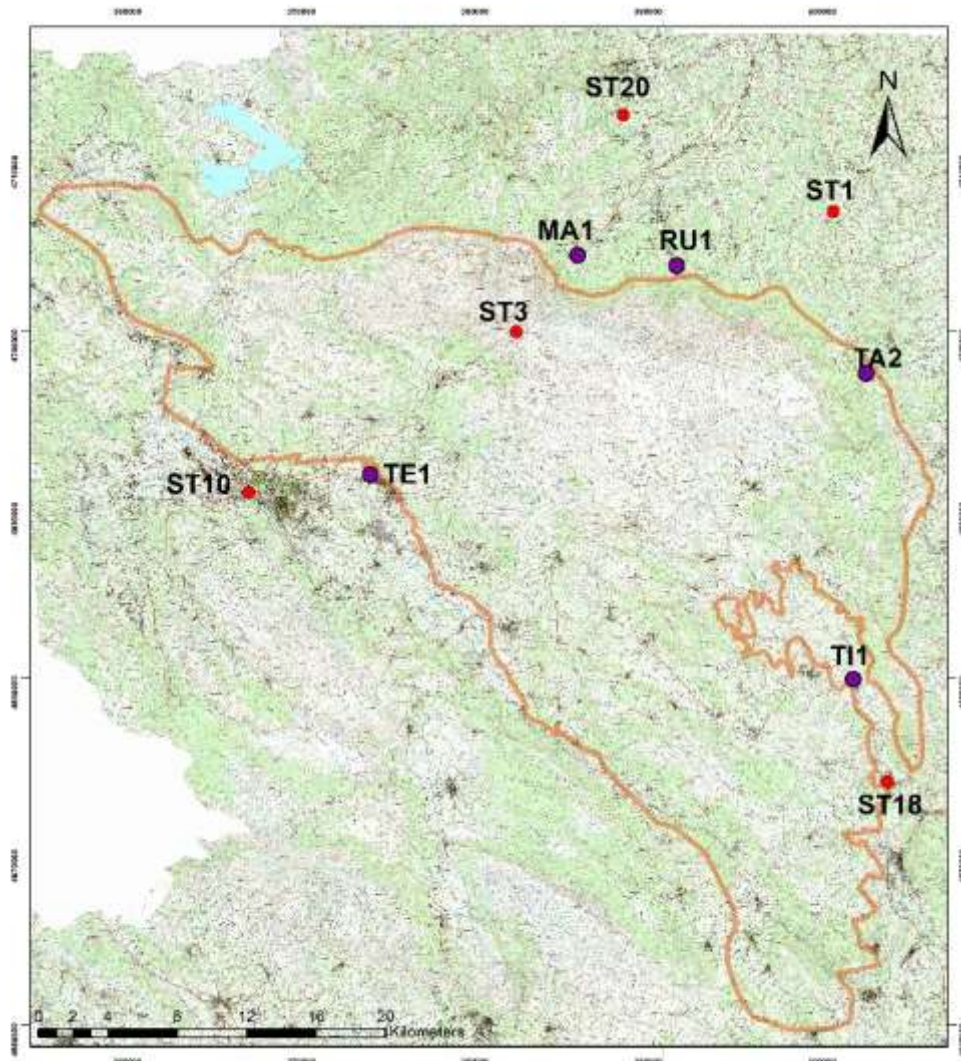


Figure 2.2. Location of hydrometric (purple circles) and thermopluviometric (red circles) gauges. MA1: Mavone-Casale S.Nicola hydrometric gauge. RU1: Ruzzo hydrometric gauge, TA2: Tavo hydrometric gauge, TI1: Tirino hydrometric gauge, TE1: Aterno-Tempera hydrometric gauge, ST1: Arsita thermopluviometric gauge, ST3: Campo Imperatore thermopluviometric gauge, ST10: L'Aquila CF thermopluviometric gauge, ST18: Popoli A. Madonnina thermopluviometric gauge, ST20: Tossicia thermopluviometric gauge.

Each gauge is composed of a casing tube open and perforated in the lower submerged portion and closed in the upper one (Figure 2.3a). An OTT ecoLog 800 multiparameter probe has been installed inside it for the continuous measurement of chemical-physical parameters (Figure 2.3b and 2.3c).



Figure 2.3. a) Hydrometric gauge; b and c) OTT ecoLog 800 multiparametric probe, for continuous acquisition and remote transmission of data, including level, temperature, and electrical conductivity.

The OTT ecoLog 800 multiparameter probe is characterised by an autonomous system for the remote transmission of measurement data relating to hydrometric level (resolution 0.001 m, error $\pm 0.05\%$), temperature (resolution 0.001°C , error 0.1°C) and electrical conductivity (resolution 0.001 mS/cm , error $\pm 0.5\%$ of measured value). The device is equipped with sensors and internal memory to store the data, allowing continuous monitoring of them. The sampling interval is set to 30 minutes for all gauges. Monitoring started in October 2020 in MA1, TA2, TI1 and TE1 gauges, while in January 2021 in RU1 gauge. All acquired data are transferred to an online data acquisition system (<https://h3o.stonebit.it/> Figure 2.4). Continuous monitoring is also supported by direct monthly flow measurements.

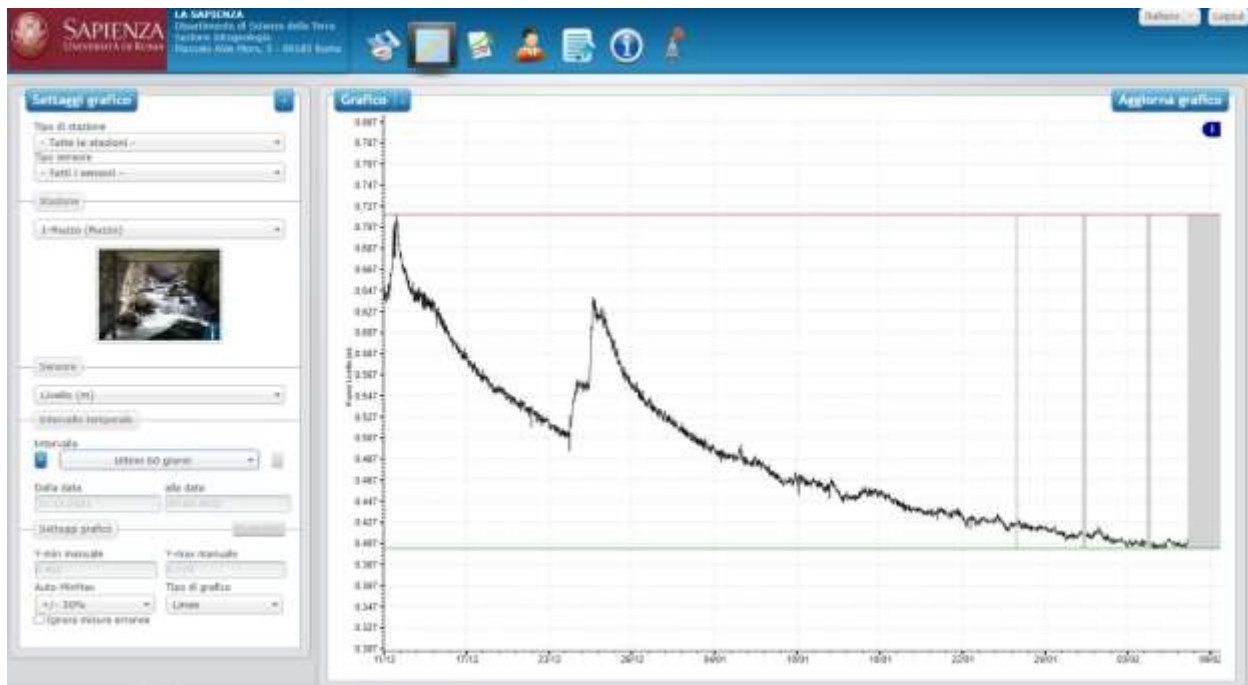


Figure 2.4. H3OCube Server.

2.3 Results and Discussion

This paragraph includes the monitoring results of hydrometric level, temperature, and electrical conductivity of five-monitoring gauges. The sample interval has been set on 30 minutes. In addition, rainfall values (collected by the nearest thermopluviometric gauges) and flow rate values are also analysed.

MA1

The MA1 gauge is located along the Mavone river in Casale San Nicola village (see location in Figure 2.2 and gauge in Figure 2.5). The monitoring in the MA1 gauge started on 14th October 2020 and is still active.



Figure 2.5. MA1 hydrometric gauge.

The Mavone river flow regime is mainly defined by discharge derived from the northern sector of the Gran Sasso drainage tunnel (overflow of the discharge withdrawn for drinking purposes). The flow regime is characterised by a steady flow rate during the years and by spike increases due to intense rainfall events. In Figure 6 the results of continuous monitoring compared with rainfall data recorded at Tossicia thermo-pluviometric gauge (ST20, 598 m a.s.l., in Figure 2.2) and direct flow rate measurements are shown. Moreover, the correlation straight line between hydrometric level and discharge measurements was calculated. The results obtained also made it possible to determine the discharge values (red line in Figure 2.6). The hydrometric regression line shows a slight increase during the monitoring period, probably related to increases in rainfall values.

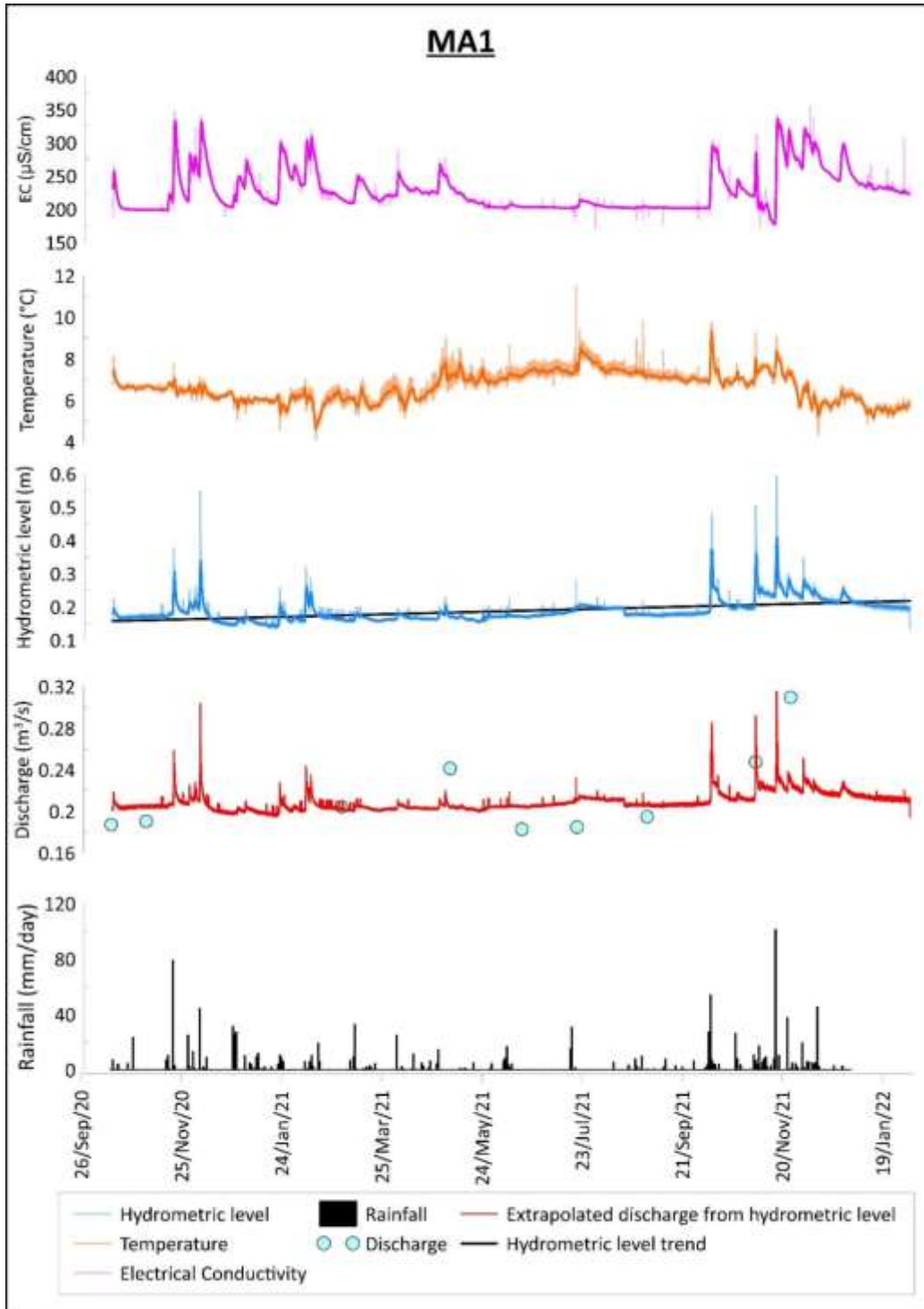


Figure 2.6. MA1 hydrometric gauge Time series.

In Table 2.1 the statistical synthesis of the parameters reported in Figure 2.6 is displayed. The standard deviation values (STD) identify stability of hydrometric level, temperature, and electrical conductivity around the mean values. In addition, in Figure 2.6, it is possible to detect a correlation between the hydrometric level and the increase in electrical conductivity with respect to intense rainfall events.

MA1	Max	Min	Mean	STD
Hydrometric level (m)	0.59	0.13	0.19	0.03
Temperature (°C)	11.5	4.1	6.6	0.7
Electrical Conductivity ($\mu\text{S}/\text{cm}$)	354	171	227	31
Discharge (m^3/s)	0.34	0.14	0.21	0.06
Rainfall (mm/day)	101.2	0	2.8	8.8

Table 2.1. Main MA1 benchmark values.

RU1

The RU1 gauge is located along the Ruzzo river in the northeastern sector of the Gran Sasso aquifer (see location in Figure 2.2 and gauge in Figure 2.7). The monitoring in the RU1 gauge started on 5th January 2021 and is still active.



Figure 2.7. RU1 hydrometric gauge.

The Ruzzo river flow rate regime is determined by the Ruzzo spring group (Mescatore, Vaceliera, Fossaceca, Peschio and Pescine springs) which represents a component of drainage of the northern sector of the Gran Sasso aquifer. However, the spring discharge is partially tapped for drinking purposes, then, the gauge RU1 represents the overflow. The flow regime is also influenced by intense rainfall events that occur in the upper Ruzzo river basin.

In Figure 2.8 the results of continuous monitoring compared with rainfall data recorded at Campo Imperatore thermo-pluviometric gauge (ST3, 2152 m a.s.l., in Figure 2.2) and direct flow rate measurement are shown. Also, in this case, the continuous discharge values were calculated from the correlation straight line between discrete flow measurements and monitored hydrometric level. As for the MA1 gauge also in the RU1 one, a mild increase of hydrometric level was recorded.

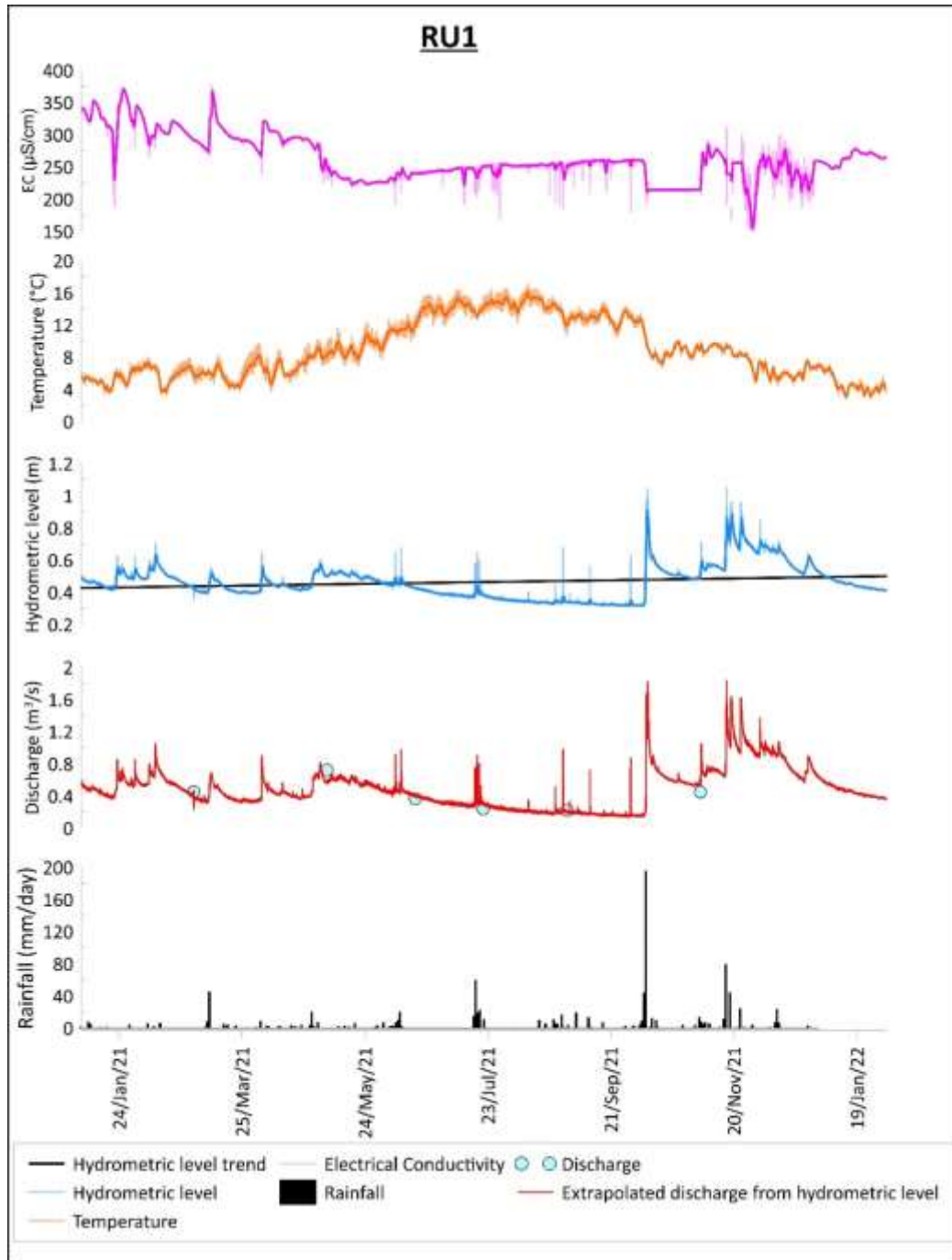


Figure 2.8. RU1 hydrometric gauge Time series.

In Table 2.2 the statistical synthesis of the parameters reported in Figure 2.8 is displayed. The standard deviation values (STD) identify a discrete variability around mean values for temperature and electrical conductivity parameters. The hydrometric level is characterised by greater variability and spike changes probably due to runoff events.

RU1	Max	Min	Mean	STD
Hydrometric level (m)	1.05	0.31	0.46	0.11
Temperature (°C)	17.1	2.8	8.9	3.6
Electrical Conductivity ($\mu\text{S}/\text{cm}$)	377	56	264	42
Discharge (m^3/s)	0.89	0.20	0.39	0.22
Rainfall (mm/day)	195.4	0	2.7	12.6

Table 2.2: Main RU1 benchmark values.

TA2

The TA2 gauge is installed in the Tavo river basin located in the northeastern part of the Gran Sasso aquifer (see location in Figure 2.2 and gauge in Figure 2.9). The monitoring in the TA2 gauge started on 14th October 2020 and is still active.



Figure 2.9. TA2 hydrometric gauge.

The Tavo river is mainly fed by Vitella D'Oro and Mortaio D'Angri springs (tapped for drinking purposes). Therefore, the TA2 gauge is influenced only by Mortaio D'Angri spring contribution (surplus flow) and by runoff events due to rainfall events and snow melting. In Figure 2.10 the monitoring compared with rainfall data recorded at Arsita thermo-pluviometric gauge (ST1, 586 m a.s.l., in Figure 2.2) and direct flow rate measurement is shown.

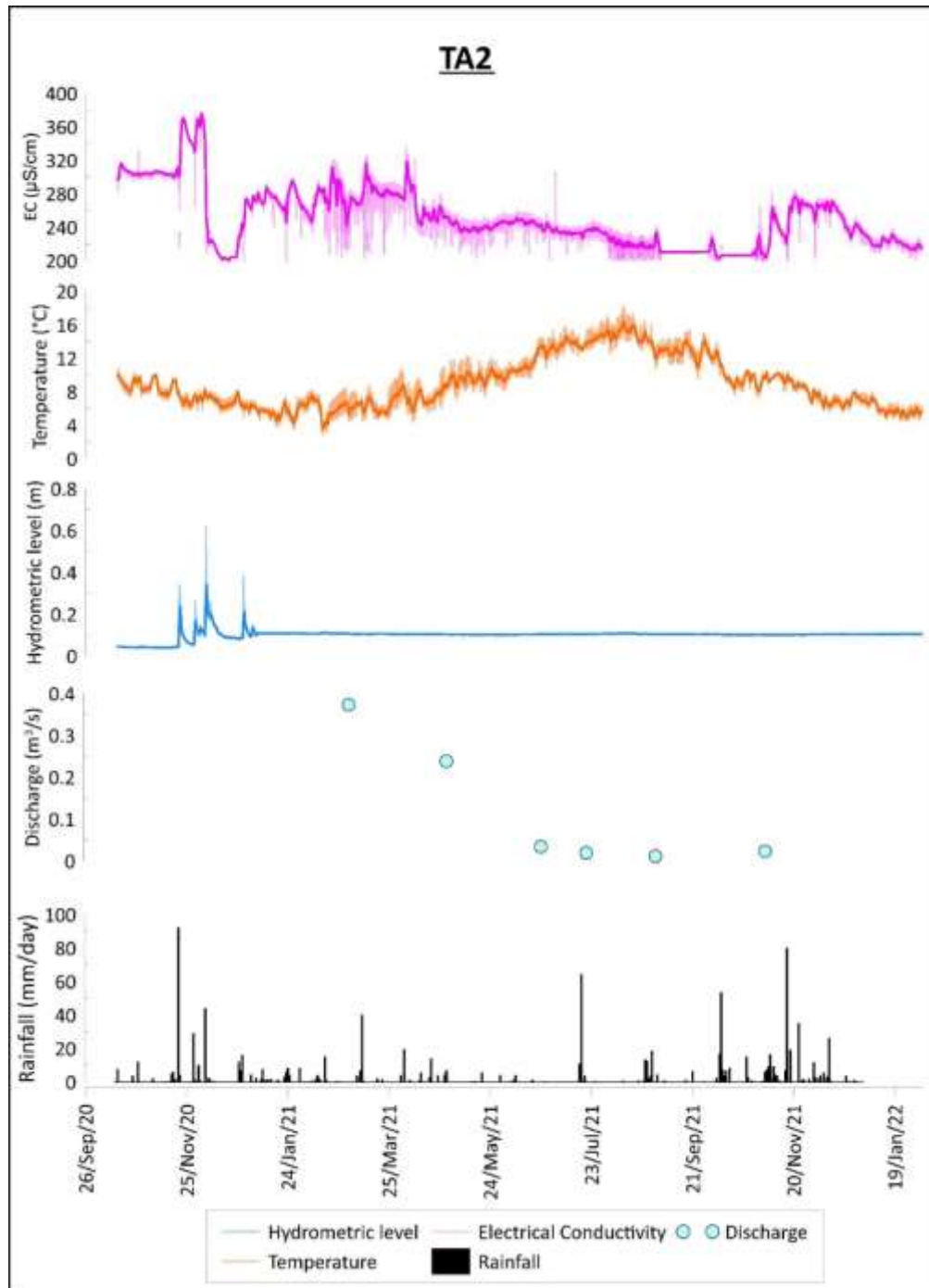


Figure 2.10. TA2 hydrometric gauge Time series.

Some malfunctioning on hydrometric level data were detected, probably due to pressure sensor damage. Indeed, no hydrometric level variation was recorded since January 2021, despite the direct flow rate measurements show increases from January to April 2021. In addition, during the summer period because of dry conditions, an emersion of the probe happened. The outliers recorded in temperature and electrical conductivity time series appear to be unrealistic. For this reason, the correlation straight line between hydrometric level and direct flow measurements cannot be assessed and the continuous discharge data were not calculated.

In Table 2.3 the statistical synthesis of the parameters reported in Figure 2.10 is displayed. As above mentioned, the maximum and minimum values of temperature and electrical conductivity are related to the low stand of hydrometric level. The low variability of hydrometric levels is attributable to probe damage.

TA2	Max	Min	Mean	STD
Hydrometric level (m)	0.62	0.04	0.10	0.03
Temperature (°C)	18.2	2.9	9.0	3.1
Electrical Conductivity ($\mu\text{S}/\text{cm}$)	591	2	255	36
Discharge (m^3/s)	0.37	0.01	0.12	0.14
Rainfall (mm/day)	92.2	0	2.2	8.3

Table 2.3: Main TA2 benchmark values.

TI1

The TI1 gauge is installed in the Tirino river basin located in the southeastern zone of the aquifer (see location in Figure 2.2 and gauge in Figure 2.11). The monitoring in the TI1 gauge started on 23rd October 2020 and is still active.



Figure 2.11. TI1 hydrometric gauge.

The Tirino river is fed by springs that represent the main basal flow of the Gran Sasso aquifer system (e.g. Capodacqua, Presciano and Basso Tirino springs). Therefore, the TI1 gauge is influenced only by Capodacqua and Presciano springs contribution. In Figure 2.12 the results of continuous monitoring compared with rainfall data recorded at Tirino a Madonnina thermo-pluviometric gauge (ST18, 313 m a.s.l., in Figure 2.2) and direct flow rate measurement are shown. The continuous discharge values were calculated from the correlation straight line between discrete flow measurements and monitored hydrometric level. The hydrometric level trend regression line shows an overall slight decrease over the monitored period, differently than at gauges MA1 and RU1. This is probably due to hydrogeological conditions of the Tirino River, which is fed by basal springs that are not significantly influenced by local meteoric events.

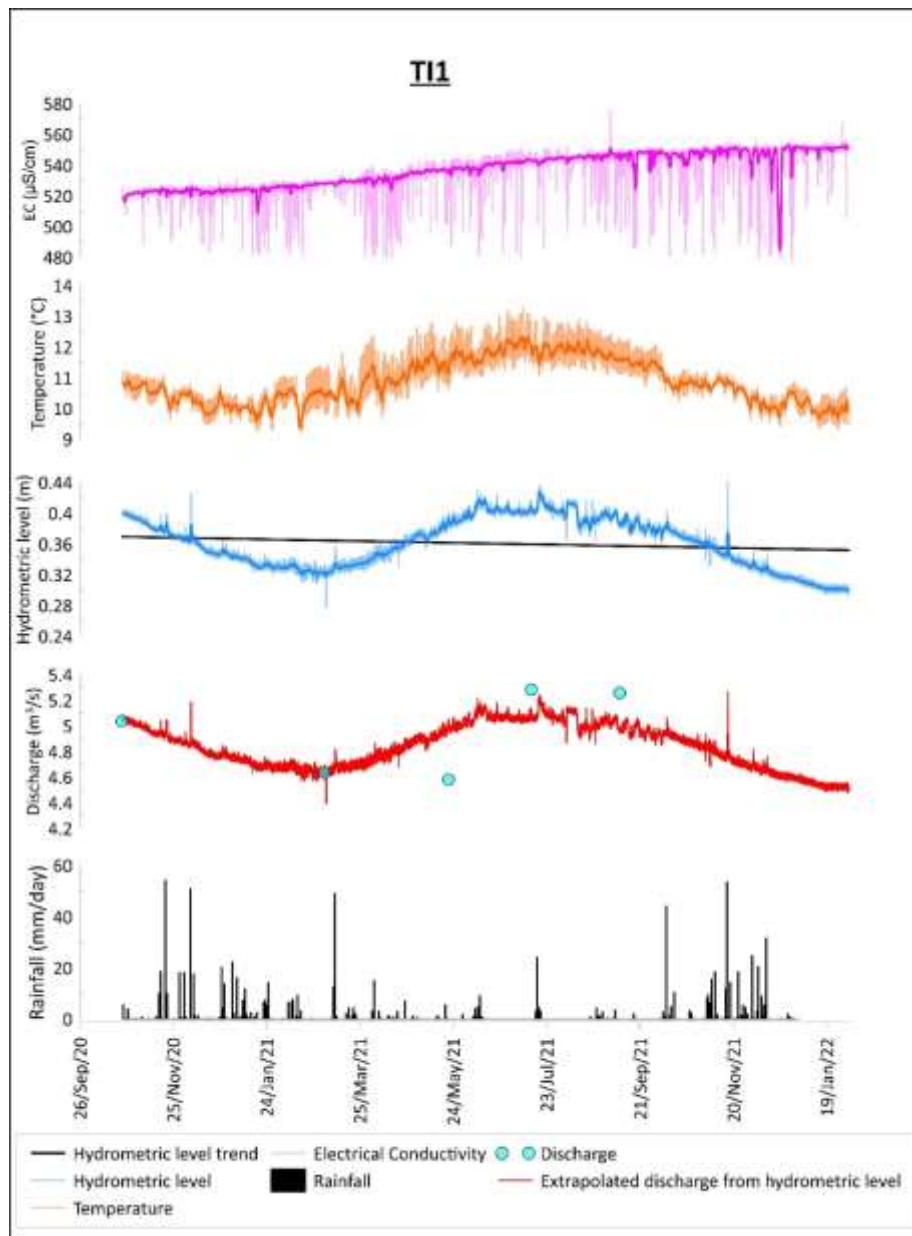


Figure 2.12. TI1 hydrometric gauge Time series.

In Table 2.4 the statistical synthesis of the parameters reported in Figure 2.12 is displayed. All standard deviation values (STD) are characterised by very low variation around the mean value. This behaviour is typical of basal springs that are characterised by long and deep flowpath in a carbonate aquifer. In addition, very small changes with respect to rainfall events or runoff were detected by the T11 gauge.

T11	Max	Min	Mean	STD
Hydrometric level (m)	0.44	0.28	0.36	0.03
Temperature (°C)	13.3	9.3	10.9	0.8
Electrical Conductivity ($\mu\text{S}/\text{cm}$)	575	347	536	16
Discharge (m^3/s)	6.31	4.78	5.27	0.49
Rainfall (mm/day)	54.2	0	2.2	6.7

Table 2.4: Main T11 benchmark values.

TE1

The TE1 gauge is installed in the Vera river at the southwestern border of the aquifer (see location in Figure 2.2 and gauge in Figure 2.13). The monitoring in the TE1 gauge started on 15th October 2020 and is still active.



Figure 2.13. T11 hydrometric gauge.

The Vera river is fed by Tempera and Vera springs that represent the main discharge of the southwestern sector of the Gran Sasso aquifer. The spring group is located in the fraction of Tempera in the Paganica town, a few kilometers from the city of L'Aquila. The Vera River has a considerably stable regime with

minimal seasonal oscillations. TE1 gauge is influenced only by Tempera spring contribution. In Figure 14 the results of continuous monitoring compared with rainfall data recorded at L'Aquila CF thermo-pluviometric gauge (ST10, 642 m a.s.l., see Figure 2.2) and direct flow rate measurement are shown. The continuous discharge values were calculated from the correlation straight line between discrete flow measurements and monitored hydrometric level.

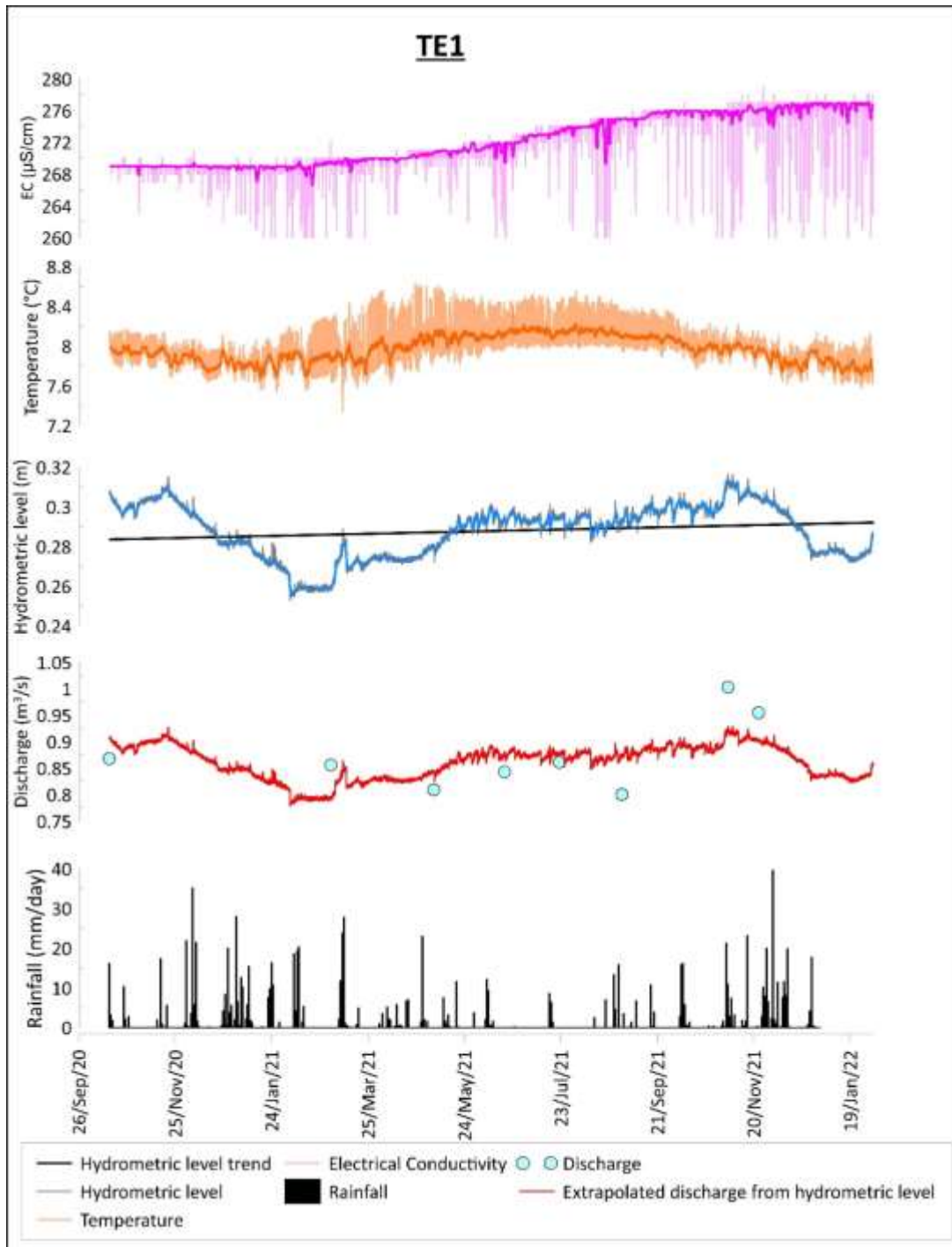


Figure 2.14. TE1 hydrometric gauge Time series.

In Table 2.5 the statistical synthesis of the parameters reported in Figure 2.14 is displayed. Also, in this case, the standard deviation values (STD) testify to very low variability of parameters around the mean value. This is in accordance with the groundwater flow model of Tempera and Vera springs, that represent the base flow for the southwestern side of the Gran Sasso aquifer (Amoruso et al., 2013).

TE1	Max	Min	Mean	STD
Hydrometric level (m)	0.32	0.25	0.29	0.01
Temperature (°C)	8.6	7.3	8.0	0.2
Electrical Conductivity ($\mu\text{S}/\text{cm}$)	279	184	272	5
Discharge (m^3/s)	1.16	0.76	0.93	0.11
Rainfall (mm/day)	39.6	0	2.2	5.4

Table 2.5. Main TE1 benchmark values.

To better understand the differences and similarities among monitoring gauges, boxplot statistical analysis was performed on the recorded time series (Figure 2.15). The box, separated into two parts by the median, represents the interquartile range (first and third quartiles). The whiskers are limited by minimum and maximum values. This statistical analysis confirms that TE1 and TI1 gauge are characterised by limited dispersion values around the median during the monitoring period concerning all recorded parameters. This means that seasonal variation at these sites is absent or at least moderate. Differently, the gauges MA1, RU1, and TA2 displayed higher dispersion around median values. This testifies greater variability due to local hydrogeological factors that can easily influence the river regime.

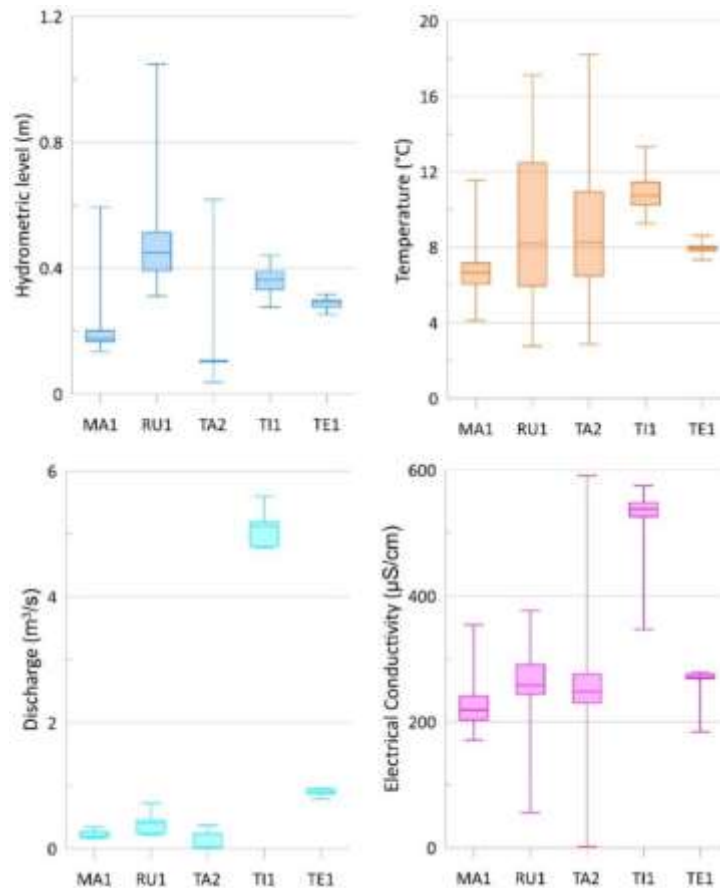


Figure 2.15. Boxplot analysis.

2.4 Bibliography

- Adinolfi Falcone, R., Falgiani, A., Parisse, B., Petitta, M., Spizzico, M., & Tallini, M., (2008). Chemical and isotopic ($\delta^{18}\text{O}\text{‰}$, $\delta^2\text{H}\text{‰}$, $\delta^{13}\text{C}\text{‰}$, ^{222}Rn) multi-tracing for groundwater conceptual model of carbonate aquifer (Gran Sasso INFN underground laboratory - central Italy). *J. Hydrol.* 357, 368–388.
- Amoruso, A., Crescentini, L., Petitta, M., Rusi, S., & Tallini, M. (2011). Impact of the 6 April 2009 L'Aquila earthquake on groundwater flow in the Gran Sasso carbonate aquifer, Central Italy. *Hydrol. Process.* 25, 1754–1764. <https://doi.org/10.1002/hyp.7933>
- Amoruso, A., Crescentini, L., Petitta, M., & Tallini, M. (2013). Parsimonious recharge/discharge modeling in carbonate fractured aquifers: The groundwater flow in the Gran Sasso aquifer (Central Italy). *J. Hydrol.* 476, 136–146
- Amoruso, L. Crescentini, S. Martino, M. Petitta, Tallini, M. (2014). Correlation between groundwater flow and deformation in the fractured carbonate Gran Sasso aquifer (INFN underground laboratories, central Italy). *Water Resour. Res.* 50, 4858-4876
- Barbieri, M., Boschetti, T., Petitta, M., & Tallini, M., 2005. Stable isotope (^2H , ^{18}O and $^{87}\text{Sr}/^{86}\text{Sr}$) and hydrochemistry monitoring for groundwater hydrodynamics analysis in a karst aquifer (Gran Sasso, Central Italy). *J. Appl. Geochem.* 20, 2063–2081.
- Monjoie, A. (1980). *Prévision et contrôle des caractéristiques hydrogéologiques dans les tunnels du Gran Sasso (Appenin, Italie)*. Livre Jubilaire, L. Calémbert, Ed. Thone, Liège.
- Petitta, M., Tallini, M. (2002). Groundwater hydrodynamic of the Gran Sasso Massif (Abruzzo): New hydrological, hydrogeological and hydrochemical surveys (19994-2001). *Boll Soc Geol It* 121, 343-363.
- Petitta, M., Caschetto, M., Galassi, D.M.P., Aravena, R. (2015). Dual-flow in karst aquifers toward a steady discharge spring (Presciano, Central Italy): influences on a subsurface groundwater dependent ecosystem and on changes related to post-earthquake hydrodynamics. *Environ. Earth Sci.* 73, 2609–2625.
- Tallini, M., Parisse, B., Petitta, M., & Spizzico, M., 2013. Long-term spatio-temporal hydrochemical and ^{222}Rn tracing to investigate groundwater flow and water-rock interaction in the Gran Sasso (central Italy) carbonate aquifer. *Hydrogeol J.* 21, 1447–1467.

3 Ubrique test site (case study Spain)

3.1 General description of the test sites

The Eastern Ronda Mountains (Fig. 3.1) test site is located in southern Spain (western area of Málaga province) where it covers a total surface of around 110 km² and presents a mean annual precipitation during the historical rainfall record (64/65-09/10) of 615 mm (Barberá, 2014). The **Merinos-Colorado-Carrasco** test site presents outcrops of Flysch sandstones and clays (Cretaceous-lower Miocene) represented in the eastern sector (Fig. 3.1), overthrust previously described geological formations. Discordant above all these upper Miocene calcareous sandstones are found, belonging to the sedimentary infilling of the Ronda basin, in the western part (Martín-Algarra, 1987).

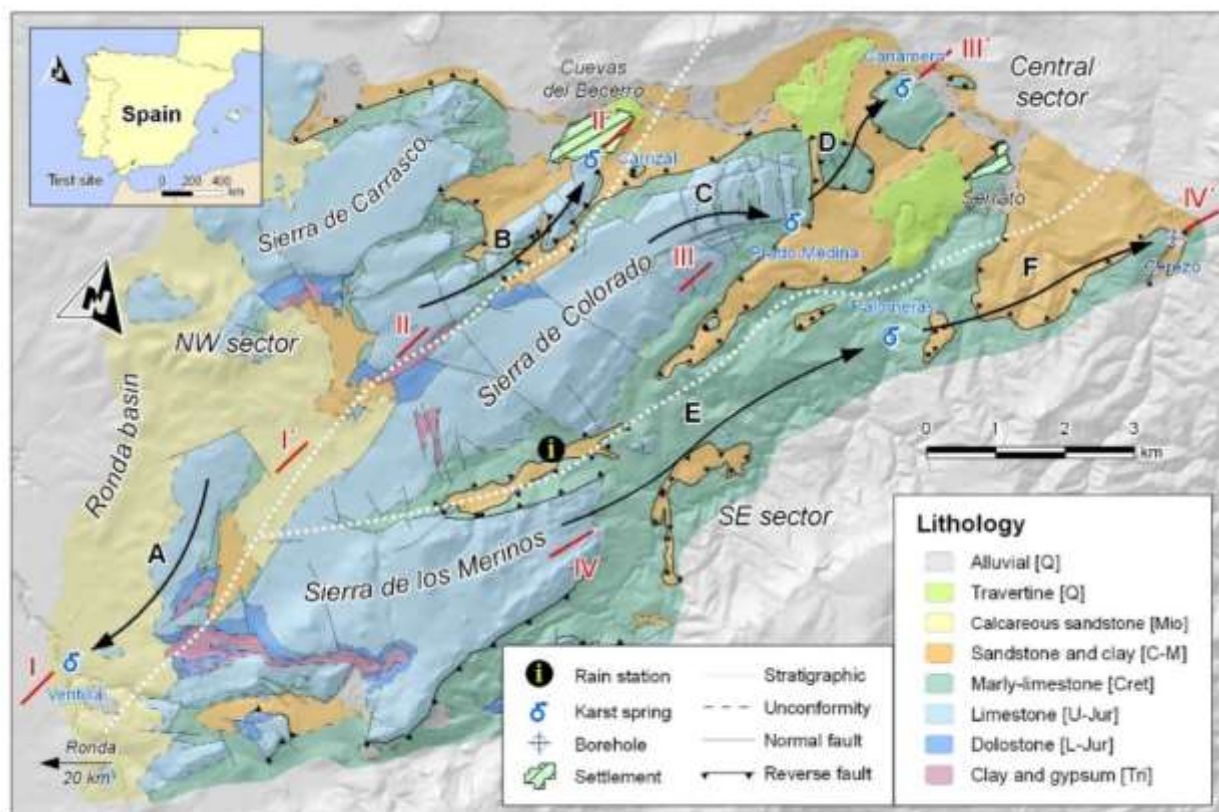


Figure 3.1. Hydrogeological setting of Merinos, Colorado and Carrasco aquifer systems (Barberá et al., 2012).

From a hydrogeological outlook, Jurassic limestones cover a large area (43 km²) in the test site and these lithologies are represented on surface, as karst exposures, or in depth, as buried aquifer segments. Dolomitic rocks, which comprise the lower levels of the Jurassic aquifers, can reach higher positions in the lithological sequence, and even appear on surface. Gypsum bearing formations (Triassic clays with gypsum), whose thickness is still imprecise, constitute the lower limit of the main aquifers and can uplift through faults. Discharge occurs through the springs of Cañamero (540 m a.s.l.) and Carrizal (740 m a.s.l.) in addition to Ventilla spring (740 m a.s.l.) (Fig. 3.1) (Barberá et al., 2012).

Sierra de Ubrique test site is placed within Sierra de Grazalema Natural Park, in the eastern part of the Cádiz province and 35 km of distance from Merinos-Colorado-Carrasco area. Sierra de Ubrique test site covers a total surface of 25 km² and the mean annual precipitation in has been estimated around 1350 mm, however, it can variate depending on the altitude and sector from 900 mm to 1800 mm (Sánchez et al. 2017). Aquifer formations in this area are also developed in Jurassic dolostones and limestones, resulting in highly fractured and karstified systems (Fig. 3.2). In the same way that happens in Eastern Ronda Mountains, clays and sandstones overthrust the previous geological formations in exception of some zones where Flysch materials structurally imbricate between Mesozoic rocks in the “Corredor del Boyar” (Martín-Algarra, 1987). This corridor provokes the individualization of two hydrogeological systems: one in the north (subbetic sector) and one in the south (penibetic sector), in which is included the Sierra de Ubrique (Fig. 3.2) (Martín-Rodríguez et al., 2016).

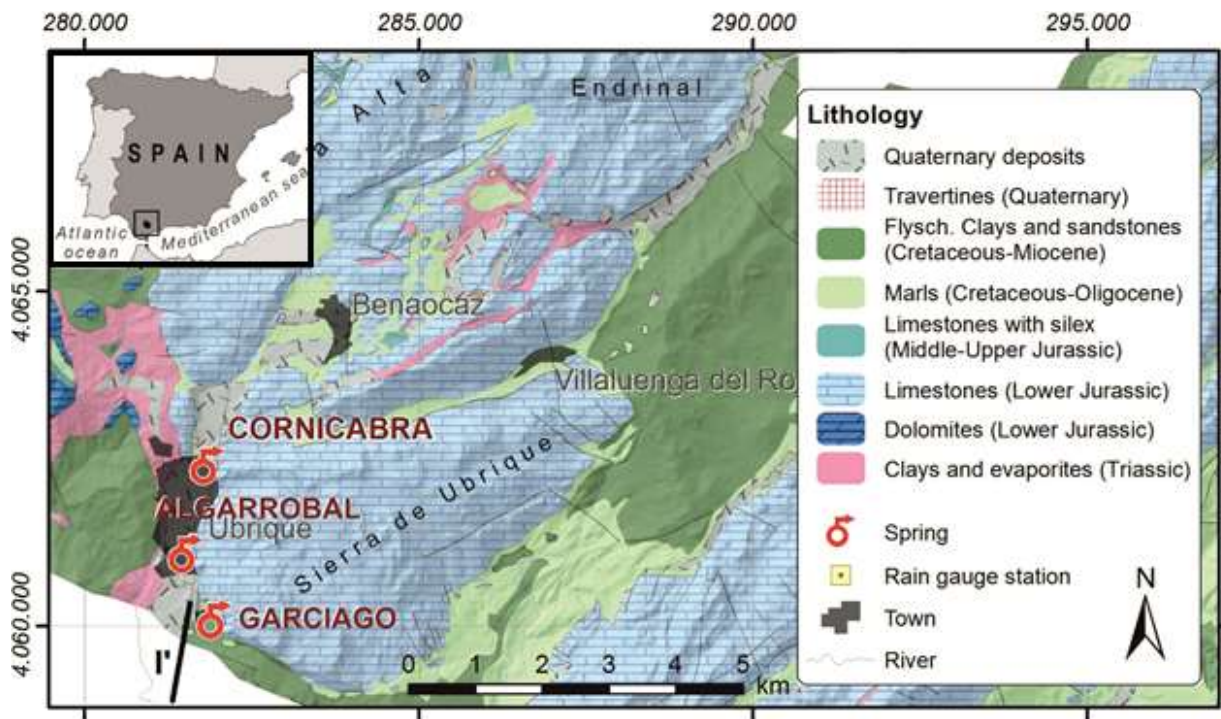


Figure 3.2. Hydrogeological setting of Sierra de Ubrique aquifer system (modified from Sánchez et al., 2017).

Drainage mainly occurs through the springs of Cornicabra (349 m a.s.l.) and Algarrobal (317 m a.s.l.) (Fig. 4) (Martín-Rodríguez et al., 2016), located in the western border of the area. In the same way that happens in the main site, other discharge points exist (such as Garciago spring, 422 m a.s.l., an overflow type associated with the previous springs).

Both Eastern Ronda Mountains and Sierra de Ubrique aquifer systems constitute representative carbonate aquifers in Spanish Mediterranean mountainous areas showing with a variable recharge and limited groundwater resources.

3.2 Equipment and methods

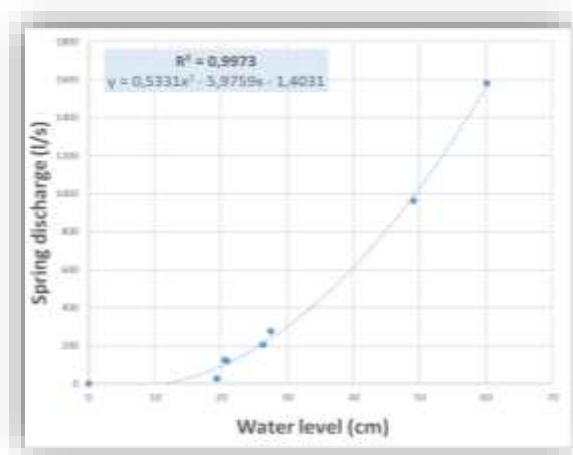
The hydrodynamic characterization has been carried out through spring discharge data analysing, both from the historical record (Barberá, 2014; Sánchez et al., 2017) as well as from the hydrodynamic data obtained during the investigation period. Spring discharge data acquisition has been realized in two ways: on the first side, spring discharge measurements during specific hydrodynamic conditions, and, on the second side, the continuous water level loggers. The data obtained from single flow measurements are used to calibrate the rating curve for each discharge point, and thus, the continuous record of spring discharge is achieved. Two methods were used for data acquisition in single measurements: current flow meter (physical), using a propeller; and salt method (chemical), using a specific probe to measure the increase in conductivity caused by the solute migration. The devices used for this task are described in Table 3.1.

<i>Parameter</i>	<i>Equipment</i>	<i>Method</i>	<i>Resolution</i>	<i>Monitoring frequency</i>
<i>Water level</i>	Odyssey® (Dataflow Systems LTD)	Piezoresistive wire and pressure compensation	±0.8 mm	1 hour (Eastern Ronda Mountains)
				15 min (Ubrique)
<i>Spring discharge</i>	SalinoMadd®	Chemical tracer	1 l/s	At specific hydrodynamic conditions
	OTT C2®	Flow velocity meter	0,1 l/s	

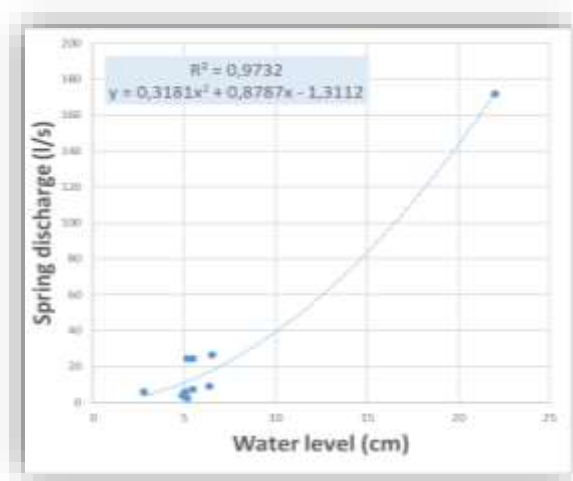
Table 3.1. Input layers for GIS processing at Merinos-Colorado-Carrasco test site (Barberá et al., 2014).

From the acquired data of water level and spring discharge, the rating curves of Eastern Ronda Mountains (Fig. 3.3) are calculated. Although it is necessary to increase the number of measurements in different hydrodynamic conditions, the rate curves are relatively well defined for Cañamero and Carrizal springs ($R^2 > 0.9$). However, in the case of Ventilla spring, a bigger dispersion of the measurements is observed ($R^2 = 0.76$). This error might be related to drainage features of the capture point, where the flow measurements are made in a pipe system.

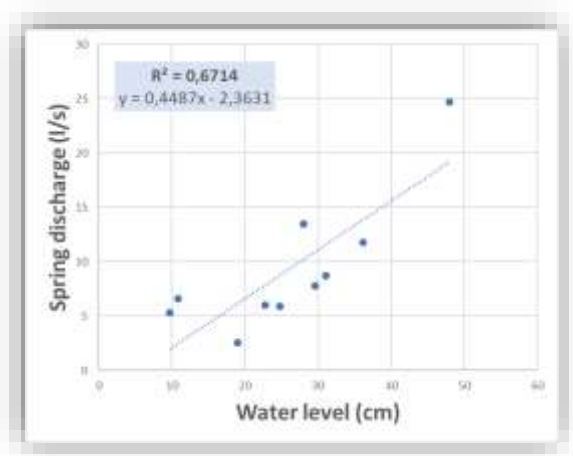
On the other hand, the rating curves at Ubrique test site (Fig. 3.4) have been developed since previous investigations started in 2013. Flow measurements at different hydrodynamic conditions were realized including maximum discharge peaks. Thus, the three rating curves show acceptable coefficient of determination ($R^2 > 0.9$) and are described through polynomial equations, except for Garciago's one which is exponential.



A



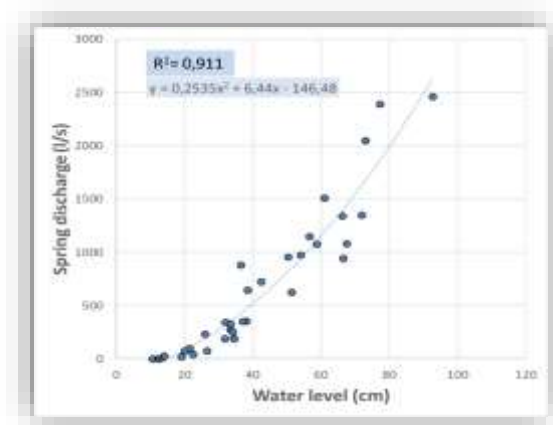
B



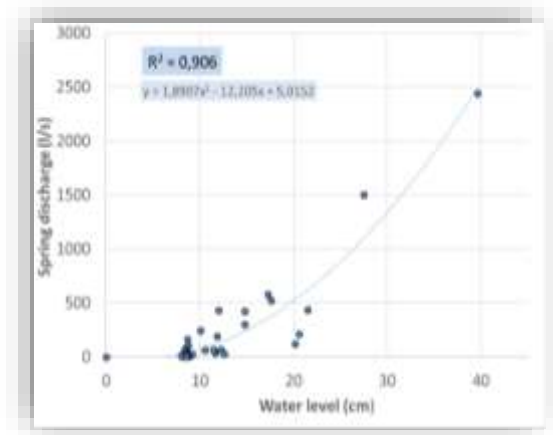
C



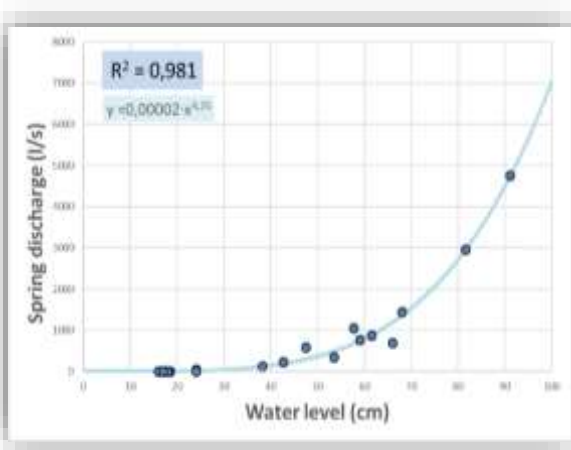
Figure 3.3. Rating curves and location of water level measurement devices at the three monitored springs at Eastern Ronda Mountains; (A) Cañamero, (B) Carrizal and (C) Ventilla.



A



B



C



Figure 3.4. Rating curves and location of water level measurement devices at the three monitored springs at Eastern Ronda Mountains; (A) Cornicabra, (B) Algarrobal and (C) Garciago.

3.3 Results

3.3.1 Main statistical descriptors of spring discharge

The continuous spring discharge monitoring during KARMA study period allowed complete hydrodynamic control of springs. The main statistical variables (minimum, maximum and mean spring discharge) are described in Table 3.2. The three springs in Eastern Ronda Mountains show similar minimum values than in previous long-term research (Barberá, 2014) but ≈ 9 times lower maximum spring discharge. Thus, the highest spring discharge during KARMA study period is 497.3 l/s for Cañamero spring, 85.5 l/s for Carrizal and 24.2 l/s for Ventilla. This is easily explainable because recharge conditions were extremely wet during the previous investigation period (2007/2010).

In the case of the three springs of Ubrique test site, the maximum spring discharge during KARMA study period is 1,604 l/s for Cornicabra spring, 917.6 l/s for Algarrobal and 4,518.5 l/s for Garciago spring. However, the maximum spring discharge values since 2013 (Andreo and Sánchez, 2013; Sanchez et al., 2017) are slightly high than those observed during KARMA study period.

Spring	KARMA study period			Previous researches		
	Min. discharge (l/s)	Max. discharge (l/s)	Mean discharge (l/s)	Min. discharge (l/s)	Max. discharge (l/s)	Mean discharge (l/s)
Cañamero	18.9	497.3	135.2	24.9	4530	374
Carrizal	2.15	85.5	22.7	0.6	783	86
Ventilla	0.5	24.2	11.5	2	163	38
Cornicabra	2	1604	123.66	0	2605.5	290.1
Algarrobal	8.23	917.6	287.5	6	2897.8	144.7
Garciago	0	4518.5	302.9	0	8977.2	151.2

Table 3.2. Main statistical descriptors (maximum, minimum and mean) of spring discharge values in the two Spanish KARMA test sites.

Time series of spring discharge measured through continuous recording equipment in the springs of the Eastern Ronda Mountains are shown in Figure 3.5. Up to 8 precipitation events were registered in this area during the first hydrological year, but the spring response is different in all of them. Cañamero spring displays 7 effective recharge events with a clear response in the spring. The shape of the unit hydrograph is narrower and sharper as more intense and abundant the precipitations are, this denotes the direct precipitation-discharge relationship due to the high degree of karstification. Hydrographs show short response times, approximately 1-2 day and the time to peak is less than a week, while concentration times are around 15 days. Ventilla spring displays as well the response to 7 effective recharge events, however, the hydrograph shape varies depending on the amount of precipitation and the intensity of the different rain episodes. The analysis of the unit hydrograph shows that the base time is approximately 1 month and the time to peak varies between 1 and 5 days.

Finally, Carrizal spring shows little variations until the month of december, when a slight increase of discharge is observed. Only 3 precipitation events produced a clear spring response. The shape of the unit hydrographs depicts sharp peaks and normally short times to peak, which are produced between 2 and 24 days, while the base times vary between 15 and 30 days. Missing data in the last two springs is due to device failure.

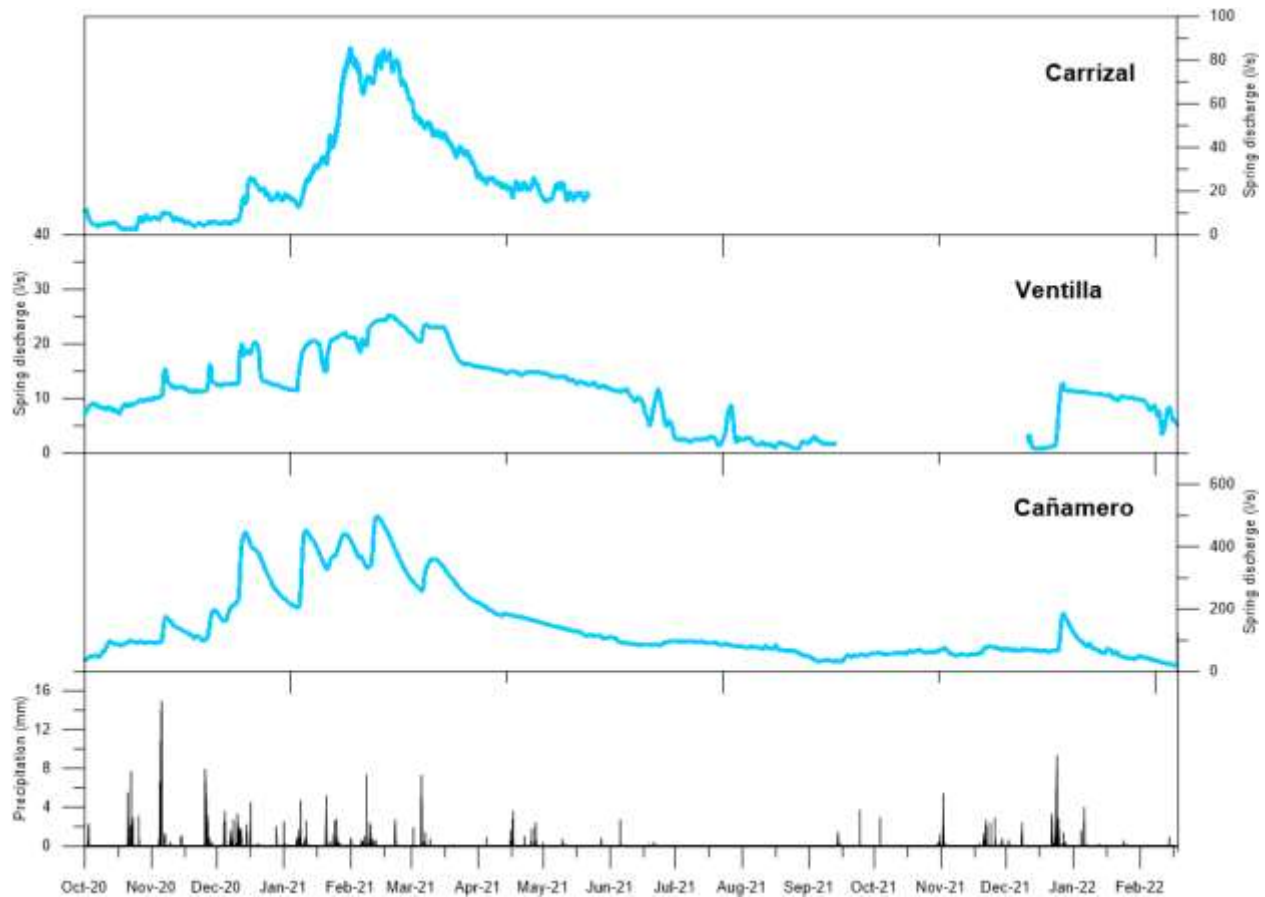


Figure 3.5. Time series of spring discharge at the main drainage points of Eastern Ronda Mountains.

Time series of spring discharge measured through continuous recording equipment in the springs of the Ubrique test site are shown in Figure 3.6. Up to 11 precipitation events were registered in this area during the first hydrological year. However, the first precipitation events of the hydrological year didn't produce any response in the drainage points, this fact is conditioned by the extremely low water content in the soil after several months without precipitation.

Cornicabra spring shows a higher sensitivity to recharge events and at least 6 clear spring responses were registered. The shape of the unit hydrograph is sharp and narrow which suggests a rapid infiltration of rainwater and fast circulation through well-developed conduits due to a high development of karstification. Hydrographs shows quite short response times, approximately 1 day and the time to peak is normally 2-4 days, while base time are around 2 weeks.

Algarrobal and Garciago springs usually respond at the same time, which reflects the direct connection between both drainage points. Algarrobal spring discharge hydrograph shows a width shape and slightly rounded discharge peaks. The response time varies between 2-5 days depending on the previous hydrodynamic conditions of the system, furthermore, the time to peak between 4-6 days and the base time is around 2 weeks. Garciago overflow spring shows really sharp hydrographs with an almost symmetric shape and the activation period is normally less than a week.

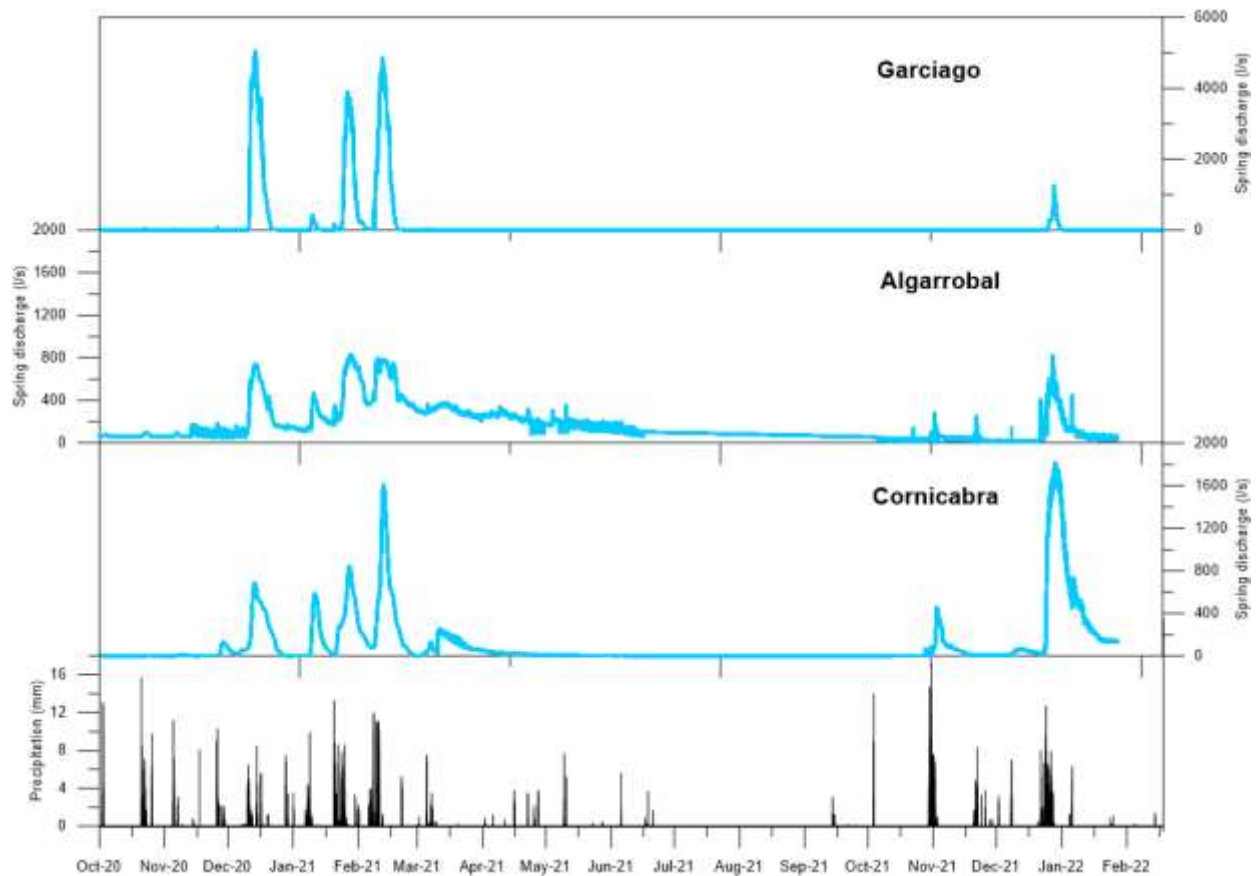


Figure 3.6. Time series of spring discharge at the main drainage points of Ubrique test site.

3.3.2 Analysis of recession curves (Mangin, 1970 1975)

Previous investigations at Eastern Ronda Mountains (Barberá, 2014) described the application of this methodology. At Ventilla spring the infiltration rate coefficient (η) resulted in 0.0455 days^{-1} and the heterogeneity coefficient (ϵ) in 0.0758 days^{-1} . These values indicate that the rate of infiltration of the water is relatively high. The value of parameter i from Mangin (1970, 1975) is 0.79. According to this author, the aquifer sector drained by the spring would be a complex and/or large system (Fig 3.7).

The infiltration rate coefficients (η) in Carrizal spring are between 0.0182 and 0.0435 days^{-1} (2007/09), values that indicate rather slow infiltration rates, probably due to of the low development of the drainage network of the unsaturated zone of the drained aquifer sector. The coefficient of heterogeneity (ϵ), which varies between 0.0636 and 0.1130 days^{-1} (2007/09) Parameter i presents values of 0.74 - 0.85 so that, according to Mangin's classification criteria the Carrizal spring would drain a complex and large system (Fig 3.7).

Finally, at Cañamero spring, the infiltration rate (η) and heterogeneity (ϵ) coefficients show mean values of 0.0330 and 0.0847 respectively, which indicate moderate drainage through the unsaturated zone of the aquifer, which occurs during periods of time of 33 days. The value of parameter i is very similar in all the decreases analyzed and is comprised between 0.79 and 0.81 (2007/09;), so the aquifer drained by the Cañamero spring would be as well complex and large (Fig 3.7).

The same approach has also been applied to Ubrique test site considering 5 recession curves from 2013 to 2020 at each spring. The mean infiltration rate coefficient (η) in Cornicabra and Algarrobal springs are 0.037 and 0.069 days⁻¹, and the coefficient of heterogeneity (ϵ), is 0.12 and 0.069 days⁻¹ respectively. The value of parameter l is 0.74 at Cornicabra and 0.75 at Algarrobal springs. On the other hand, slightly differences are found in parameter k , which shows a value of 0.28 at Cornicabra spring and 0.14 at Algarrobal. So that, according to Mangin's classification criteria both springs would drain a complex and large system (Fig 3.7). The different parameters determined from the analysis of the hydrograph by the methodology of Mangin (1970, 1975) are summarized in Table 3.3.

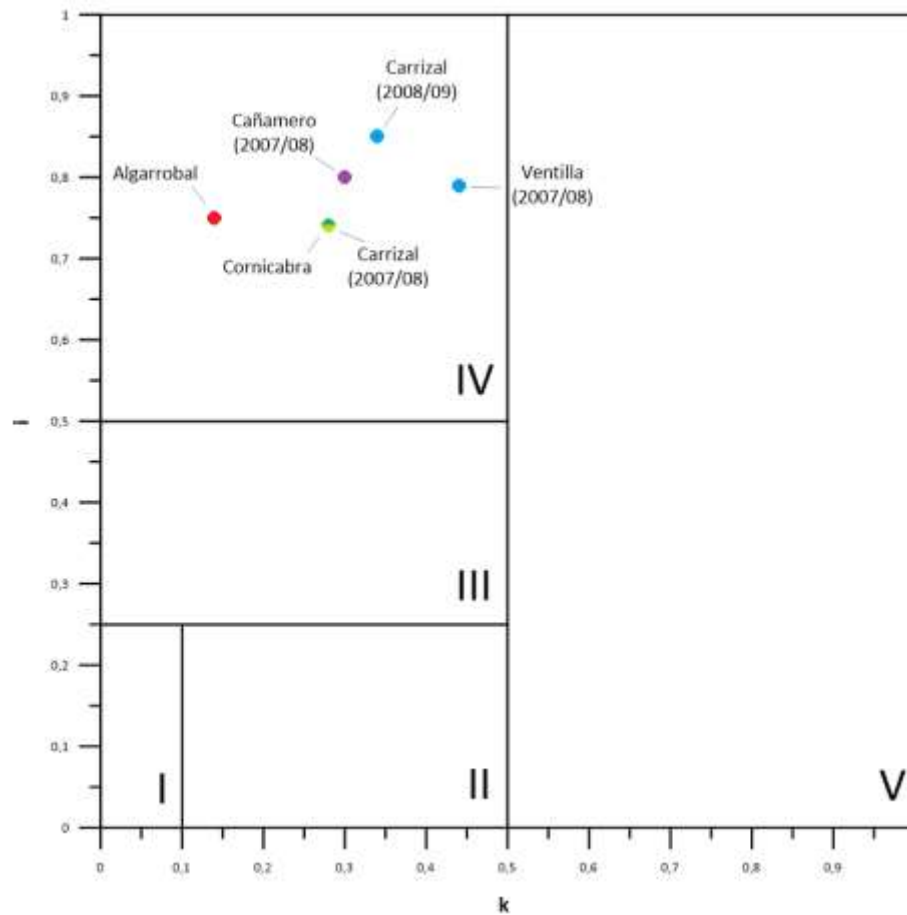


Figure 3.7. I-k graph (Mangin, 1970; 1975) for the study of karstic aquifers from the analysis of the recession curves applied to Eastern Ronda Mountains springs. Modified from (Barberá, 2014).

Spring	Hydrological year	Dd	η	ϵ	i	Da	a	Vd	Vt	k
Ventilla	2007/2008	22	0,0455	0,0758	0,79	103	0,0031	0,08	0,19	0,44
Carrizal	2007/2008	23	0,0435	0,113	0,74	81	0,0276	0,14	0,5	0,28
Carrizal	2008/2009	55	0,0182	0,0636	0,85	143	0,0095	0,84	2,46	0,34
Cañamero	mean (2007/10)	33	0,033	0,0847	0,8	97	0,0147	6,47	25,15	0,3
Cornicabra	(2013/2020)	35	0,037	0,12	0,74	89	0,0459	0,86	2,73	0,28
Algarrobal	(2013/2020)	16	0,069	0,069	0,75	38	0,0199	0,61	5,37	0,14

Table 3.3. Results obtained from the analysis of the recession curves at the 5 main springs of Spanish KARMA test sites: Ventilla, Carrizal, Cañamero (Barberá, 2014), Cornicabra and Algarrobal.

3.4 Discussion and conclusion

The gauging methods used in this investigation are well known in karst hydrogeology and allow to measure spring discharge with high accuracy. The rating curves of the springs in Spanish KARMA research areas are properly defined, especially in Ubrique test site. The three springs in Eastern Ronda Mountains showed a totally different hydrogeological functioning regarding discharge rates and hydrograph shapes. Ventilla spring hydrographs suggest a complex hydrodynamic functioning which is conditioned by the groundwater transfer from the Jurassic formations to the Miocene basin of the Ronda depression and the discharge through calcareous sandstone. Carrizal spring, in contrast, appears to show a more inertial behaviour and lower karstification degree. Finally, Cañamero spring shows the highest discharge rates of Eastern Ronda Mountains and the typical karst behaviour, with steep rising limbs and softer recession curves. The analysis of spring discharge at Ubrique test site suggest a well-developed conduit system through which the rapid circulation of groundwater occurs and it is reflected in narrow and sharp hydrographs.

Although both study areas (Eastern Ronda Mountains and Ubrique Test Site) have different hydrodynamic characteristics, the analysed recession curves are classified within the same type. However, Ubrique test site springs show a lower value of i parameter, which suggest a slightly more developed karst network in the vadose zone.

3.6 References

- Andreo, B and Sánchez, D. (2013) Caracterización hidrogeológica y evaluación de los recursos hídricos de la Sierra de Grazalema (Cádiz) para su potencial implementación como reserva estratégica de cabecera de la Demarcación Hidrográfica del Guadalete-Barbate. Informe de resultados del periodo de control noviembre 2012-noviembre 2013. Junta de Andalucía
- Barberá, J.A. and Andreo, B. (2012). Functioning of a karst aquifer from S Spain under highly variable climate conditions, deduced from hydrochemical records. *Environ Earth Sci* 65, 2337–2349.
- Barberá, J.A. (2014). Investigaciones hidrogeológicas en los acuíferos carbonáticos de la Serranía Oriental de Ronda (Málaga). PhD Thesis. University of Málaga, Spain. 591 p.
- Mangin, A. (1970). Contribution à l'étude des aquifères karstiques à partir de l'analyse des courbes de décrue et tarissement. *Annales Spéologie* 25 (3), 581-610.
- Mangin, A. (1975). Contribution à l'étude hydrodynamique des aquifères karstiques (I). PhD Thesis. Dijon University (France). *Annales Spéologie* 29 (3), 283-332; 29 (4), 495-601; 30 (1), 21-214.
- Martín-Algarra, M. (1987). Evolución geológica alpina del contacto entre las Zonas Internas y Externas de la Cordillera Bética. PhD Thesis, University of Granada, Spain. 1171 p.

Martín-Rodríguez, J.F., Sánchez-García, D., Mudarra-Martínez, M., Andreo-Navarro, B., López-Rodríguez, M., and Navas-Gutiérrez, M.R. (2016). Evaluación de recursos hídricos y balance hidrogeológico en acuíferos kársticos de montaña. Caso de la Sierra de Grazalema (Cádiz, España). Book chapter on Las aguas subterráneas y la planificación hidrológica, 163-170. Spanish-Portuguese Congress. IAH Spanish Chapter. Madrid (Spain), November 2016.

Sánchez, D., Barberá, J.A., Mudarra, M. and Andreo, B. (2017). Hydrogeochemical tools applied to the study of carbonate aquifers: examples from some karst systems of southern Spain. *Environmental Earth Sciences*, 74, 199–215.

4 The Lez Karst Catchment (case study France)

4.1 General description of the test site

The Lez system, located north of Montpellier, is a major Cretaceous and Jurassic limestone karstic aquifer that supplies drinking water to about 350 000 inhabitants of metropolitan Montpellier area. This large karst system located in the Mediterranean basin, South East of France, is referred to as the Lez aquifer because it feeds the Lez spring (mean discharge ~ 2200 l/s). The present water management scheme allows pumping at higher rates than the natural spring discharge during low-flow conditions, while supplying a minimum discharge rate (~ 230 l/s) into the Lez river to ensure ecological flow downstream, and reducing flood hazards via rainfall storage in autumn (Avias, 1995, Jourde et al., 2014).

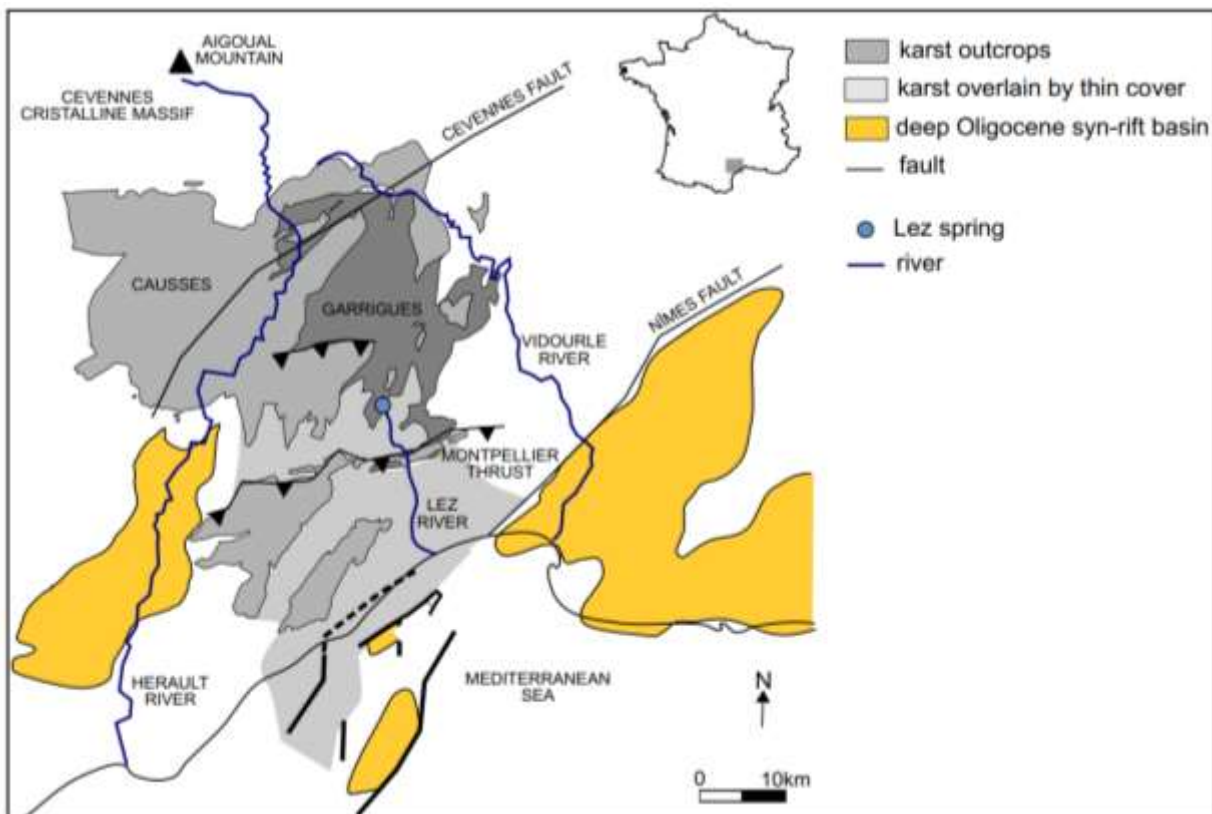


Figure 4.1. General situation of the Lez karst aquifer system. From Mazzilli, 2011, simplified after Camus, 1999.

The Lez aquifer is located in the karst Garrigues area, which is encompassed between the Hercynian basement of the Cévennes to the north and the Mediterranean Sea to the south (Fig. 4.1). The boundaries of the karst system comprising the Lez aquifer can be roughly materialized by the Hérault and Vidourle rivers (western and eastern sides) and by the Cévennes fault and Montpellier faults (southern and northern sides). It is ranked between the Cévennes crystalline massive at the north, and the littoral plain at the south. The topography rises gently from the south to the north of the area. The topographical heights range from 15 m.a.s.l (Vidourle's banks) to 658 m.a.s.l (Saint-Loup mountain). The northern part of the study area is little urbanized. Carbonate facies are predominant. Soils are either inexistent, or shallow and little developed. The residues of limestone dissolution may fill topographic lows and open

fractures. This area is mostly covered by low scrublands and woods that are well suited to drought. The south-eastern part of the study area is characterized by vineyards and an increased urbanization.

The area is characterized by a typical Mediterranean climate with dry summers and rainy autumns. The temperatures are hot in summer (mean temperature about 22 °C) and mild in winter (mean temperature about 5 °C). Rainfall is characterized by both monthly and annual irregularity. Annual rainfall is bi-seasonal, occurring primarily from September to December and in a lesser extent from March to May (Fig. 4.2). Precipitations may range from about 600 mm (dry year) to about 1500 mm (wet year). The intense rainfall events in autumn are the main contributors to the annual recharge. Rainfall is also spatially variable with an increase from south to north due to the rising topography and the proximity of the Cevennes hills (Fig. 4.1).

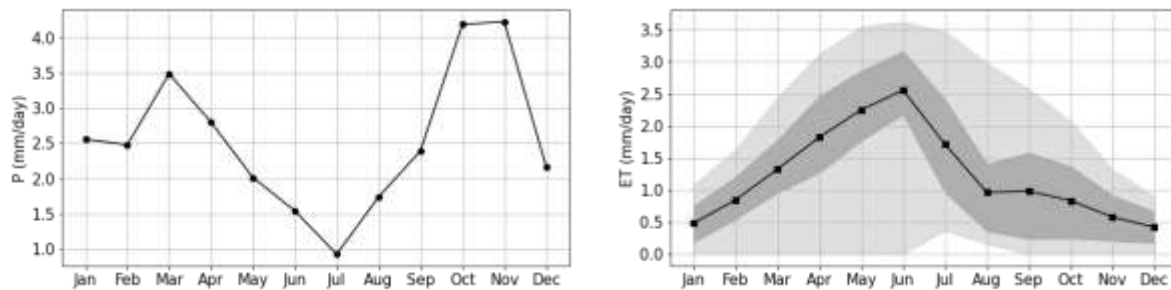


Figure 4.2. Variability of the precipitation and evapotranspiration (ET) over the Lez spring catchment estimated for the 2008-2021 period.

At a more local scale, the geographic situation of the study area bears important consequences on the rainfall repartition. The mean annual cumulated precipitations increase from the south to the north of the study area due to the rising topography and the proximity of the Cevennes massive. The region is also prone to intense convective rain events during the autumn season, the so-called Cevenols or Mediterranean episodes. The cumulated daily rainfall may reach several hundreds of mm (e.g. 473 mm recorded at the Ceyrac rain gauge on the 08/09/2002, 272 mm recorded at the Montpellier rain gauge on the 22/09/2003). Many tracer tests have been conducted in the basin since the 1960s to determine the hydraulic connections and underground water transit times. However, the findings of most of these tests are questionable because of the detection methods used at this time (mainly active carbon and visual detection). In the framework of the 'Lez karst catchment multipurpose management' project (Jourde et al. 2011; Leonardi et al. 2013), further tracing tests were conducted to check some uncertain tracings and outline the limits of the Lez spring hydrogeological basin under natural flow regime (Fig. 4.3).

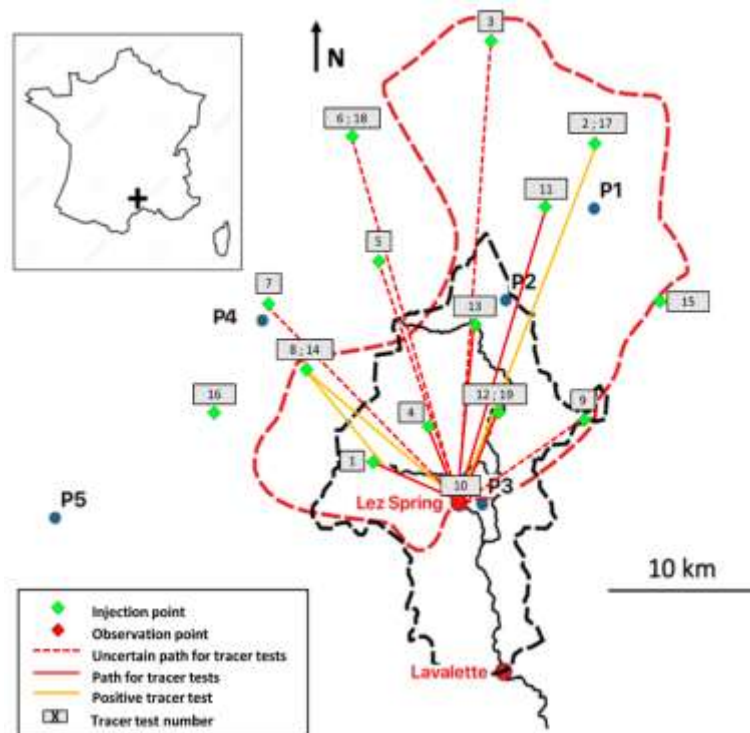


Figure 4.3. Lez River watershed at Montpellier - Lavalette (black dashed line), Lez spring hydrogeological basin under natural flow regime boundaries (red dashed line), and pattern of artificial tracer tests (modified after Leonardi et al., 2013).

The Lez spring (Fig. 4.4) is located about 15 km north of Montpellier. It is of Vaclusian-type with an overflow level at 65 m.a.s.l, and a maximum discharge of approximately 15 m³/s. The aquifer also discharges into several seasonal overflowing springs, the largest corresponding to the Lirou Spring (85 m.a.s.l), where high turbidity occurs during high discharge events (Fig. 4.3).



Figure 4.4. Specific recharge (m³/m²/year) on the Lez catchment for an intermediate water year (1955-1956).

After a period during which only the natural overflow of the Lez spring was used for Montpellier water supply (from 1864 to 1965), groundwater was pumped in the spring down to -6.50 m below the overflow level of the spring (65 m.a.s.l). In 1982, an underground pumping plant was built, and four deep wells were drilled (Fig. 4.5) to intercept the karst conduit feeding the spring, 48 m below the overflow level of

the spring (17 m.a.s.l). Pumping these wells allows up to 1800 l/s to be withdrawn under low-flow conditions (with an authorized maximum drawdown of 30 m), while the average annual pumping flow rate is about 1020 l/s (over the 2008-2020 period). This type of groundwater management is possible as long as the mean pumped flow rate does not exceed the mean annual discharge of the spring under natural regime (Avias, 1995). Due to the pumping management of the aquifer, which supplies about 30 to 35 Mm³ of water per year to the metropolitan area of Montpellier, the discharge at the Lez spring is often small or nil. During low-flow conditions, when the pumping rates exceed the natural discharge of the karst aquifer, the water level in the karst conduit and in the spring drops below the overflow level. Pumping then causes a drawdown of almost 30 m at the end of the low-water period, and the spring dries up (Fig. 4.5).

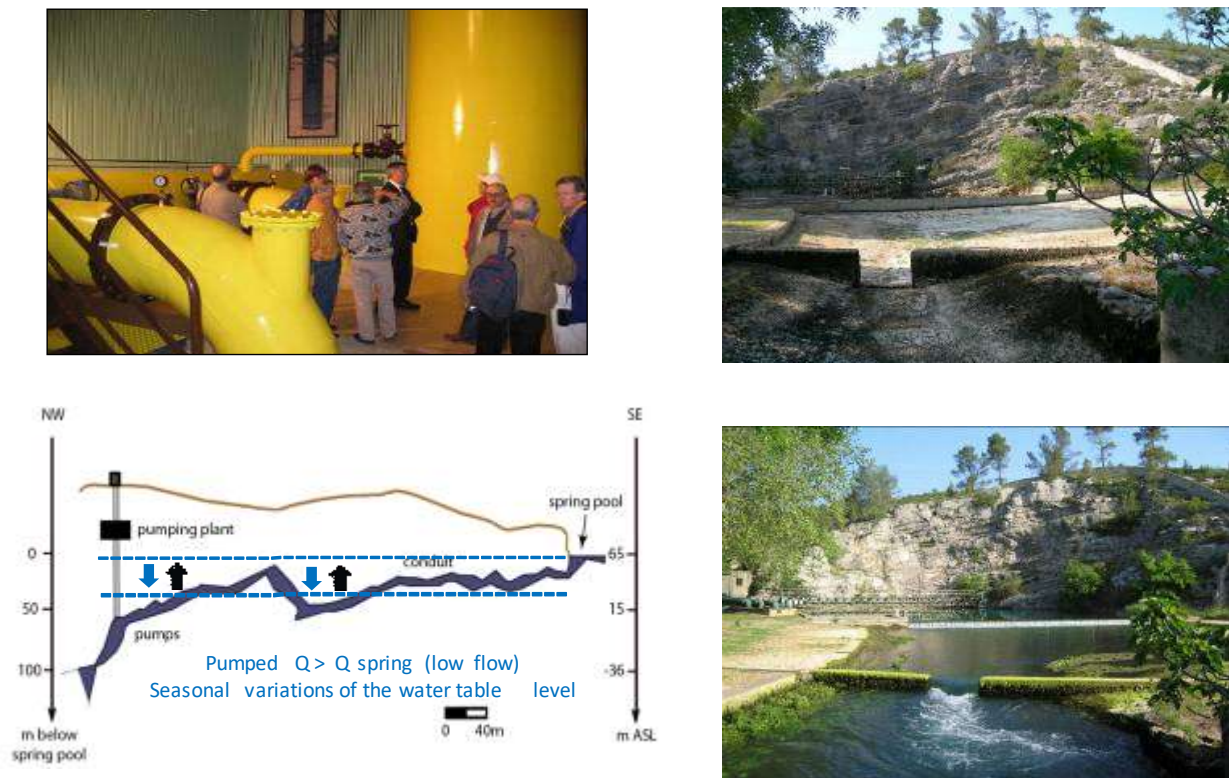


Figure 4.5. Lez spring during low flow and high flow conditions. Underground Pumping station and seasonal variation of the water table level (Lez spring simplified topography from Mazzilli, 2011).

During autumn and winter, the karst aquifer is recharged and its reserves are renewed. The present water management scheme allows pumping at higher rates than the natural spring discharge during low-flow conditions, while supplying a minimum discharge rate into the Lez river for ecological concerns, and reducing flood hazards via rainfall storage in autumn (Jourde et al., 2014).

The water quality of the Lez spring is good, except for bacteriological contaminations due to some leaks from wastewater treatment plants infiltrating within the aquifer during flood events. Pumped groundwater is supplied by pipes and treated at the Arago purification plant in Montpellier. Water is cleared of suspended particles by flocculation/decantation (if turbidity > 4 NTU) and disinfected with Cl₂ gas after filtering.

4.1.2 Characteristics of the monitoring station at Lez spring

The monitoring at the Lez spring (Fig. 4.6) has been performed by the MEDYCYSS Observatory (OSU OREME, SNO KARST, OZCAR-THEIA) since 2006 and encompasses the following data:

- Water level (every 15 minutes from 2007), natural organic matter (including humic and proteic fluorescence signal, every 15 minutes from 2015), physico-chemical (water temperature, conductivity, pH, turbidity, dissolved oxygen and chlorides; every hour from 2015), Radon-222 (every hour from 2016), and other parameters (TOC, DOC, NO₃⁻, every 15 minutes from 2021), continuously recorded at the perennial Lez spring.
- Regular sampling for physico-chemical parameters and water samples are carried out every two weeks and with a short time span during flood events. The chemical (major elements, TOC, DOC, NOM, trace elements), isotope (water stable isotopes) and biological (Total coliforms and E. Coli) analyses are performed at HydroSciences Montpellier laboratory of the University of Montpellier, France.

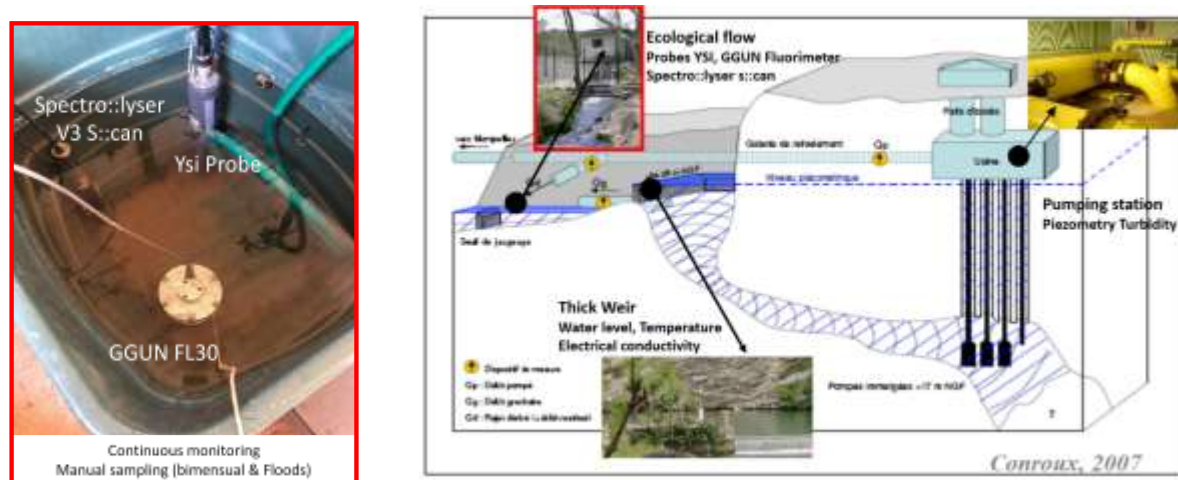


Figure 4.6. Monitoring at Lez spring (weir), upstream (pumping station) and downstream (ecological flow).

The Lez spring is characterized by a complex mixing of mineralized waters with long residence times which derive from Jurassic and deeper aquifers, and recently infiltrated waters less mineralized and affected by anthropogenic contaminants (Bicalho et al., 2012). The different origins of the waters are: (1) superficial circulation within the main aquifer (Upper Jurassic and Cretaceous limestones), (2) surface-water interactions and interactions with the marls of the Valanginian cover of the aquifer, (3) water coming from deep circulation within Middle Jurassic and deeper compartments (Trias/Paleozoic) which can move up thanks to the major regional fault of Corconne-Les Matelles. The proportions of these different water types vary during the hydrological cycle and depend on the hydrodynamical state of the aquifer. Previous studies showed that Lez spring waters have a good chemical quality even if they can be affected by punctual contaminations during flood events or very dry periods and may show peaks for faecal bacteria at these periods. The major anthropogenic impacts on the water quality of the Lez spring are summarized below:

- In the Lez spring catchment, many areas have low permeable covers of low thickness, or present fractured and karstified calcareous outcrops which induce infiltration of water through the aquifer. Urbanized areas represent about 5% of the basin. As other Mediterranean areas, the population of the basin doubled between 1990 and today. In the northern part of the basin, urbanization has increased significantly in some areas, but the infrastructure to treat urban or domestic wastewater is not sufficient. Thus, peaks in bacterial pathogen content can be measured at the Lez spring during flood events or very dry conditions. The more vulnerable areas for water quality are sink-holes located in temporary streams where concentrated infiltration occurs during flood periods. Moreover, some are located near wastewater treatment plants which discharge effluents in these temporary streams, without dilution of the residual nutrients or bacterial contaminants after treatment. Wastewaters of the cities located in the southern part of the basin are collected and treated by the regional treatment plant of MAERA.
- Agricultural activities correspond to approximately 25% of the surface area of the basin (Batiot et al., 2013). Vulnerable areas linked to these activities are essentially vineyards. These may explain the excess of the potability standards for phytosanitary products during high flows. Concerning agricultural contamination, regular analyses during a hydrological cycle (September 2010 to September 2011) of 16 pesticides in the waters of the Lez spring indicate a level of very low contamination (<25 ng/l). For some compounds, the concentration variations showed a seasonal use such as herbicides. These results have been compared with those resulting from others punctual samplings at the Lez spring (ADES data, 1997-2011). The average and maximum observed concentrations are generally low (respectively <30 ng/l and 50 ng/l) for all molecules. Punctually, compounds such as simazine or diuron may exceed 100 ng/l. As a result, the Lez aquifer does not appear to be chronically contaminated with pesticides, even if some molecules may exceed the potability standard set at 100 ng/l during flood events.

4.1.3 Objectives

The fluorescence of Dissolved Organic Matter in karst systems is a suitable tool for tracing the origin and type of karst waters in addition to the more conventional hydrochemical parameters. The decomposition of the DOM fluorescence signal is a pertinent indicator for better analysing the total signal. Indeed, the signal emitted by the humic-like compounds is better appropriate for the monitoring of rapid infiltration flows during high-flow periods. The fluorescence of protein-like compounds thus provides further information on direct infiltration flows and their specific organic matter inputs. As the signal may be related to faecal bacteria, it highlights fast infiltration flows arriving at the outlet of the Lez spring, after a few days, and demonstrates its vulnerability to contaminant flows, mainly related to domestic wastewater pollution. Accordingly, TOC, NO₃, NOM fluorescence, turbidity and 222-Rn could be used as EWS indicators evidence fast infiltration within the aquifer and potential pollutions. Finally, chloride may be relevant to monitor the contribution of waters coming from deeper compartments which are not impacted by anthropogenic pollution.

4.2 Equipment and methods used

Groudwater at the lez spring overflow a 21 m long weir, which has a 10 cm thickness (Fig. 4.7). The height of the water overflowing the threshold has been measured with different sensors since 2008, and the one presently in use, is an OTT Ecolog (0-10 m span, 0.05% (5 mm) precision). The use of a basic hydraulic formula then allows determining the overflowing Lez spring discharge from the threshold (65 m.a.s.l).



Figure 4.7. Water level monitoring in the Lez spring basin near the thick weir, for continuous discharge estimates.

Many gauging have been performed (Fig. 4.8), either with flowmeter or with Acoustic Current Doppler Profilers (ADCPs) in the Lez river channel, a few hundred meters downstream the Lez spring. Based on these measurements a modified threshold formula was propose to better estimate the discharge :

$$Q = C\sqrt{2g} \times L \times h^{3/2}$$

with C the coefficient characteristic of the weir, L the weir's length, and h the height of the water overflowing the threshold.

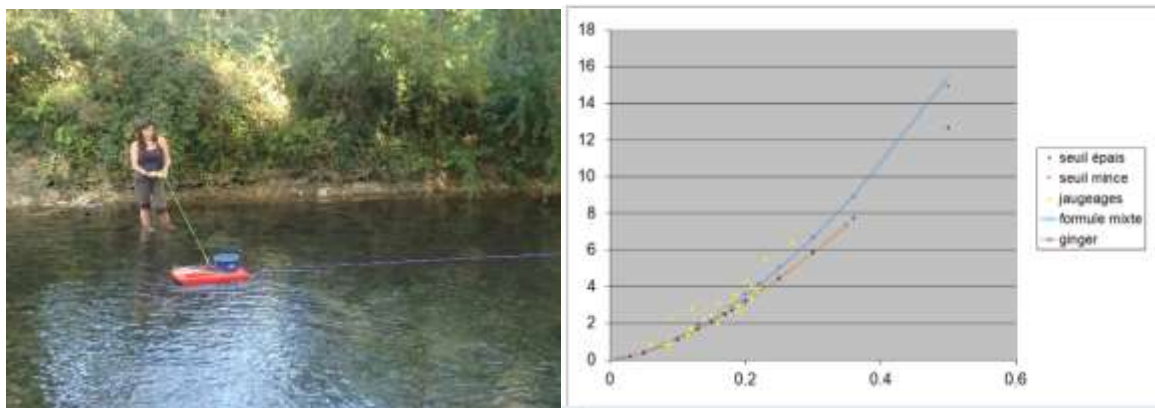


Figure 4.8. Gauging downstream the Lez spring (left) and gauging curve (right) - Q(m³/s) versus water level (m).

There is a relative dispersion of the gauging values that can be related to the very fast variations of flow of the spring (Fig. 4.8). Indeed, as previously mentioned, the spring is pumped upstream for water supply of the city of Montpellier at very high rate (up to 1.8 m³/s). Start and stop of the pumping are causing very rapid changes of the level at the gauging station, and thus of the spring discharge, which can affect the result of gauging. The uncertainty of Lez discharge value has been estimated to be about +/- 10%.

Data monitoring	Equipment specifications	Monitoring frequency	Time frame	Field regular sampling/measurement
Piezometry, EC, T°C	SDEC CTD probe	1 min	Ongoing from 2012	
T°C, pH, EC, DO, Cl	YSI6920 V2-2-SV probe	60 min	Ongoing from 2015	Twice a month + flood events
NOM fluorescence/turbidity	GGUN FL620	15 min	Ongoing from 2015	Twice a month for 3D fluorescence
TOC, DOC, NO ₃ , Turbidity	Spectro::lyser s::can	15 min	Installation in November 2020. Calibration in progress	Twice a month + flood events for TOC, NO ₃
Radon-222	RAD7 Durrige	60 min	Ongoing from 2016	Twice a month + flood events

Table 4.1: Physical-chemical parameters measured at the Lez spring with high frequency monitoring.

Three probes were installed downstream the Lez spring where the ecological flow feeds back the Lez river. In this way a continuous monitoring of physical-chemical parameters (Table 4.1) is assured with the following probes: YSI (EC, DO, T, Cl, pH), GGUN fluorimeter (Humic NOM, proteic NOM, fluorescein, Turbidity), Spectro::lyser s::can (Turbidity, UV 254, TOC, DOC, NO₃).

4.3 Results

4.3.1 Time Series of the Lez spring karst system

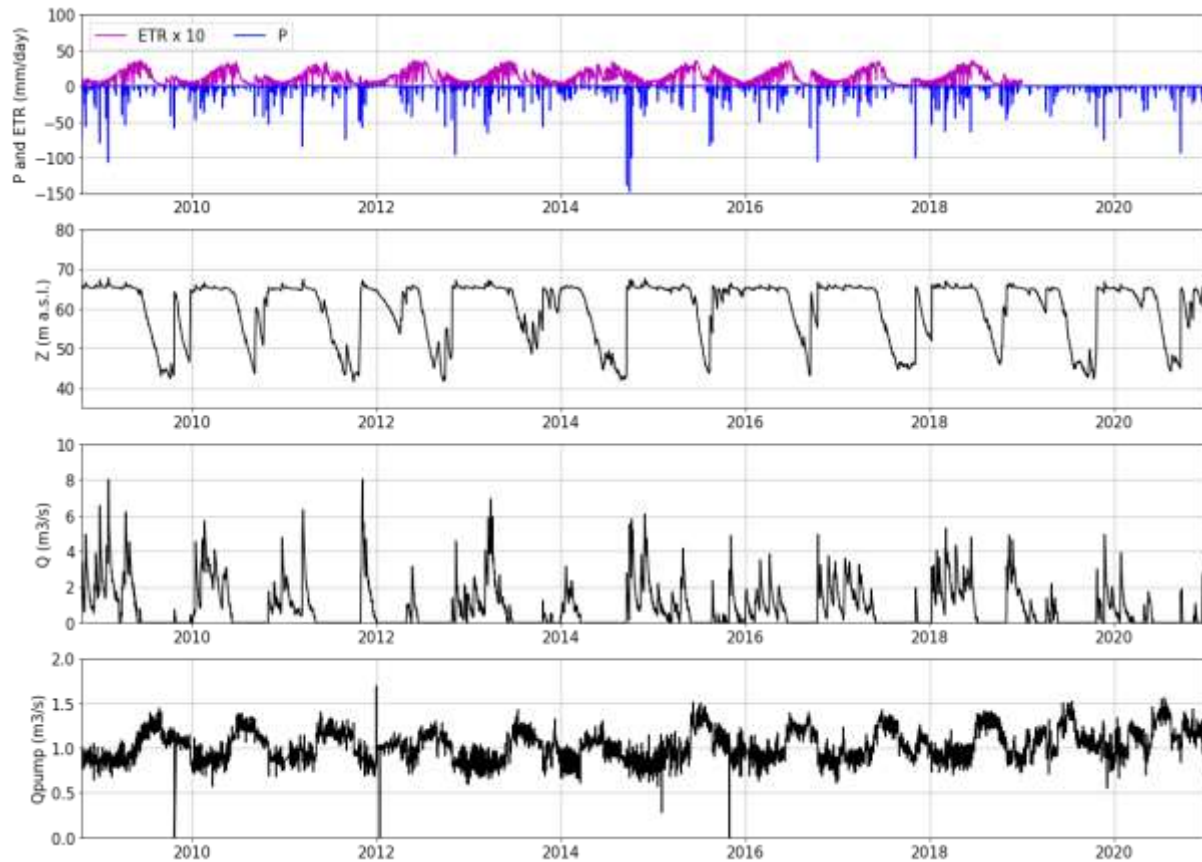


Figure 4.9. Time series for the Lez spring catchment (2008–2021 period): precipitation P (mm/day), real evapotranspiration ETR (mm/day), piezometric head Z at the pumping station (m a.s.l.), spring discharge Q (m³/s) and groundwater abstraction Q_{pump} (m³/s).

Discharge at Lez spring is regularly null during dry periods due to the pumping into the saturated zone of the aquifer (Fig. 4.9). This anthropogenic perturbation disrupts the functioning of the aquifer, thus the monitored time series of the Lez spring discharge is not representative of the natural dynamics and draining of the Lez karst system. This can particularly hinder the results of (i) the recession curve analysis, due to the nearly absence of low flows and proper recession period, and (ii) the correlation and spectral analyses, due to the high occurrence of null values which induces a correlation bias.

4.3.1.1 Main statistical description

Table 4.2 presents the results of statistical analyses applied on the discharge time series of the Lez spring. Over the 2008–2021 period, the mean discharge at the Lez spring was estimated to be 0.84 m³/s, while the mean discharge during overflow periods only was estimated to be about 1.65 m³/s.

	Count	Mean	Std	Min	25%	50%	75%	Max	CV
Whole period	4455	0,84	1,22	0	0	0,11	1,35	8,02	1.44
Period of overflow	2272	1,65	1,25	0,003	0,70	1,32	2,34	8,02	0.75

Table 4.2: Main statistical description of Lez spring discharge over the 2008-2021 period.

The pumping discharge represents more than 50% of the total volume with a mean pumping of about $1.02 \text{ m}^3 \cdot \text{s}^{-1}$ and a mean discharge at the spring of about $0.84 \text{ m}^3 \cdot \text{s}^{-1}$ when considering the whole time series. The coefficient of variation CV is significant and translates a rather reactive response of the system to precipitation events. The minimum and maximum observed discharges over the monitored period are 0 and about $8.2 \text{ m}^3 \cdot \text{s}^{-1}$ respectively. The 25th and 75th quantiles of discharges are of 0 and about $1.35 \text{ m}^3 \cdot \text{s}^{-1}$, respectively. It highlights the scale of the dry periods -in fact, the discharge at the spring is null nearly 50% of the time.

4.3.1.2 Yearly discharge analysis

Fig. 4.10 presents the yearly analysis of the Lez spring discharge time series. The graph shows that the mean pumping is quite steady around $1 \text{ m}^3 \cdot \text{s}^{-1}$. The mean discharge at the spring is variable, with a maximum annual mean of $1.5 \text{ m}^3 \cdot \text{s}^{-1}$ in 2018 and a minimum of $0.33 \text{ m}^3 \cdot \text{s}^{-1}$ in 2012 and 2020. It is mainly correlated with precipitation, although the year of minimum annual precipitation (2017 with 560 mm) does not correspond to the minimum annual mean discharge in 2012 (for which annual precipitation was about 692 mm). Due to the short length of the time series (12 years), it is difficult to identify long term (i.e. interannual) trend.

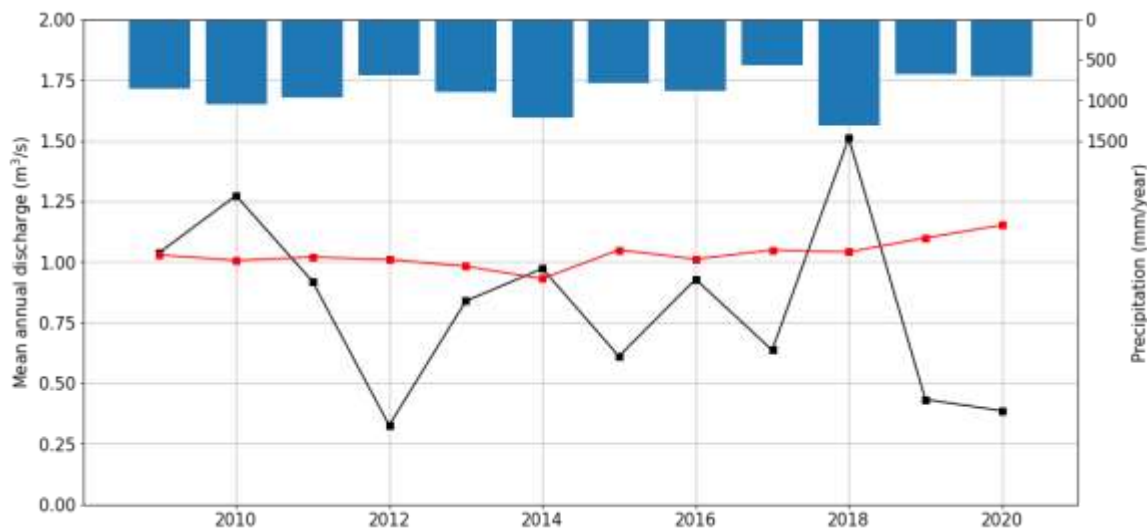


Figure 4.10. Yearly precipitation over the Lez spring catchment and discharge analysis. Discharge at the spring is in black and pumped discharge is in red.

4.3.2 Recession curves analysis

We performed the analysis of recession curves on the discharge time series of Lez spring. The response at the Lez spring is greatly impacted by the anthropogenic pressure on the natural functioning of the karst system. This results into pronounced dry periods and less pronounced recession periods, which bring some uncertainties into the recession curves analysis.

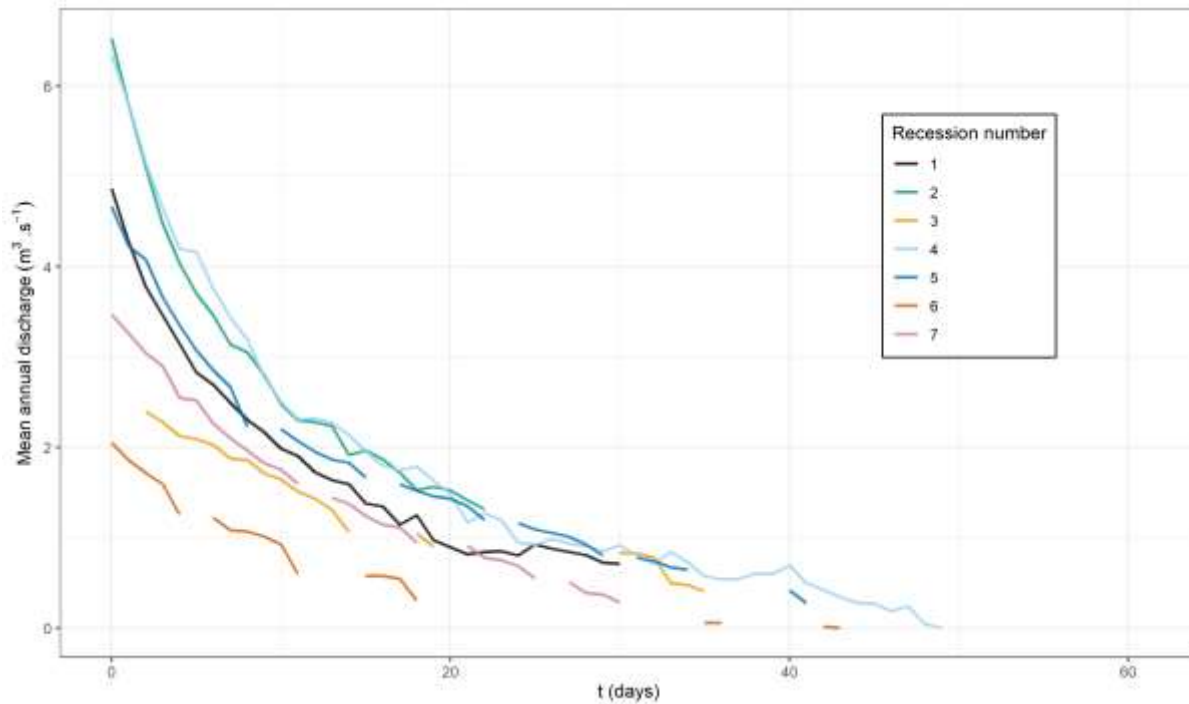


Figure 4.11. Selected recession curves for the analysis on the Lez spring discharge time series.

Over the 10 years discharge time series, we selected 7 recession curves (Fig. 4.11) for performing the Mangin recession analysis (Mangin, 1975). The recession curves differ in total duration and initial discharge peaks. This ensures that the analysis consider the functioning of the karst system in different hydrological conditions. We chose to remove spikes on the recession curves, which usually correspond to the system's response to small precipitation events and can be considered as noise for the modelling. Table 4.3 shows the values of the indicators k , i and α for the retained recession curves. k is between 0.01 and 0.2, i is between 0.43 and 0.89 and α is between 0.01 and 0.08.

Recession number	k	i	α
1	0.20	0.75	0.01
2	0.11	0.57	0.05
3	0.07	0.89	0.02
4	0.06	0.61	0.06
5	0.11	0.43	0.05
6	0.01	0.82	0.08
7	0.07	0.79	0.08

Table 4.3: Results of the Mangin recession analysis.

According to the classification of Cinkus et al. (2021), the Lez system is classified C1 with a k_{max} of 0.2, an α_{mean} of 0.05 and an IR (i Range) of 0.46. This class characterize a system with a poor capacity of

dynamic storage (k_{max}), a fast draining of the capacitive function (α_{mean}) and a substantial variability of the hydrological functioning (IR). The results from the classification seem very different from the actual scientific knowledge of the natural functioning of the Lez karst system. This is likely due to the impact of pumping, which strongly reduces the capacity of dynamic storage, and increases the draining of the capacitive function. Thus, the recession periods are shorter and less pronounced. The analysis of recession curves shows that the Lez karst system functioning is heavily impacted by the anthropogenic forcing due to the pumping in the saturated zone of the aquifer. This pressure induces a faster draining of the capacitive function than expected, reducing the length of recession periods.

4.3.3 Description of hydrological cycle

The summer periods are characterised with a low precipitation rate. The evapotranspiration shows a maximum value during the late spring / early summer period. Such meteorological may induce dry periods at the Lez spring, where no overflow can be observed during almost 4 complete months from June to September (Fig. 4.12).

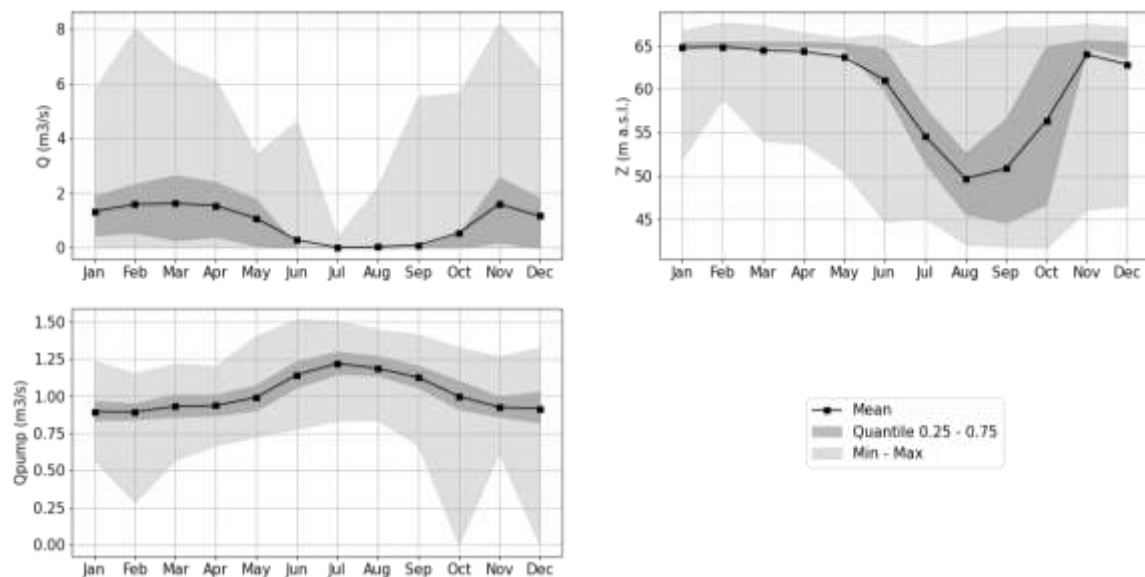


Figure 4.12. Variability of the spring discharge, piezometric head, and groundwater abstraction along with the month of the year.

This is in accordance with a mean piezometric level lower than 65 m.a.s.l. (elevation of Lez spring overflow level). Also, such dry period is exacerbated with a significant increase of groundwater abstraction during summer period, where the mean discharge of groundwater abstraction may rise up to 1.25 m³.s⁻¹ in July against 0.9 m³.s⁻¹ the rest of the year. Fig. 4.12 shows the variability with the month of the year for the different variables of interest. The precipitation shows an annual cycle with two rainy periods during spring and autumns periods. Fig. 4.13 shows the probability density function of rainfall, evapotranspiration, spring discharge and piezometric head, the later highlighting the modification of statistical distribution depending on the piezometric head and the spring elevation (65 m a.s.l.).

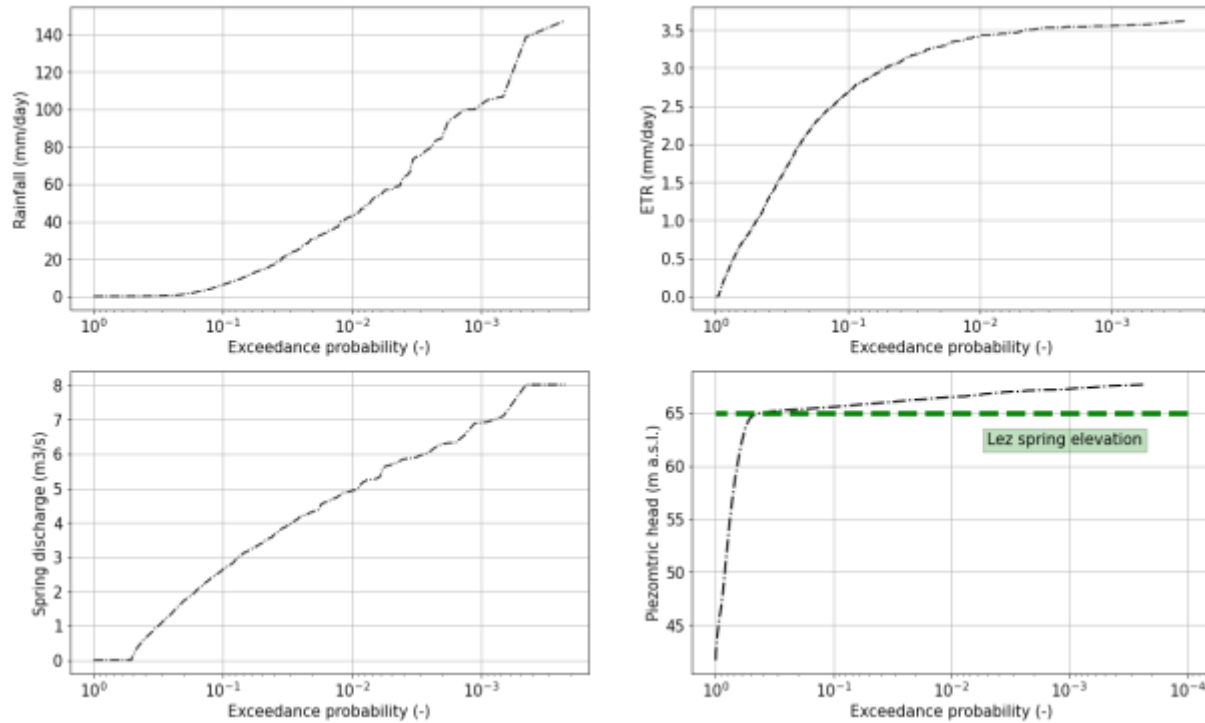


Figure 4.13. Probability of exceedance for rainfall, evapotranspiration, spring discharge and piezometric head.

4.3.4 Correlation analysis

In karst hydrology, the auto-correlation function (ACF) is frequently used to characterize the temporal structure of hydrological signals under the linear-stationary hypothesis (Labat et al., 2000; Larocque et al., 1998; Mangin, 1984; Padilla and Pulido-Bosch, 1995; Panagopoulos and Lambrakis, 2006). In addition, the cross-correlation function (CCF) between rainfall and spring discharge provides an approximation of the impulse response (Mangin, 1984) when assuming the rainfall consists of a random process (white noise). Also, it describes the capacity of a system to transform the rainfall into discharge. The higher the CCF peak, the more the system acts as a piston.

Fig. 4.14 shows the ACF calculated for both the spring discharge and the piezometric head time series. The piezometry show a high inter-annual self-dependence, where secondary peaks in the ACF occurs on an annual basis, with correlation value above 0.4. Considering the spring discharge, the ACF shows a memory effect of 58 days. Nonetheless, such analysis is biased due to the occurrence of dry period, with no overflow at Lez spring, when piezometric head is lower than 65 m a.s.l. Then to avoid such bias the ACF and CCF are estimated within periods of at least 90 continuous days of outflow at the Lez spring (Fig. 4.15). The estimated memory effect varies from 8 to 18 days, with a mean of 10 days. Also, the rainfall-discharge CCF peaks varies from 0.3 to 0.5 with response time of 1 day, testifying of a significant piston effect, where rainfall contributes to quick piezometric head variation within the catchment and so discharge at the spring. The latter is also suggested with the analysis of the piezometric-discharge CCF showing peaks values close to 1. One should note the influence of pumping, that may impact the relation between piezometric variations and spring discharge.

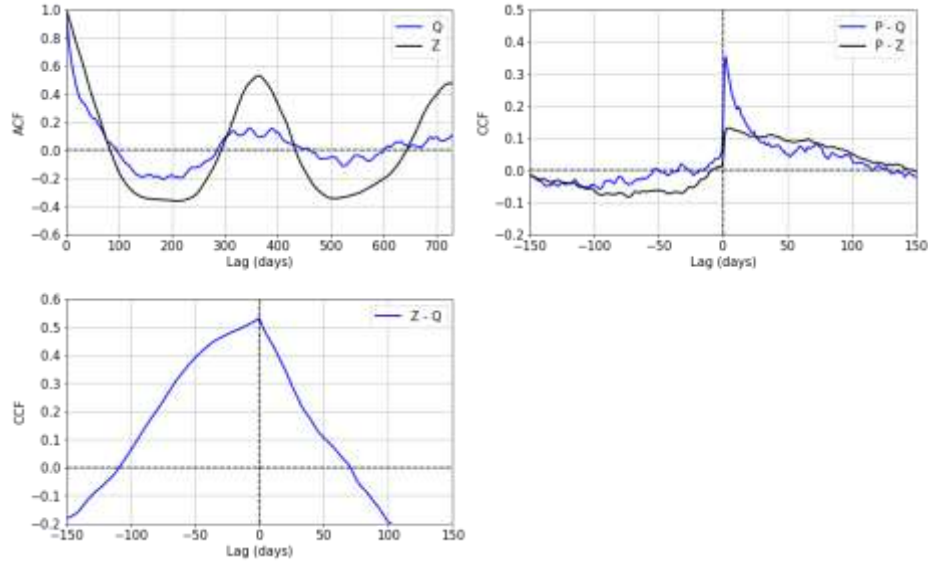


Figure 4.14. ACF of discharge (Q) and piezometric head (Z) at the Lez spring, as well as precipitation-discharge and precipitation - piezometric head CCF.

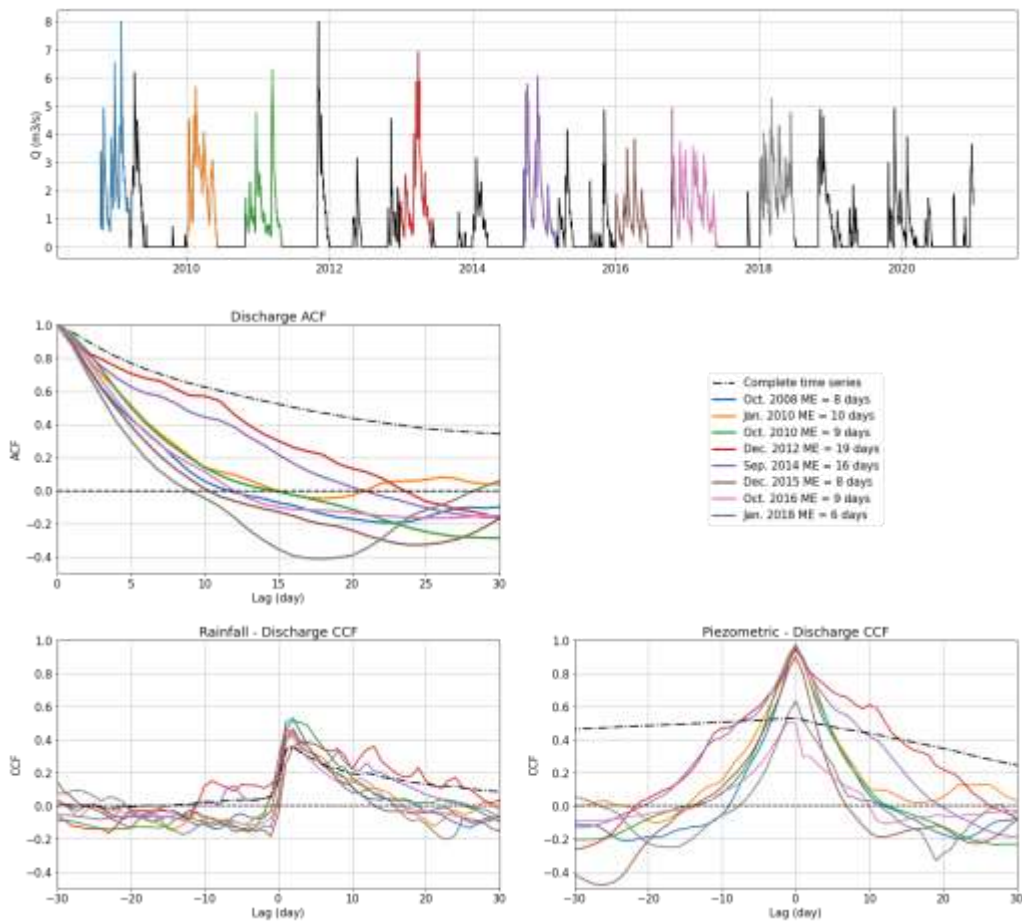


Figure 4.15. ACF and CCF estimated for periods of outflow at the Lez spring and memory effect (ME) estimation (Mangin, 1975). Only periods of at least 90 days are considered so the ACF and CCF still significant for lag value up to 30 days.

4.3.5 Spectral analysis

The Fourier spectrum of a signal/process represents the distribution of energy/variance E of the process depending on the frequency ω . It is observed a relation $E = \omega^\beta$ where the β coefficient corresponds to the Fourier spectrum slope in a log-log plot. The β coefficient can give information on the signal (Hardy and Beier 1994). Indeed $\beta = 0$ is characteristic of a white noise (energy and frequency are independent), $\beta = -1$ is a pink noise (natural phenomenon of large spatial and temporal scales), $\beta = -2$ is characteristic of a red noise (the successive points are independent for one another but they follow a statistical law), $\beta < -3$ is black noise (the signal is not statistical but characteristic of exceptional events interrupting periods when another law was applying).

Fig. 4.16 shows the Fourier spectra calculated based on the spring discharge and piezometric head time series. The β coefficient for the spring discharge within the period from 2 to 64 days is estimated around -2, characteristic of a red noise. The β coefficient for the piezometric head is estimated around -2.3, showing a higher influence of event with a significative change in statistical distribution. Then, the cell effect at the Lez spring pool, gives a physical meaning in the modification of statistical distribution depending on the piezometric head and the spring elevation (65 m a.s.l.).

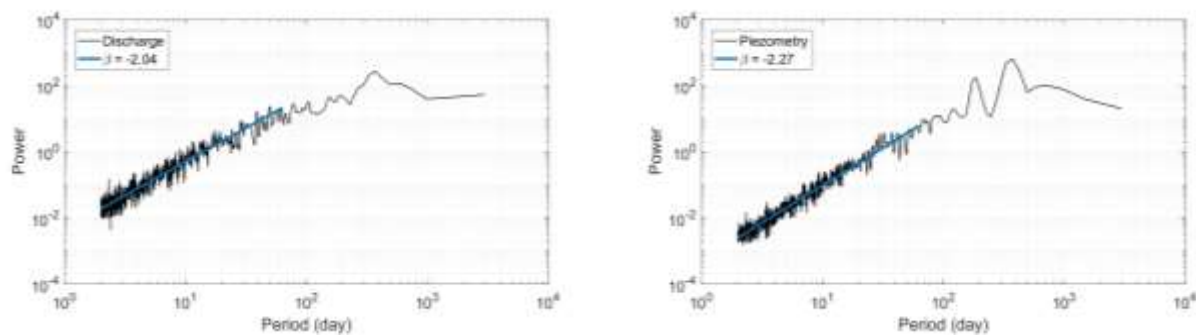


Figure 4.16. Fourier spectra for both spring discharge and piezometric head time series.

4.4 Discussion

Fig. 4.17 shows the Mean Water Level Drop (MWLD) based on the piezometric head time series, considering period without influence of recharge. The MWLD is considered within 1-meter thick slice to investigate the influence of effective porosity with depth. The profile with depth shows different media: the MWLD increase up to 0.3 m/day at a depth of 60 m a.s.l., remains constant until an elevation around 55 m a.s.l., then the MWLD decrease for mean piezometric head lower than 51 m a.s.l.. One should note the influence of groundwater abstraction, where the mean volume depends on the period of the year (Fig. 4.12). It is observed that the influence of groundwater abstraction is constant with depth, until an elevation of 46 m a.s.l.

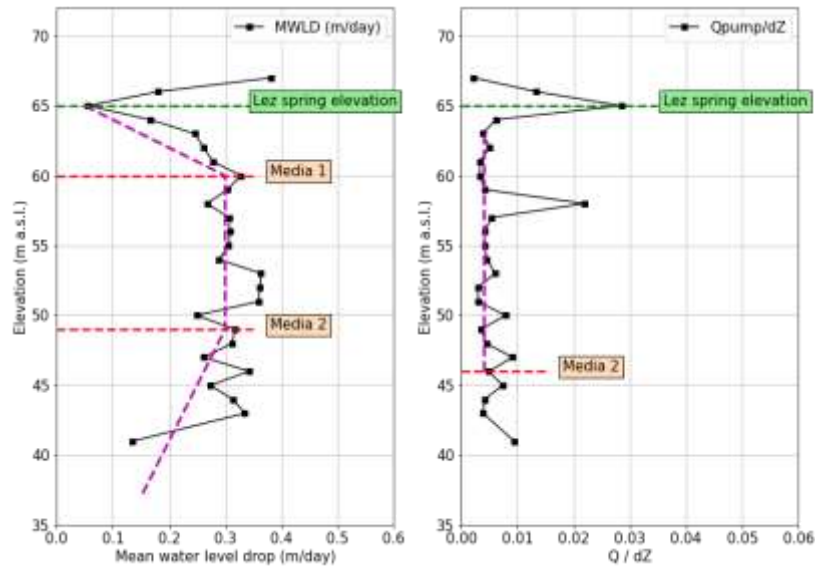


Figure 4.17. Mean Water Level Drop and influence of groundwater abstraction depending as a function of the piezometric head –time series 2008 – 2020.

4.5 References

- Avias J. V., 1995 - Gestion active de l'exsurgence karstique de la source du Lez, Hérault, France, 1957-1994. Hydrogeologie (Orléans) 1995: 113-127
- Batiot-Guilhe, C., Ladouche, B., Seidel, J.-L., Maréchal, J.-C., 2013 - Caractérisation hydrochimique et qualité des eaux de l'aquifère karstique du Lez (SE de la France), Karstologia 62, 23-32.
- Bicalho C.C., Batiot-Guilhe C., Seidel J. L., Van Exter S., Jourde H. (2012). Hydrodynamical changes and their consequences on groundwater hydrochemistry induced by three decades of intense exploitation in a Mediterranean Karst system. Environmental Earth Sciences, Volume 65, Issue 8, 2311-2319, <https://doi.org/10.1016/j.jhydrol.2012.04.059>
- Camus, H. (1999). L'organisation des réseaux de drainage à différents stades de l'évolution du paysage karstique de la bordure carbonatée sub-cévenole (de l'Aigoual à la basse vallée de l'Hérault). In: Karst 99 - Livret guide des excursions Grands Causses - Vercors. Ed. by Y. Perrette and J.-J. Delannoy. Cahiers savoisiens de Géographie, p 55-74.
- Cinkus, G., Mazzilli, N., Jourde, H., 2021. Identification of relevant indicators for the assessment of karst systems hydrological functioning: Proposal of a new classification. Journal of Hydrology 603, 127006. <https://doi.org/10.1016/j.jhydrol.2021.127006>
- Erostate M., Batiot-Guilhe C., Bailly-Comte V., Durepaire X. (2016). Relationships between natural fluorescence and organic matter content based on sampling and in-situ monitoring of groundwater. Application to the karst systems of the Lez and Fontaine de Nîmes springs, 43rd IAH Congress, 25-29th September, 2016, Montpellier, France.
- Jourde, H., Dörflinger, N., Maréchal, J.-C., Batiot-Guilhe, C., Bouvier, C., Courrioux, G., Desprats, JF., Fullgraf, T., Ladouche, B., Leonardi, V., Malaterre, PO., Prié, V., Seidel, J.-L., 2011. Projet gestion multi-

usages de l'hydrosystème karstique du Lez - Synthèse des connaissances récentes et passées (BRGM No. RP-60041-FR).

Jourde H., Lafare A., Mazzilli N., Belaud G., Neppel L., Dörfli N. And Cernesson F., 2014 - Flash flood mitigation as a positive consequence of anthropogenic forcing on the groundwater resource in a karst catchment. *Environmental Earth Sciences*: 1-11 doi: 10.1007/s12665-013-2678-3

Labat, D., Ababou, R., Mangin, A., 2000. Rainfall–runoff relations for karstic springs. Part I: convolution and spectral analyses. *Journal of Hydrology* 238, 123–148. [https://doi.org/10.1016/S0022-1694\(00\)00321-8](https://doi.org/10.1016/S0022-1694(00)00321-8)

Larocque, M., Mangin, A., Razack, M., Banton, O., 1998. Contribution of correlation and spectral analyses to the regional study of a large karst aquifer (Charente, France). *Journal of Hydrology* 205, 217–231. [https://doi.org/10.1016/S0022-1694\(97\)00155-8](https://doi.org/10.1016/S0022-1694(97)00155-8)

Leonardi, V., Jourde, H., Dausse, A., Dörfli N., Brunet, P., Maréchal, J.-C., 2013. Apport de nouveaux trçages et forages à la connaissance hydrogéologique de l'aquifère karstique du Lez. *KARSTOLOGIA* 62, 7–14.

Mangin, A., 1975. Contribution à l'étude hydrodynamique des aquifères karstiques (PhD thesis). Université de Dijon, France.

Mangin, A., 1984. Pour une meilleure connaissance des systèmes hydrologiques à partir des analyses corrélatoire et spectrale. *Journal of Hydrology* 67, 25–43. [https://doi.org/10.1016/0022-1694\(84\)90230-0](https://doi.org/10.1016/0022-1694(84)90230-0)

Mazzilli N. (2011). Sensitivity and uncertainty associated with the numerical modelling of groundwater flow within karst systems. PhD, Université Montpellier 2, France.

Padilla, A., Pulido-Bosch, A., 1995. Study of hydrographs of karstic aquifers by means of correlation and cross-spectral analysis. *Journal of Hydrology* 168, 73–89. [https://doi.org/10.1016/0022-1694\(94\)02648-U](https://doi.org/10.1016/0022-1694(94)02648-U)

Panagopoulos, G., Lambrakis, N., 2006. The contribution of time series analysis to the study of the hydrodynamic characteristics of the karst systems: Application on two typical karst aquifers of Greece (Trifilia, Almyros Crete). *Journal of Hydrology* 329, 368–376. <https://doi.org/10.1016/j.jhydrol.2006.02.023>

Quiers M., Batiot-Guilhe C., Bicalho CC., Perrette Y., Seidel J.L., S. Van Exter. (2014). Characterisation of rapid infiltration flows and vulnerability in a karst aquifer using a decomposed fluorescence signal of dissolved organic matter. *Environmental Earth Sciences*, 71, 2, 553-561. DOI 10.1007/s12665-013-2731-2.

Rohde Y. (2020). Use of emerging tracers to characterize groundwater flow and vulnerability in Mediterranean karst aquifers. The Lez spring karst aquifer. Study Project. Water Science and Engineering M.Sc., Karlsruher Institut für Technologie, Matriculation number: 2238397, 64 pages.

5 Hochifen-Gottesacker karst area (test site in Austria)

5.1 General description of the monitoring network for spring discharge monitoring

The test site is located in the Northern Alps at the border between Austria and Germany and belongs to the Helvetic zone of the Alps (Fig. 5.1a). The altitude varies between 1035 m asl (Sägebach Spring) and 2230 m asl (summit of Mt. Hochifen). The most important rock formation is the Cretaceous Schrattenkalk limestone, which forms the surface of the Gottesacker terrain (Goldscheider, 2005) and constitutes a karst aquifer of about 100 m thickness above a marl formation of about 250 m acting as an aquitard (Fig. 5.1b and 5.c). Previous research (Goldscheider, 2005; Goepfert and Goldscheider, 2008) has shown that the orientation of underground flow paths is structurally controlled (Fig. 5.1c). The mountain range SE of the Schwarzwasser valley is formed by sedimentary rocks of the Flysch zone and is characterized by low permeability and surface drainage. The karst aquifer receives autogenic recharge from precipitation and snowmelt, and allogenic recharge from the Flysch zone (Chen & Goldscheider, 2014).

The nearest permanent weather station in the Breitach valley (1140 m asl) gives a mean annual rainfall of 1840 mm and an air temperature of 5.7 °C. In the elevated parts of the study site, the precipitation is certainly higher and a large proportion falls as snow. Assuming a vertical temperature gradient of 0.6 °C/100 m (e.g. Veith, 2002) a mean annual temperature of 0 °C is expected at an altitude of 2100 m.

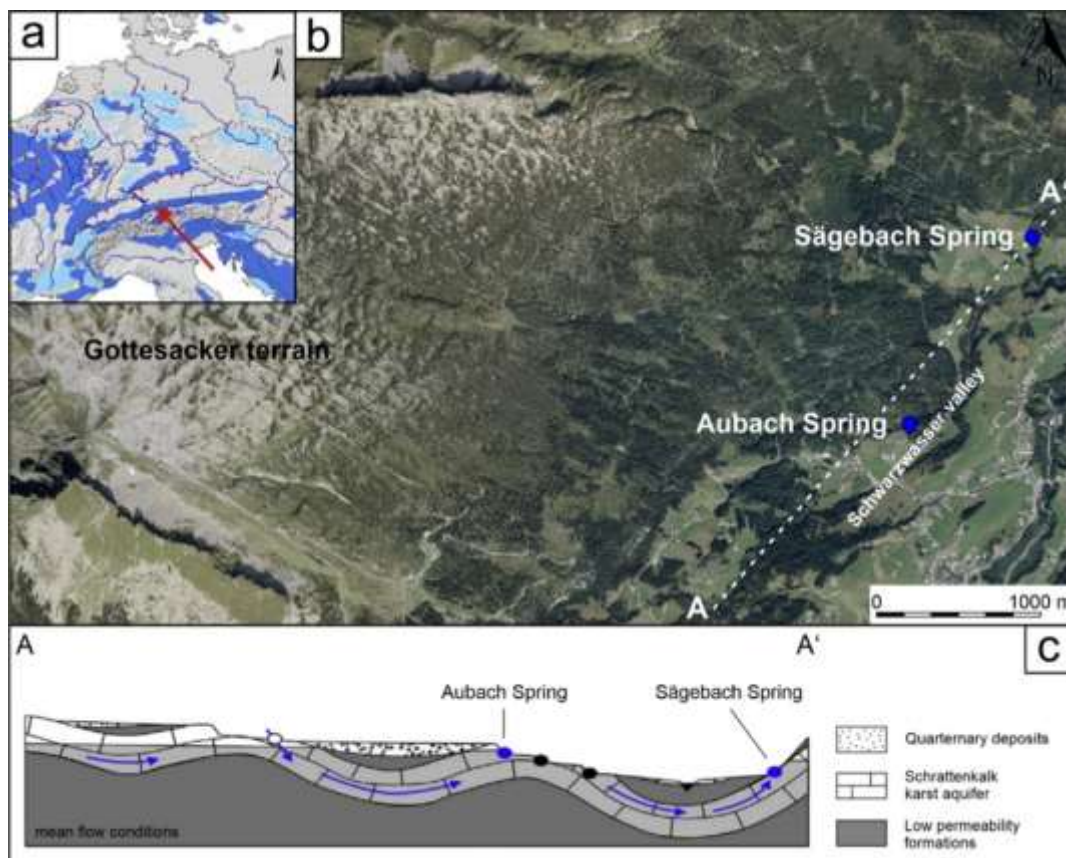


Fig. 5.1. a) Location of the test site shown on a section of the World Karst Aquifer Map (Chen et al., 2017) with carbonate rocks in blue b) Detail of the test site with the Gottesacker area and Aubach- and Sägebach Spring (basemap: Land Vorarlberg – data.vorarlberg.gv.at) and c) schematic cross-section with flow paths at mean flow conditions (Goldscheider, 2005) (modified after Goepfert et al., 2020).

Two springs in the Schwarzwasser valley were investigated (Fig. 5.1b and 5.1c). The first one is the large but intermittent Aubach Spring (QA), which discharges up to 8000 L/s but runs completely dry in long dry periods and in winter. Further downstream, the Sägebach Spring (QS) presents the largest permanent spring (base-flow spring) in the valley and discharges up to about 3500 L/s (Chen & Goldscheider, 2014). A relatively constant amount of the spring discharge, usually about 135 L/s, is used by a hydropower plant that takes water directly at the spring. The total size of the catchment area of QA and QS is about 35 km² (Chen & Goldscheider, 2014). Both investigated springs are not used for drinking water supply and show high variability regarding discharge and water quality.

5.2 Equipment and methods used

For the discharge at QA, high-resolution data from the Water Management Department of Vorarlberg were used, which are continuously recorded since 1999. The Water Management Department of Vorarlberg also provides precipitation data for the weather station at Walmendinger Horn, around 10 km SW of both springs, since 2000.

At QS, the water level was recorded with an OTT Orpheus Mini logger with an accuracy of $\pm 0.05\%$ of the full scale. Discharge measurements were done using the salt dilution method with point injection and a stage-discharge relation was derived. Using this stage-discharge relation, continuous discharge for each water level was then calculated. Note, that in order to obtain the complete discharge of QS, the discharge of the extracted water by the power plant need to be added. Data concerning the amount extracted water were provided by the Water Management Department of Vorarlberg.

5.3 Results

Fig. 5.2 and Fig. 5.3 show the discharge and rainfall data for QA and QS from 30.06.2020 until 25.08.2020, a time period which is not affected by snowmelt in the catchment. At both springs, distinct reaction of discharge after rainfall events were recorded. The maximum discharge of 6183 L/s (QA) and 3670 L/s (QS) were reached after a heavy rain event on 04.08.2020, while the minimum discharge at QA and QS with 149 L/s and 204 L/s, respectively, were measured between the rainfall events. On average, the discharge for QA is 677 ± 919 L/s and for QS 463 ± 812 L/s. It is noticeable, that the rainfall event between 21.07.2020 and 25.07.2020 was only recognizable in the discharge of QS, while the discharge at QA showed no reaction (Fig. 5.2 and Fig. 5.3). Therefore, this specific rainfall event was likely extremely focused in the catchment of QS.

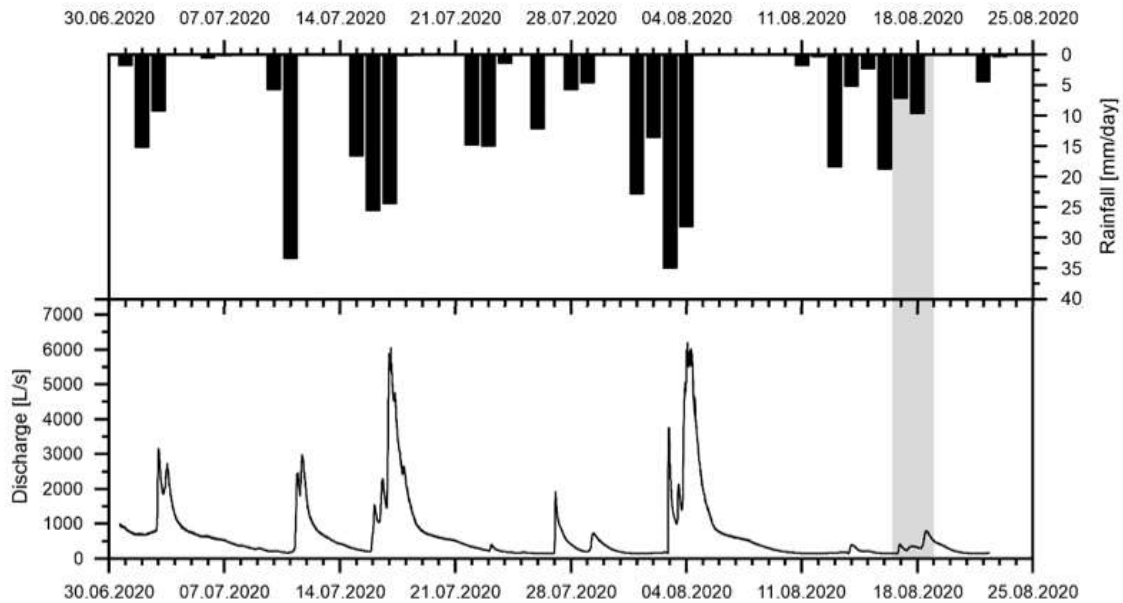


Fig. 5.2. Temporal patterns of discharge at Aubach Spring and rainfall data from the nearest permanent weather station in the Breitach valley (1140 m asl). The grey bar indicates a detailed monitoring period for water quality (modified after Frank et al., submitted).

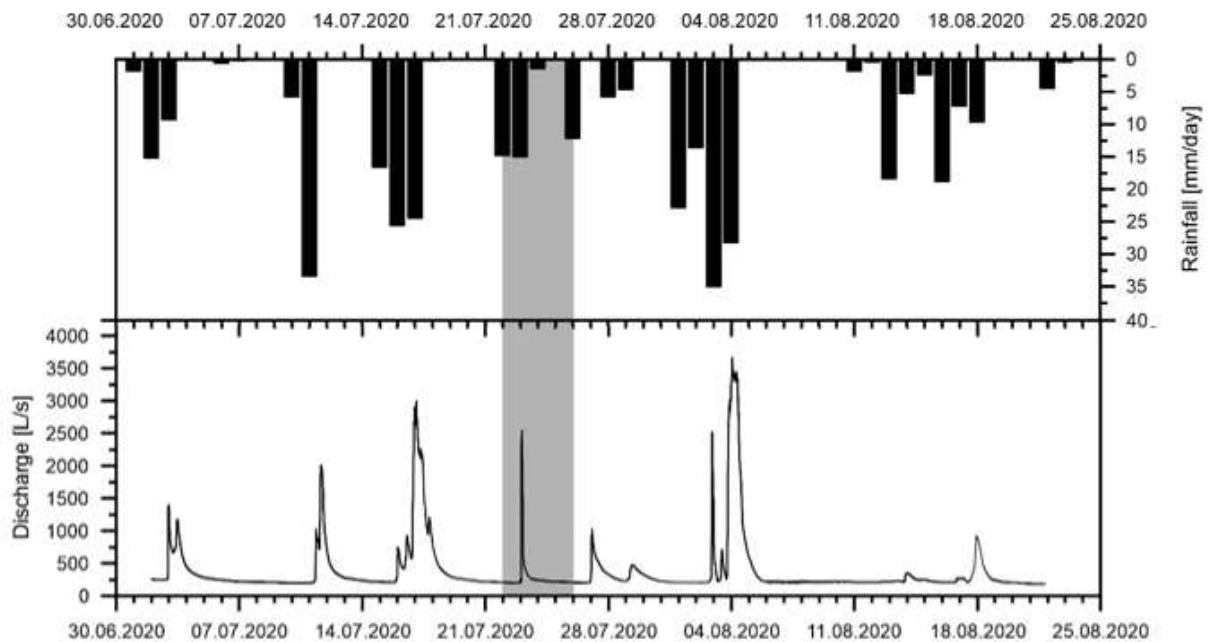


Fig. 5.3. Temporal patterns of discharge at Sägebach Spring and rainfall data from the nearest permanent weather station in the Breitach valley (1140 m asl). The grey bar indicates a detailed monitoring period for water quality (modified after Frank et al., submitted).

5.4 Discussion

The salt dilution method in combination with pressure probes is a well-known technique in the field of hydrogeology to distribute discharge and gives reliable results. The discharge at QA and QS show a fast response to rainfall events, highlighting the fast groundwater dynamics in karst systems, which make them highly vulnerable to climate change. The prediction is, that climate change will lead to lower spring discharge in the entire Hochfifen-Gottesacker area, even if the impacts on different springs are distinct (Chen et al., 2018). However, for describing the relationship between discharge and precipitation and for more accurate predictions about the discharge of different springs, spatially high-resolution meteorological data are needed. The meteorological data provided by nearby weather stations are only true for a very small area, especially regarding the highly variable topography in the alps. This fact is also illustrated by the lack of discharge reaction at QA for the rainfall event between 21.07.2020 and 25.07.2020, as it only took place in the QS catchment.

The lack of information is also shown in the work of Wunsch et al., 2021, in which the discharge at QA between January and November 2020 was simulated with deep learning models using meteorological input data such as precipitation, temperature, evaporation, snowmelt, snowfall and volumetric soil water. Wunsch et al., 2021 showed, that the model derived by only using meteorological data from the nearest weather stations does not perform satisfactorily for discharge at QA. The best fit was reached by combining raster data from ERA5-Land (Muñoz Sabater, 2019) and spatially higher resolved RADOLAN data (DWD Climate Data Center (CDC)) as model inputs (Fig. 5.4). However, for the very small catchment of QA, even this model has its limits (Wunsch et al., 2021).

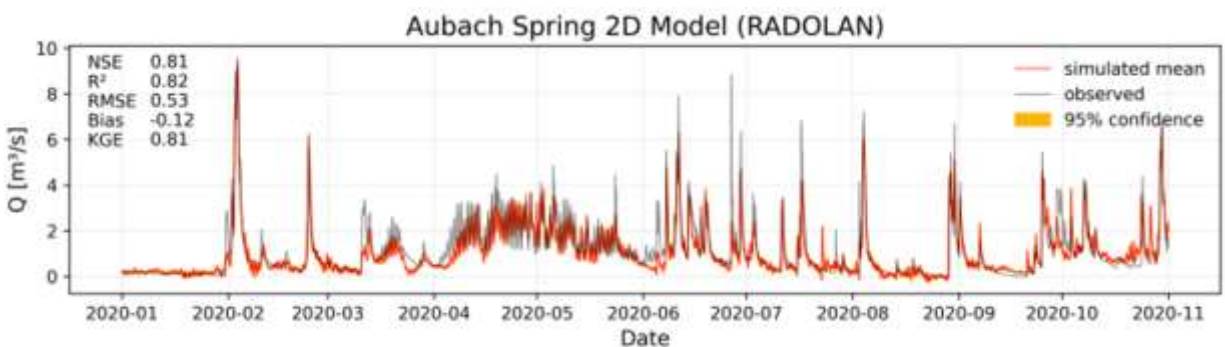


Fig. 5.4. Simulation results for the year 2020 at Aubach Spring with a 2D-model with combination of ERA5-Land data and RADOLAN precipitation input (Wunsch et al., 2021).

5.5 Conclusions

The discharge of two alpine karst springs in Austria were monitored during July and August 2020 (8 years of data are available for QA), with multiple rainfall events of varying intensity occurring. A fast and marked response of discharge to rainfall events was observed at both springs. Even though, extremely focused rainfall events can occur in the different catchments, that therefore do not affect the discharge of all other springs. To achieve further knowledge about the reaction of discharge at different springs, it is important to overcome missing climate data due to unsatisfactory spatial coverage of weather station. Gridded meteorological data have a better spatial and temporal coverage and resolution and thus offer a better option. But even these data do not provide a good enough spatially resolution for very small catchment

areas. Therefore, the development of higher spatial resolution systems for meteorological data promises more precise results and predictions, in particular to accurately assess spring discharge observations in relation to climate change.

5.3 Literature

Chen Z, Goldscheider N (2014) Modeling spatially and temporally varied hydraulic behavior of a folded karst system with dominant conduit drainage at catchment scale, Hochifén–Gottesacker, Alps. *Journal of Hydrology*. 514: 41-52

Chen Z, Auler A, Bakalowicz M, Drew D, Griger F, Hartmann J, Jiang G, Moosdorf N, Richts A, Stevanovic Z, Veni G, Goldscheider N (2017) The world karst aquifer mapping project: Concept, mapping procedure and map of Europe. *Hydrogeol. J.* 25 (3), 771-785

Chen Z, Hartmann A, Wagener T, Goldscheider N (2018) Dynamics of Water Fluxes and Storages in an Alpine Karst Catchment under Current and Potential Future Climate Conditions, *Hydrol. Earth Syst. Sci.*, p. 17, <https://doi.org/10.5194/hess-22-3807-2018>

DWD Climate Data Center (CDC): Historical and Current Hourly RADOLAN Grids of Precipitation Depth (Binary). Version V001, https://opendata.dwd.de/climate_environment/CDC/grids_germany/hourly/radolan/

Frank S, Fahrmeier N, Goeppert N, Goldscheider N (submitted) High-resolution multi-parameter monitoring of microbial water quality and particles at two alpine karst springs as a basis for an early-warning system

Goeppert N, Goldscheider N (2008) Solute and colloid transport in karst conduits under low- and high-flow conditions. *Groundwater* 46 (1), 61-68

Goeppert N, Goldscheider N, Berkowitz B (2020) Experimental and modeling evidence of kilometer-scale anomalous tracer transport in an alpine karst aquifer. *Water research*, 178.

Goldscheider N (2005) Fold structure and underground drainage pattern in the alpine karst system Hochifén-Gottesacker. *Eclogae geol. Helv.* 98 (1), 1–17

Muñoz Sabater J (2019) ERA5-Land Hourly Data from 2001 to Present. Copernicus Climate Change Service (C3S) Climate Data Store (CDS), <https://doi.org/10.24381/CDS.E2161BAC>, 2019.

Veith H (2002) *Die Alpen: Geoökologie und Landschaftsentwicklung*, 1st ed. Verlag Eugen Ulmer, Stuttgart

Wunsch A, Liesch T, Cinkus G, Ravbar N, Chen Z, Mazzilli N, Jourde H, Goldscheider N (2021) Karst spring discharge modeling based on deep learning using spatially distributed input data. *Hydrol. Earth Syst. Sci. Discuss.* [preprint], <https://doi.org/10.5194/hess-2021-403>, in review, 2021.

6 Jebel Zaghouan aquifer

6.1 Study area

The Jebel Zaghouan is the most important Jurassic of the Zaghouan massif and it is located at about fifty kilometers from Tunis (Tunisia). This massif is constituted by monoclinals of limestone overlapping one on the other. It is also made of marls of the Cretaceous and Eocene (Castany, 1951). The Jebel Zaghouan is characterized by the presence of southern and transverse faults that have created individualized blocks. These faults allow the infiltration. The Zaghouan karst aquifer is about 19.6 km² area (Figure 6.1). It has an eastern part favorable to the storage of seepage water, contrary to its western part, its western part where marl deposits strongly decrease the storage coefficient (Djebbi et al., 2001).

The geology of Jebel Zaghouan has made it an important water reserve used since antiquity for the water supply of Carthage, then Tunis. The Roman aqueduct (120 A.D.), still very well preserved, which connects the water temple to the city of Carthage, can be seen along the road linking Tunis to Zaghouan. Currently, the aquifer is exploited by mainly 9 boreholes and galleries intended for the drinking water supply of the city of Zaghouan and the surrounding rural agglomerations. Three of these wells used as commercialized mineral water.

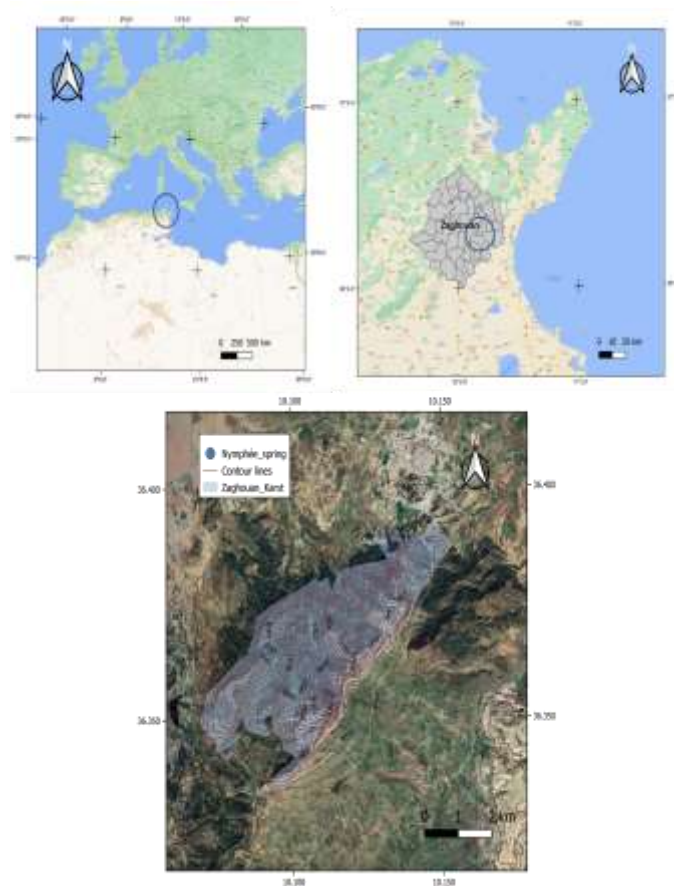


Figure 6.1. Location of the Jebel Zaghouan karst aquifer.

The massif is drained by 14 springs. The most important springs are on massif north-western slope among them: Nymphaea, Ain Ayed, Ain ElGuelb, Gallerie 44 and Gallerie 47 and Ain Haroun, shown in Figure 6.2.

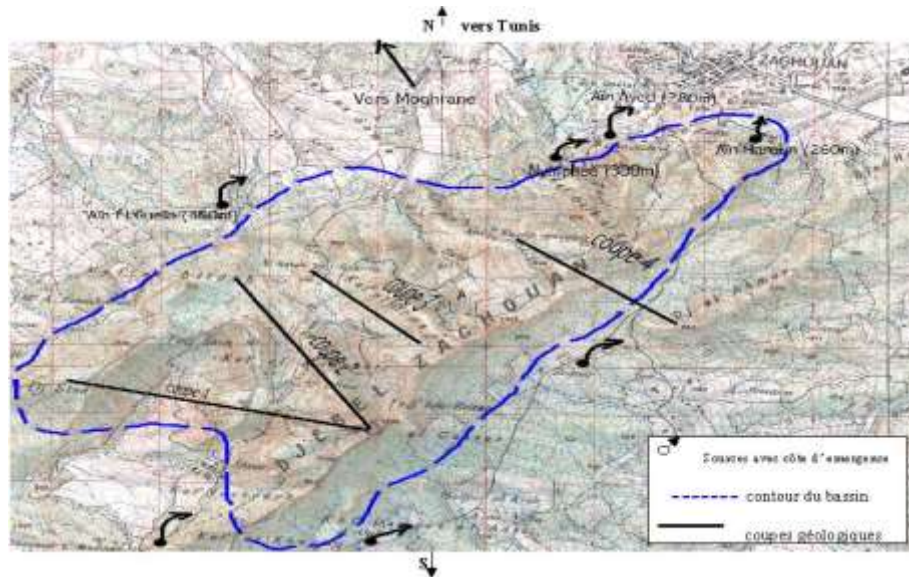


Figure 6.2. Springs location map.

6.2 Water resources

Djebel Zaghouan limestone aquifer is the one of the most important water resources of good quality in the region. Since the roman era, the karst springs of Zaghoaun, supplied drinking water for the local cities and for the capital (Carthage then Tunis) through an aqueduct of 132 km. Due to the drought of the forties, three galleries (known as 44 and 47) were drilled in the system (Figure 6.3) to drain the natural resurgences. These two galleries are about 300 m long. They are all equipped with control valves that allow consumers to be served according to their needs. A series of boreholes were also installed from the nineties.



Figure 6.3. Photos of Galleries 44 and 47 (field trip February 2019 and Dziri, 2016).

6.3 Historical flow data

The available flow data corresponding to the natural flow period was recorded from 1915 to 1943 at irregular time scales. Discharges measurements were taken on a weekly, twice-weekly, or once-monthly basis rather than daily. Since the installation of the valves to control the flows supplied by the galleries, the system is no longer natural. The flows observed from 1958 to 1962 and from 1971 to 1995 are very random and indicate that they are highly dependent on the openings of the gates. These openings depend on several contingencies, in particular the daily demands made by SONEDE to meet the water needs of its users.

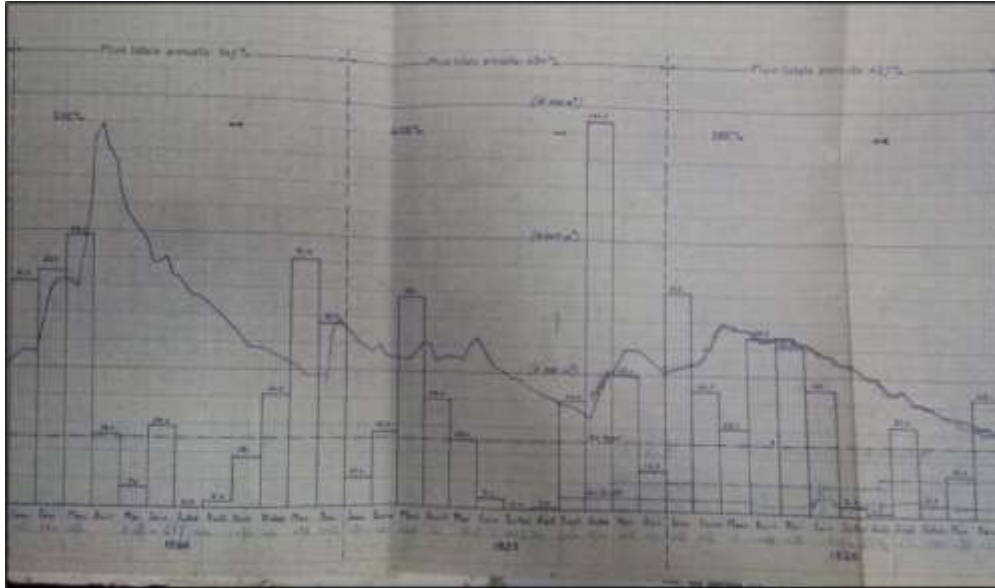


Figure 6.4. Examples of non-digitized discharge.

6.4 Current situation

Currently, the aquifer is exploited by mainly 9 boreholes and galleries intended for the drinking water supply of the city of Zaghouan and the surrounding rural agglomerations. Three of these wells used as commercialized mineral water (Cristaline, Aqualine and Prestine). Since galleries 44 and 47 are dry and to cope with water shortage that Zaghouan city suffers from, two other boreholes (Water temple and Ain Haroun 3bis) were drilled in 2017 and 2018.

With the help of SONEDE and CRDA, we are currently collecting the daily amounts of water extracted from these boreholes.

6.5 References

Castany, G., 1951. Djebel Zaghouan, carte géologique. Dans: S. g. d. Tunisie-Tunis, éd. Étude géologique de L'Atlas Tunisien Oriental. Tunis: Tunisie. Service géologique. Éditeur scientifique, p. 1.

Djebbi M. , Sagna J. and Besbes M. (2001). Sources karstiques de Zaghouan : Recherche d'un opérateur Pluie - Débit. Sciences Et Techniques De L'Environnement Mémoire Hors-Serie,

Dziri R., Chkir N., Emblanch C., Zouari K. and Gallali A. (2016). Geochemical and hydrodynamic characteristics of the karstic system of Jbal Zaghouan (Northeastern-Tunisia). I-DUST 2016: inter-Disciplinary Underground Science & Technology Avignon

7 The Qachqouch aquifer (Case study-Lebanon)

7.1 Introduction

Qachqouch Spring (Figure) is located within the Nahr el Kalb Catchment, and originates from the Jurassic karst aquifer at about 64 meters above sea level. During low flow periods, the spring is used to complement the water deficit in the capital city Beirut and surrounding areas. Its total yearly discharge reaches 35-55 Mm³ based on high resolution monitoring of the spring (2014-2019; *Dubois et al., submitted*, Dubois, 2017). Flow maxima reach a value of 10 m³/s for a short period of time following flood events; it is about 2 m³/s during high flow periods and 0.2 m³/s during recession periods.

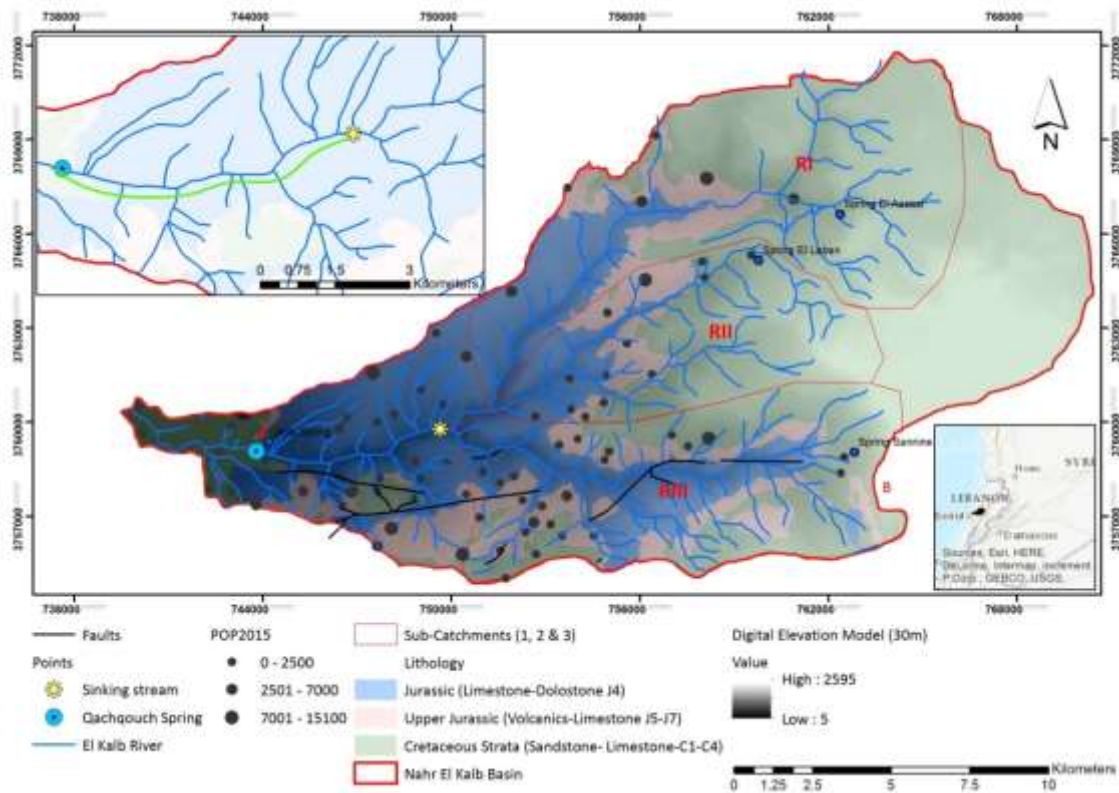


Figure 7.1. Investigated Spring (Qachqouch) and River (Nahr el Kalb) watersheds showing the relationship between a sinking stream on the river and the spring (Aoun, 2019).

The lithology of the surface water and groundwater catchments mostly consists of Jurassic karstified limestone to dolomitic limestone (in the higher plateaus) grading into more massive micritic limestone in the lower portion of the catchment. Formations of middle cretaceous age are exposed on the upper parts of the catchment (Figure 7.1, Dubois, 2017).

The Qachqouch spring is a karst spring characterized by a duality of flow in a low permeability matrix and high permeability phreatic conduit system (Dubois, 2017). It is highly reactive to rain events with recession coefficient ranging between 0.005 and 0.1 depending on the event responses (Dubois, 2017). About 3% of the river infiltrates into the Qachqouch spring based on multiple tracer test experiments conducted in the river during different flow periods. The estimated transport velocities vary between 0.02 and 0.05 m/s (Aoun, 2019).



a



b

Figure 7.1 a) Qachqouch spring during high flow (picture taken February 2020); b) Nahr el Kalb River- a pressure transducer was installed in November 2019 (picture taken January 2020)

The total yearly precipitation is estimated from two stations deployed over the surface and groundwater catchment to about 950-1500 mm on average (2014-todate; local high-resolution monitoring). The latter includes the snow component contributing locally to the river in March and April of each hydrological year (Dubois 2017).

Qachqouch spring is highly polluted due to excessive waste discharge located in its urbanized catchment upstream, in addition to the input from the river through a sinking stream. Raw wastewater is either directly discharged into the river system or bottomless cesspits or overflowing in valleys, as there are no effective wastewater treatment plants (WWTPs) on the studied catchment area (Doummar and Aoun, 2018b).

Nahr El Kalb River is originating from springs in the highlands of Kesrouane area, in addition to interflow and runoff occurring shortly after rain events and snowmelt. Its catchment is about 249 km² and extends from the outlet of the river on the coast to about 22 km to the east in the Lebanese Mountains (Margane, A. & Stoeckl, L., 2013). Its southern and northern boundaries were delineated based on topography highs. The river consists of three sub-catchments (RI -Nahr El Salib; RII-Nahr el Ouadi, and RIII- Nahr Abou Mizane; Figure) joining together to form the main branch of the river. Its peak discharge reaches a maximum of 22 m³/s, with a yearly discharge volume of 80.0- 230 Mm³ (based on River measurements from 2014-2017). Most of the River runoff is generated as a response to precipitation events between December and March, from snowmelt in the highlands (1200-2200 m above sea level) occurring between March and April of the same hydrological year. From August till October, the River flow does not exceed 0.8 m³/s at its outlet; while the three upper tributaries (RI, RII, and RIII) run dry (Doummar and Aoun, 2018b).

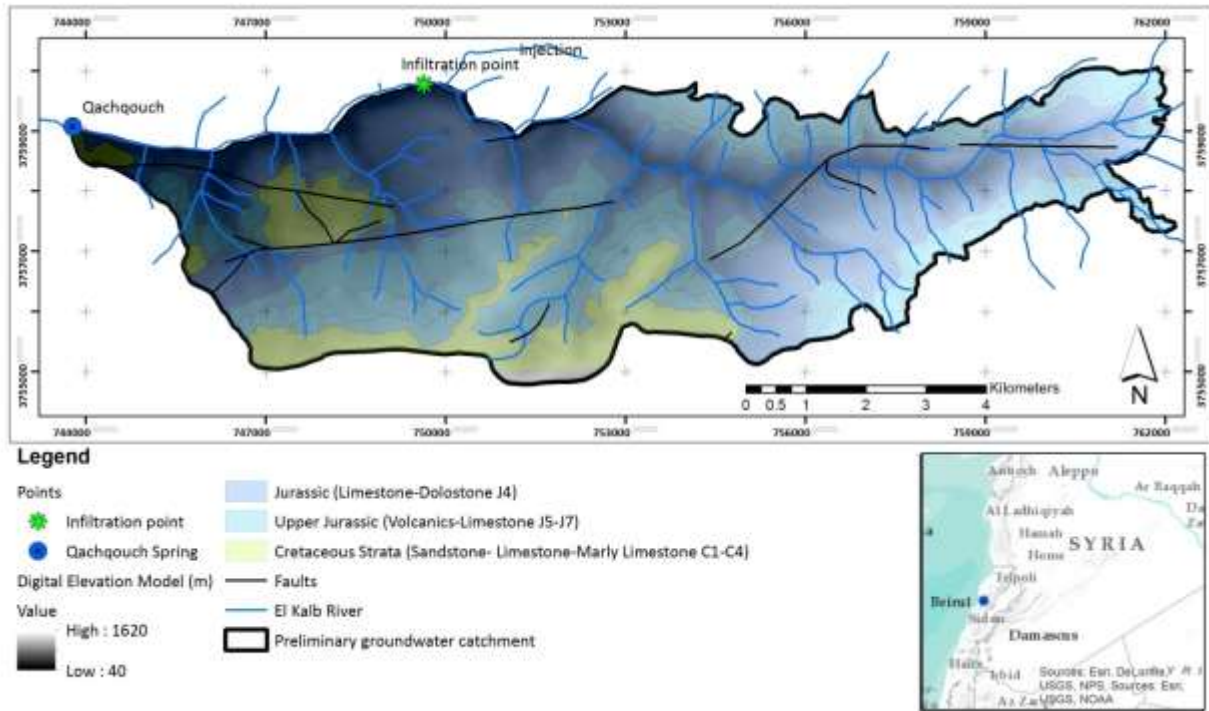
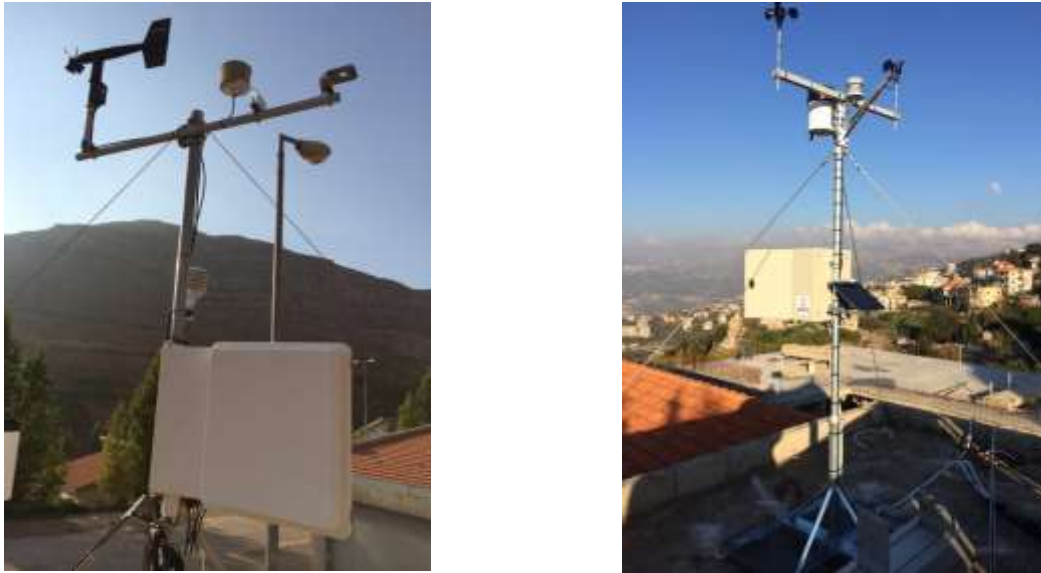


Figure 7.2. Geological map of the Qachqouch spring catchment outlined to date based on tracer experiments, geological boundaries and topography (Doummar and Aoun, 2018a).

7.2 Equipment and methods

- Climatic stations for the measurement of precipitation (including snow) at two different altitude (950 and 1700 m above sea level) for the assessment of potential evapotranspiration and input precipitation (frequency of 15 -60 min).
- Flow monitoring in both River and spring is done using pressure transducers for water level measurement. Discharge is estimated using a rating curve (Figure 7.4) based on monthly measurement of discharge. Concerns arise during high flow where accessibility to both spring and River is constrained. A multi-parameter probe measuring turbidity (TU), Electrical Conductivity (EC), temperature (TEMP), and water level (WL) is installed in the spring. Data time series collected in-situ to date include in addition to *flow rates (Q)*, *Electrical Conductivity (EC)*, *Temperature (T)*, *Turbidity (TU)*, *Dissolved Oxygen (DO)*. Flow calculations have a high level of uncertainty above 4 m³/s, therefore the constraining of high flow values was achieved with discharge rate frequency classification.

Data related to water balance is currently being collected on the Qachqouch catchment as follows (Table 7.1; Doummar et al., 2021).



a

b

Figure 7.3. a) Climatic Station at 1700 m (above sea level; asl); b) At 950 m (asl) installed in the framework of a USAID (PEER Science supported project).

Table 7.1. Collected data from the monitoring equipment, frequency and duration of monitoring.

Data monitoring	Frequency of monitoring	Time frame
Precipitation and other climatic series (x2 at elevations 950 m and 1700 m)	15- 60 min	Continuing (since 2014)
River time series (discharge, level, and temperature)	1 hour	Nov, 15, 2019- continuing
Spring discharge (Qachqouch)	30 min	Sept 2014- continuing
Isotope analysis (spring)	Every 3 days	Nov 27, 2019- continuing

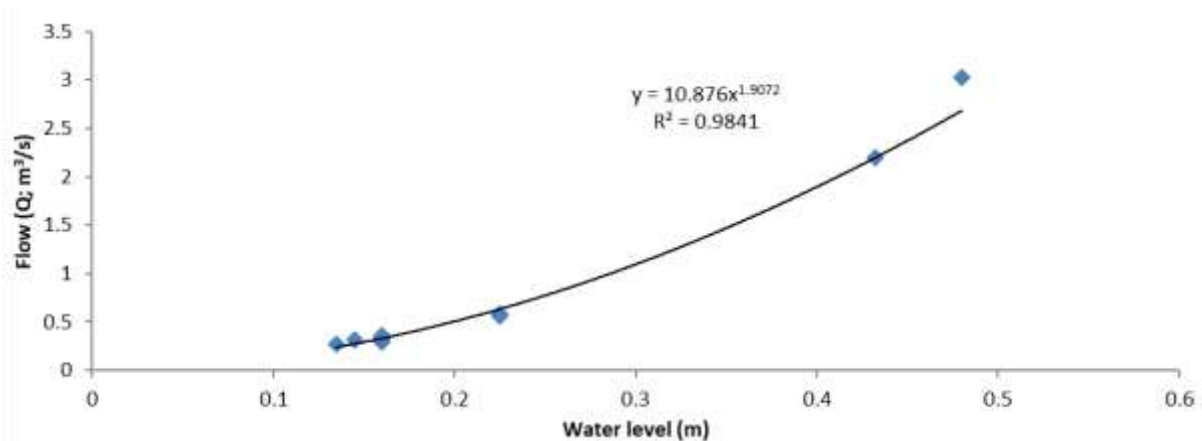


Figure 7.4. Rating curve that correlates water level observed with the pressure transducer and the flow rate (A high uncertainty is observed above 4 m³/s).

7.3 Results

7.3.1 Time series

A representation of the collected time series is shown on Figure 7.5 and Figure 7.6

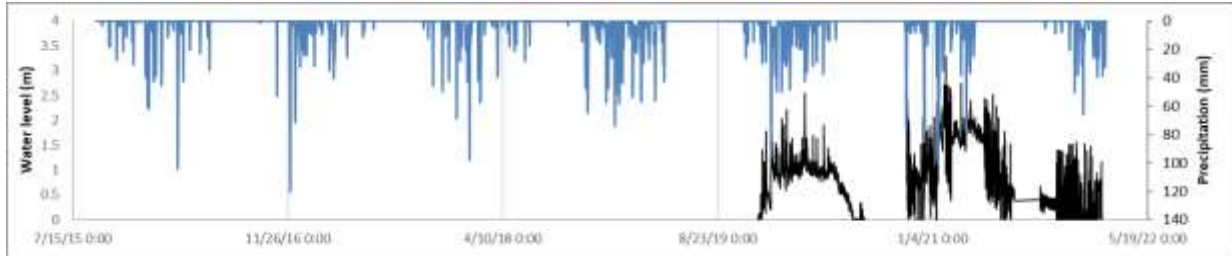


Figure 7.5. Time series of precipitation (elevation: 1700 masl) and level in the Nahr El Kalb River collected in the period 2019- 2022 during the course of the KARMA project.

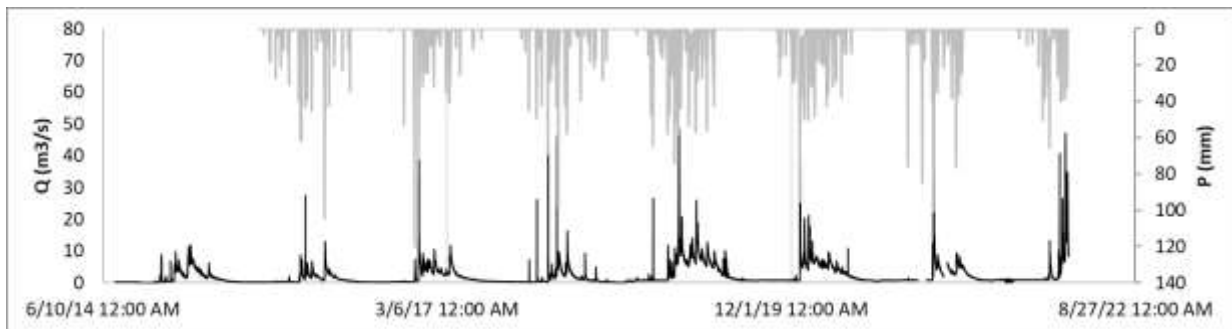


Figure 7.6. Time series of precipitation (elevation: 1700 masl) and flowrates at the Qachqouch spring collected in the period 2014-2022, with 2019- 2022 were collected during the course of the KARMA project.

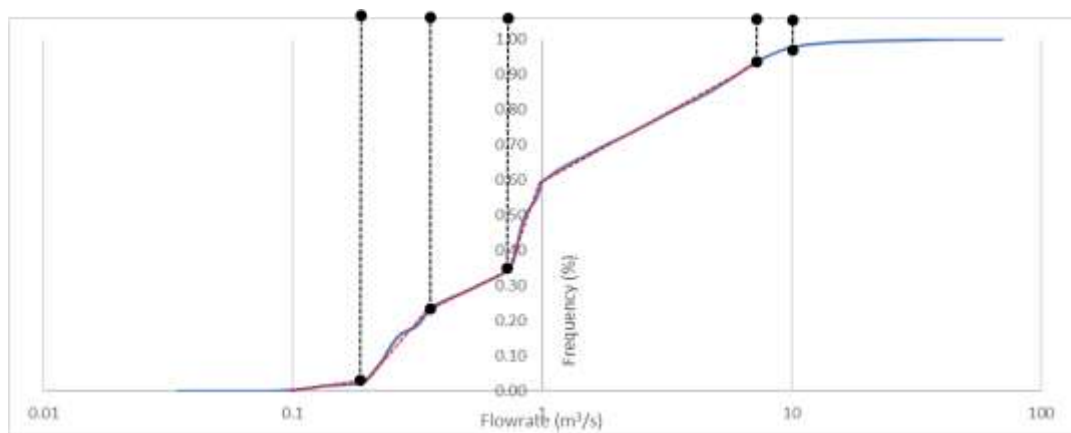


Figure 7.7. Classified flow rates on the Qachqouch spring (inflection points and changing slopes are noted at 0.20, 0.35, 0.75, 1.05, 7.7, and 10.5).

A classification of the flowrates (recorded between 2015-2022) according to their cumulative probability of occurrence yield at least four slope discontinuities and inflection points, noting different storage reservoirs in the system, this analysis is consistent with the analysis done by Dubois et al., 2020 on a dataset 2015-2017. Classified flow rates on the Qachqouch spring (inflection points and changing slopes are noted at 0.20, 0.35, 0.75, 1.05, 7.7, and 10.5). By summarizing these different behaviors, we can

determine that the source is alimeted by precedent storage during the depletions of the dry season (until 0.35 m³/s). Flowrates from 0.75 m³/s until 7.7 m³/s have about 60% frequency of occurrence. For the higher flow, 7.7 until around 10.5 m³/s, part of the flow should come from another system. For the flow rates higher than 9 m³/s, it is assumed that the gauging station is overflowed.

7.3.2 Data Correction

Flowrates below 0.09 and above 10.5 m³/s, have a very low likelihood of occurrence, therefore, discharge above 10.5 m³/s recorded by rating curve during high flow periods can be further corrected or cut off at 14.2 m³/s (likelihood of occurrence of 99%). These corrections allow to correct the total recorded volumes at the spring and refine the water balance components.

Flow correction for values below 10.5 m³/s, the flow parameters for the Qachqouch Spring including (slope and Manning coefficient) were calibrated based on mean flow velocity calculated on the rating curve. At a later stage value above 10.5 m³/s were calculated following the Manning-Strickler equation for observed water heights using the same channel parameters estimated on lower discharge rates. This correction allowed to reduce the uncertainties at flood rates and to minimize the error for domains where the rating curve is not applicable. Figure 7.9 shows the data post and pre-correction. Table 7.2 shows the errors in annual spring volumes before and after the correction especially for highly wet years.

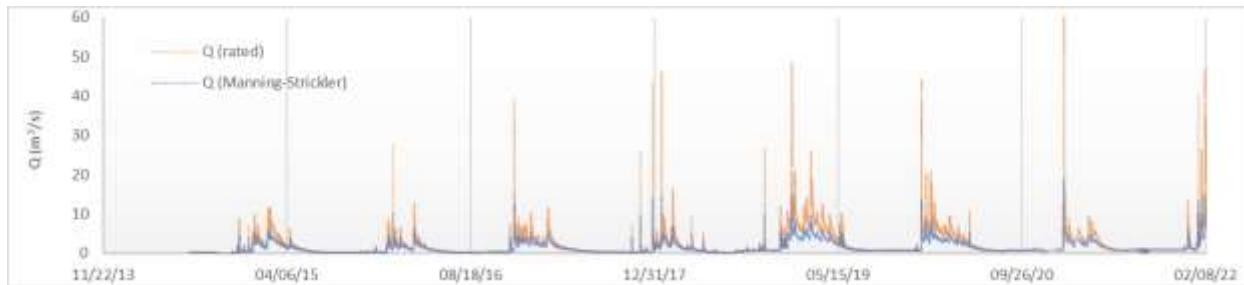


Figure 7.8. Discharge above 10 m³/s corrected and calculated based on manning- Strickler flow in an open channel with channel parameters (Slope $S= 0.012$ and Manning coefficient $n=0.025$) calibrated based on spring discharges calculated with the rating curve ($R^2= 0.99$ and $RMSE= 0.083$ m³/s).

Table 7.2. Total annual flow calculated based on the rating curve and based on the corrected discharge for values above 10 m³/s especially in very wet years.

Total Precipitation (mm) Value at 950 m asl	Discharge	
	Qr (rating curve) without correction	Corrected Qc (Qachqouch) and error ((Qr-Qc)/Qr)
921 mm (2015-16)	35 Mm ³ (2015-16)-652 mm (70%)	29 Mm ³ - 17%
1034 mm (2016-17)	47 Mm ³ (2016-17)- 839 mm (81%)	43 Mm ³ - 8%
1089 mm (2017-18)	50 Mm ³ (2017-18)- 892 mm (81%)	33 Mm ³ - 34%
1838 mm (2018-19)	105 Mm ³ (? Too high) High uncertainties in high flow measurements	76 Mm ³ - 27%
1405 mm (2019-20)	81.3 Mm ³ (? Too high)- High uncertainties in high flow measurements	59 Mm ³ - 27%
1160 mm (2020-21)	49.8 Mm ³ 890 mm (77%)	50 Mm ³ - 0%

7.3.3 Discharge auto- and cross correlation

Using the simple correlation (time dependency) allows to estimate the memory effect of a signal (when $r(k)=0.2$). Based on Figure 7.9, the below is noted in the autocorrelation analysis and memory effect (Dubois 2017):

- 3.4 hours for rain
- 61.5 days for the flow rates
- 73.5 days for the temperature
- 83.9 days for the Electrical Conductivity
- 16.1 days for the Nahr El-Kalb River.

The Qachqouch Spring has a significant memory effect, a relatively longer regulation time and a very low cut off frequency. According to Mangin's classification, the system is very inertial, which is inversely proportional to the karstification degree. The system stocks the water from the precipitations to give it back in annual (or longer) cycle, despite its high reactivity to rain events (Dubois et al., 2020).

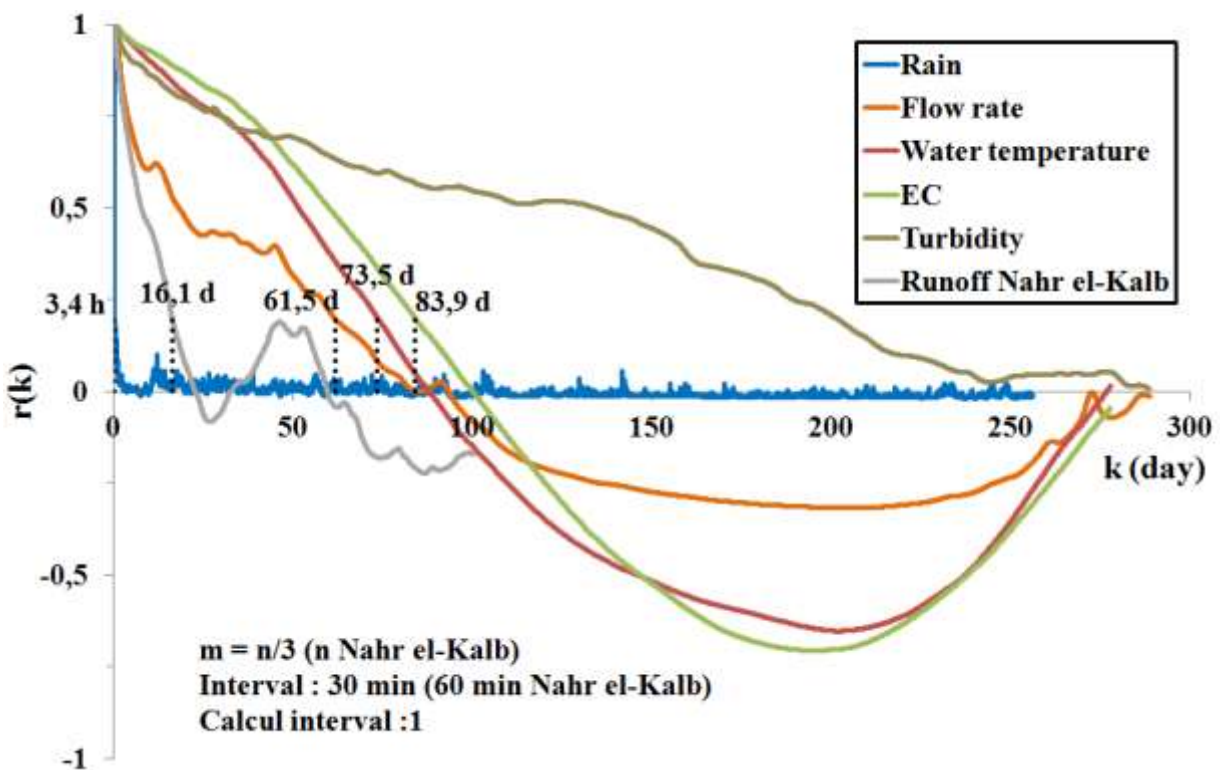


Figure 7.9. Simple correlation function of the sampled parameters (short term analysis – $m=n/3$; Dubois et al., 2020)

The rain could be assimilated to a random signal by the really short memory effect (< 4 hours) while the other signals (output) have a very long memory effect (>60 days), meaning that the system has latent inertia.

7.4 Conclusions

Spring monitoring undertaken during the project period allowed a collection of further data over 3 years additional years and river water level data. The timeseries were processed, and analyzed: water level at the spring were converted to flowrate based on a rating curve. The values above 10.5 m³/s appear to be anomalous value, where the rating curve is no longer applicable. Unfortunately, it remains very difficult to access the spring under these high flow periods. A correction of the time series for extensively wet years was done to minimize the error in the calculation of total yearly volumes observed at the spring.

The cross correlation and autocorrelation helped identify the memory effect of the spring of 60 days indicating a latent behavior of the spring (probably due to snow melt). Other more advanced correlations and inference of system dynamics and geometry were further validated based on recent time series as in Dubois et al., 2020.

7.5 References

Doummar J., et al., 2021. Assessment of water quality and quantity of springs at a pilot-scale: Applications in semi-arid Mediterranean areas in Lebanon. ESSOAR Preprint. <https://doi.org/10.1002/essoar.10508719.1>

Doummar, J. and Aoun, M. Occurrence of selected domestic and hospital emerging micropollutants on a rural surface water basin linked to a groundwater karst catchment, *Environmental Earth Sciences*, 77(9), 351, doi: 10.1007/s12665-018-7536-x, 2018b.

Dubois E., Doummar J., Pistre S., Larocque M. Calibration of a semi-distributed lumped model of a karst system using time series data analysis: the example of the Qachqouch karst spring. *Hydrol. Earth Syst. Sci.*, 24, 4275–4290, doi.org/10.5194/hess-24-4275-2020, 2020.

Dubois, E. Analysis of high-resolution spring hydrographs and climatic data: application on the Qachqouch spring (Lebanon), Master thesis, American University of Beirut, Department of Geology, Beirut, Lebanon. 2017. [online] Available from: https://www.researchgate.net/profile/Emmanuel_Dubois5/publication/320237930_Analysis_of_high_resolution_spring_hydrographs_and_climatic_data_application_on_the_Qachqouch_spring_Lebanon/links/59d69a76a6fdcc52aca7d05c/Analysis-of-high-resolution-spring-hydrographs-and-climatic-data-application-on-the-Qachqouch-spring-Lebanon.pdf, 2017

8 Conclusions

During the development of KARMA project, spring discharge has been successfully measured at the main discharge points of the different study areas. The obtained results are representative from different hydro-climatological conditions and recharge features of karst systems in the Mediterranean area: (1) minimum annual recharge is found in Eastern Ronda Mountains (Spain) and Lez study area (France) with 733 and 916 mm of and maximum that range from 1259 mm in Gran Sasso area (Italy) to 1840 mm in Hochifen-Gottesacker test site (Austria). (2) Recharge areas range from small sizes like 19.6 km² in Jebel Zaghouan aquifer (Tunisia) to medium size areas like 130 km² in Lez study area or 1034 km² in Gran Sasso area (Italy). However, the obtained results are somehow conditioned by the length of the record (e.g. historical vs. KARMA time span) and the hydrogeological knowledge acquired in previous investigations.

The 14 monitored springs of KARMA project showed a mean discharge flow of 0.81 m³/s and maximum spring discharge values vary between 0.085-0.89 at Carrizal (Spain) or RU1 (Italy) and 6-15 m³/s in permanent and overflow springs such as TI1 (Italy), Garciago (Spain), Lez (France) or Aubach (Austria). Minimum discharge varies between 0.005 and 0.2 m³/s at springs like Ventilla (Spain), Sägebach (Austria) or RU1 (Italy). The case of Djebel Zaghouan is quite special, as natural drainage does not exist anymore and groundwater exploitation is made through 9 boreholes and galleries intended for the drinking water supply

The analysis of recession curves through Mangin (1970, 1975) methodology in Lez spring showed values of the parameters k , i and α where k is found between 0.01 and 0.2, i is between 0.43 and 0.89 and α is between 0.01 and 0.08. In Spanish test sites, k parameter is established between 0.14 and 0.44, i is between 0.74 and 0.85 and α is between 0.003 and 0.45. However, the application of these methods to some springs might be affected by pumping or catchments for water supply of different scale populations.

The continuous monitoring of spring discharge added to previous good quality long-term data series and precipitation records has served as main input for other tasks such as water budget estimation (Deliverable 2.1). The acquired knowledge about aquifer functioning, water availability and spring discharge database constitutes an important input for the application and validation of modeling tools (Deliverables 4.2-4) and prediction of different climate scenarios.

8.1 References

Mangin, A. (1970) Contribution à l'étude des aquifères karstiques à partir de l'analyse des courbes de décrue et tarissement. *Annales Spéléologie* 25 (3), 581-610.

Mangin, A. (1975) Contribution à l'étude hydrodynamique des aquifères karstiques (I). PhD Thesis. Dijon University (France). *Annales Spéléologie* 29 (3), 283-332; 29 (4), 495-601; 30 (1), 21-214.